

Tunneling in Luttinger Liquids

ラッティンジャー流体におけるトンネル効果

古崎 昭

①

Tunneling in Luttinger Liquids

*submitted to the Department of Physics, The University of Tokyo
as a thesis for the degree of Doctor of Science*

by

Akira Furusaki

*Department of Applied Physics
Faculty of Engineering
The University of Tokyo*

April 1993

Acknowledgements

I would like to acknowledge Prof. N. Nagaosa for his continual guidance and encouragement during the course of the present work. I have learned from him most of field-theoretical methods used in this thesis; without his instructive suggestions I could not have completed this work. I am also grateful to my former supervisor, Prof. M. Tsukada, who introduced me to this fertile field in physics, i.e., physics of tunneling phenomena. I am pleased to thank Dr. T. Ogawa for helping my understanding of the orthogonality catastrophe in studying the Fermi-edge singularities in Luttinger liquids and Dr. M. Ueda for stimulating my interest in the Coulomb blockade in small tunnel junctions. I also wish to acknowledge Dr. M. P. A. Fisher for useful discussions during the ISQM '92. I am indebted to Prof. P. A. Lee for informing me of preprints by Dr. C. L. Kane and Dr. M. P. A. Fisher when I told him an idea of the tunneling in a Luttinger liquid. Thanks are extended to all the members of the theoretical condensed-matter group at the Department of Applied Physics as well as at the Department of Physics.

Last but not least, I wish to thank my parents for their continual encouragement.

Contents

1	General Introduction	1
1.1	Introduction	1
1.2	Language of the text	2
1.3	The author's intention	3
2	Worked Example 1: Simple Circuit	10
2.1	Introduction	10
2.2	Problem Statement	11
2.3	Solution	12
2.4	Discussion	13
2.5	Conclusion	14
3	Worked Example 2: Simple Circuit	15
3.1	Introduction	15
3.2	Problem Statement	16
3.3	Solution	17
3.4	Discussion	18
3.5	Conclusion	19
4	Worked Example 3: Simple Circuit	20
4.1	Introduction	20
4.2	Problem Statement	21
4.3	Solution	22
4.4	Discussion	23
4.5	Conclusion	24
5	Worked Example 4: Simple Circuit	25
5.1	Introduction	25
5.2	Problem Statement	26
5.3	Solution	27
5.4	Discussion	28
5.5	Conclusion	29
6	Worked Example 5: Simple Circuit	30
6.1	Introduction	30
6.2	Problem Statement	31
6.3	Solution	32
6.4	Discussion	33
6.5	Conclusion	34
7	Worked Example 6: Simple Circuit	35
7.1	Introduction	35
7.2	Problem Statement	36
7.3	Solution	37
7.4	Discussion	38
7.5	Conclusion	39
8	Worked Example 7: Simple Circuit	40
8.1	Introduction	40
8.2	Problem Statement	41
8.3	Solution	42
8.4	Discussion	43
8.5	Conclusion	44
9	Worked Example 8: Simple Circuit	45
9.1	Introduction	45
9.2	Problem Statement	46
9.3	Solution	47
9.4	Discussion	48
9.5	Conclusion	49
10	Worked Example 9: Simple Circuit	50
10.1	Introduction	50
10.2	Problem Statement	51
10.3	Solution	52
10.4	Discussion	53
10.5	Conclusion	54
11	Worked Example 10: Simple Circuit	55
11.1	Introduction	55
11.2	Problem Statement	56
11.3	Solution	57
11.4	Discussion	58
11.5	Conclusion	59
12	Worked Example 11: Simple Circuit	60
12.1	Introduction	60
12.2	Problem Statement	61
12.3	Solution	62
12.4	Discussion	63
12.5	Conclusion	64
13	Worked Example 12: Simple Circuit	65
13.1	Introduction	65
13.2	Problem Statement	66
13.3	Solution	67
13.4	Discussion	68
13.5	Conclusion	69
14	Worked Example 13: Simple Circuit	70
14.1	Introduction	70
14.2	Problem Statement	71
14.3	Solution	72
14.4	Discussion	73
14.5	Conclusion	74
15	Worked Example 14: Simple Circuit	75
15.1	Introduction	75
15.2	Problem Statement	76
15.3	Solution	77
15.4	Discussion	78
15.5	Conclusion	79
16	Worked Example 15: Simple Circuit	80
16.1	Introduction	80
16.2	Problem Statement	81
16.3	Solution	82
16.4	Discussion	83
16.5	Conclusion	84
17	Worked Example 16: Simple Circuit	85
17.1	Introduction	85
17.2	Problem Statement	86
17.3	Solution	87
17.4	Discussion	88
17.5	Conclusion	89
18	Worked Example 17: Simple Circuit	90
18.1	Introduction	90
18.2	Problem Statement	91
18.3	Solution	92
18.4	Discussion	93
18.5	Conclusion	94
19	Worked Example 18: Simple Circuit	95
19.1	Introduction	95
19.2	Problem Statement	96
19.3	Solution	97
19.4	Discussion	98
19.5	Conclusion	99
20	Worked Example 19: Simple Circuit	100
20.1	Introduction	100
20.2	Problem Statement	101
20.3	Solution	102
20.4	Discussion	103
20.5	Conclusion	104
21	Worked Example 20: Simple Circuit	105
21.1	Introduction	105
21.2	Problem Statement	106
21.3	Solution	107
21.4	Discussion	108
21.5	Conclusion	109
22	Worked Example 21: Simple Circuit	110
22.1	Introduction	110
22.2	Problem Statement	111
22.3	Solution	112
22.4	Discussion	113
22.5	Conclusion	114
23	Worked Example 22: Simple Circuit	115
23.1	Introduction	115
23.2	Problem Statement	116
23.3	Solution	117
23.4	Discussion	118
23.5	Conclusion	119
24	Worked Example 23: Simple Circuit	120
24.1	Introduction	120
24.2	Problem Statement	121
24.3	Solution	122
24.4	Discussion	123
24.5	Conclusion	124
25	Worked Example 24: Simple Circuit	125
25.1	Introduction	125
25.2	Problem Statement	126
25.3	Solution	127
25.4	Discussion	128
25.5	Conclusion	129
26	Worked Example 25: Simple Circuit	130
26.1	Introduction	130
26.2	Problem Statement	131
26.3	Solution	132
26.4	Discussion	133
26.5	Conclusion	134
27	Worked Example 26: Simple Circuit	135
27.1	Introduction	135
27.2	Problem Statement	136
27.3	Solution	137
27.4	Discussion	138
27.5	Conclusion	139
28	Worked Example 27: Simple Circuit	140
28.1	Introduction	140
28.2	Problem Statement	141
28.3	Solution	142
28.4	Discussion	143
28.5	Conclusion	144
29	Worked Example 28: Simple Circuit	145
29.1	Introduction	145
29.2	Problem Statement	146
29.3	Solution	147
29.4	Discussion	148
29.5	Conclusion	149
30	Worked Example 29: Simple Circuit	150
30.1	Introduction	150
30.2	Problem Statement	151
30.3	Solution	152
30.4	Discussion	153
30.5	Conclusion	154
31	Worked Example 30: Simple Circuit	155
31.1	Introduction	155
31.2	Problem Statement	156
31.3	Solution	157
31.4	Discussion	158
31.5	Conclusion	159
32	Worked Example 31: Simple Circuit	160
32.1	Introduction	160
32.2	Problem Statement	161
32.3	Solution	162
32.4	Discussion	163
32.5	Conclusion	164
33	Worked Example 32: Simple Circuit	165
33.1	Introduction	165
33.2	Problem Statement	166
33.3	Solution	167
33.4	Discussion	168
33.5	Conclusion	169
34	Worked Example 33: Simple Circuit	170
34.1	Introduction	170
34.2	Problem Statement	171
34.3	Solution	172
34.4	Discussion	173
34.5	Conclusion	174
35	Worked Example 34: Simple Circuit	175
35.1	Introduction	175
35.2	Problem Statement	176
35.3	Solution	177
35.4	Discussion	178
35.5	Conclusion	179
36	Worked Example 35: Simple Circuit	180
36.1	Introduction	180
36.2	Problem Statement	181
36.3	Solution	182
36.4	Discussion	183
36.5	Conclusion	184
37	Worked Example 36: Simple Circuit	185
37.1	Introduction	185
37.2	Problem Statement	186
37.3	Solution	187
37.4	Discussion	188
37.5	Conclusion	189
38	Worked Example 37: Simple Circuit	190
38.1	Introduction	190
38.2	Problem Statement	191
38.3	Solution	192
38.4	Discussion	193
38.5	Conclusion	194
39	Worked Example 38: Simple Circuit	195
39.1	Introduction	195
39.2	Problem Statement	196
39.3	Solution	197
39.4	Discussion	198
39.5	Conclusion	199
40	Worked Example 39: Simple Circuit	200
40.1	Introduction	200
40.2	Problem Statement	201
40.3	Solution	202
40.4	Discussion	203
40.5	Conclusion	204
41	Worked Example 40: Simple Circuit	205
41.1	Introduction	205
41.2	Problem Statement	206
41.3	Solution	207
41.4	Discussion	208
41.5	Conclusion	209
42	Worked Example 41: Simple Circuit	210
42.1	Introduction	210
42.2	Problem Statement	211
42.3	Solution	212
42.4	Discussion	213
42.5	Conclusion	214
43	Worked Example 42: Simple Circuit	215
43.1	Introduction	215
43.2	Problem Statement	216
43.3	Solution	217
43.4	Discussion	218
43.5	Conclusion	219
44	Worked Example 43: Simple Circuit	220
44.1	Introduction	220
44.2	Problem Statement	221
44.3	Solution	222
44.4	Discussion	223
44.5	Conclusion	224
45	Worked Example 44: Simple Circuit	225
45.1	Introduction	225
45.2	Problem Statement	226
45.3	Solution	227
45.4	Discussion	228
45.5	Conclusion	229
46	Worked Example 45: Simple Circuit	230
46.1	Introduction	230
46.2	Problem Statement	231
46.3	Solution	232
46.4	Discussion	233
46.5	Conclusion	234
47	Worked Example 46: Simple Circuit	235
47.1	Introduction	235
47.2	Problem Statement	236
47.3	Solution	237
47.4	Discussion	238
47.5	Conclusion	239
48	Worked Example 47: Simple Circuit	240
48.1	Introduction	240
48.2	Problem Statement	241
48.3	Solution	242
48.4	Discussion	243
48.5	Conclusion	244
49	Worked Example 48: Simple Circuit	245
49.1	Introduction	245
49.2	Problem Statement	246
49.3	Solution	247
49.4	Discussion	248
49.5	Conclusion	249
50	Worked Example 49: Simple Circuit	250
50.1	Introduction	250
50.2	Problem Statement	251
50.3	Solution	252
50.4	Discussion	253
50.5	Conclusion	254
51	Worked Example 50: Simple Circuit	255
51.1	Introduction	255
51.2	Problem Statement	256
51.3	Solution	257
51.4	Discussion	258
51.5	Conclusion	259
52	Worked Example 51: Simple Circuit	260
52.1	Introduction	260
52.2	Problem Statement	261
52.3	Solution	262
52.4	Discussion	263
52.5	Conclusion	264
53	Worked Example 52: Simple Circuit	265
53.1	Introduction	265
53.2	Problem Statement	266
53.3	Solution	267
53.4	Discussion	268
53.5	Conclusion	269
54	Worked Example 53: Simple Circuit	270
54.1	Introduction	270
54.2	Problem Statement	271
54.3	Solution	272
54.4	Discussion	273
54.5	Conclusion	274
55	Worked Example 54: Simple Circuit	275
55.1	Introduction	275
55.2	Problem Statement	276
55.3	Solution	277
55.4	Discussion	278
55.5	Conclusion	279
56	Worked Example 55: Simple Circuit	280
56.1	Introduction	280
56.2	Problem Statement	281
56.3	Solution	282
56.4	Discussion	283
56.5	Conclusion	284
57	Worked Example 56: Simple Circuit	285
57.1	Introduction	285
57.2	Problem Statement	286
57.3	Solution	287
57.4	Discussion	288
57.5	Conclusion	289
58	Worked Example 57: Simple Circuit	290
58.1	Introduction	290
58.2	Problem Statement	291
58.3	Solution	292
58.4	Discussion	293
58.5	Conclusion	294
59	Worked Example 58: Simple Circuit	295
59.1</		

Contents

1	General Introduction	1
1.1	Introduction	1
1.2	Tomonaga-Luttinger model	3
1.3	Localization problem in dirty Luttinger liquids	10
2	Tunneling through a Single Barrier	15
2.1	Introduction	15
2.2	Effective action	16
2.3	Weak barrier potential	17
2.3.1	Scaling equations	17
2.3.2	Conductance	20
2.4	Strong barrier potential	23
2.4.1	Duality mapping and scaling equations	23
2.4.2	Conductance	27
2.5	Summary	30
3	Resonant Tunneling	33
3.1	Introduction	33
3.2	Effective action	36
3.3	Weak barrier potential	37
3.3.1	Scaling equations	37
3.3.2	Conductance	39
3.4	Strong barrier potential	41
3.4.1	Scaling equations and phase diagram	41
3.4.2	Conductance	46
3.5	Asymmetric Barriers	50
3.6	Summary	51
4	Anderson Localization	53
4.1	Introduction	53
4.2	Effective action	54
4.3	Implications to transport properties	55
4.4	Summary	57
5	Concluding Remarks	59
5.1	Conclusions	59
5.2	Related problems	60

Appendices	61
A.1 Derivation of Eq. (2.27)	61
A.2 Derivation of Eq. (2.29)	62
A.3 Conductance from $\langle \hat{\theta}(\omega_n) \hat{\theta}(-\omega_n) \rangle$	63
A.4 Equivalence between two models	70
A.5 Derivation of Eqs. (3.43) and (3.45)	71

General Introduction

1.1 Introduction

The purpose of this book is to provide a comprehensive treatment of the theory of stochastic processes and their applications. The book is divided into two main parts: the first part deals with the theory of stochastic processes, and the second part deals with their applications. The first part is divided into three chapters: Chapter 1 deals with the theory of stochastic processes, Chapter 2 deals with the theory of stochastic processes, and Chapter 3 deals with the theory of stochastic processes. The second part is divided into two chapters: Chapter 4 deals with the applications of stochastic processes, and Chapter 5 deals with the applications of stochastic processes.

The book is intended for students and researchers in the field of stochastic processes and their applications. It is a comprehensive treatment of the theory of stochastic processes and their applications. The book is divided into two main parts: the first part deals with the theory of stochastic processes, and the second part deals with their applications. The first part is divided into three chapters: Chapter 1 deals with the theory of stochastic processes, Chapter 2 deals with the theory of stochastic processes, and Chapter 3 deals with the theory of stochastic processes. The second part is divided into two chapters: Chapter 4 deals with the applications of stochastic processes, and Chapter 5 deals with the applications of stochastic processes.

Chapter 1

General Introduction

1.1 Introduction

The subject of this thesis is the tunneling through potential barriers in one-dimensional (1D) interacting electron systems. The electronic transport in mesoscopic devices has been intensively studied over the past decade. With progress in the micro-fabrication techniques, it is now becoming possible to design devices intentionally in nanometer or even atomic scale. Clearly, as the system size is reduced, the Coulomb interaction between electrons becomes more important, and hence the electronic transport or tunneling is strongly affected by the Coulomb repulsion [1, 2]. A well-explored example of this effect is the Coulomb blockade: in small-capacitance tunnel junctions the tunneling is suppressed due to a large charging energy. However, even in these systems in which the Coulomb blockade effect has been observed, electron density in leads (wires) is large enough to screen the Coulomb repulsion, thereby making the Hartree-type approximation valid. Then a question arises: What happens if the leads themselves are very narrow and if the electron density is so low that the Coulomb interaction can no longer be screened off? More precisely, how is the tunneling affected by the electron-electron interaction in such a *single*-channel quantum wire? This is the problem addressed in this thesis.

Single-channel quantum wires may be viewed as a 1D system. It is well known that the electron-electron interaction is of crucial importance in 1D; an interacting electron system is in general described not as a Fermi liquid but as a Luttinger liquid [3] provided that the system has a gapless excitation. This was shown in weak-coupling regime by using abelian bosonization methods in the 1970's [4, 5, 6, 7]. The validity of the Luttinger-liquid picture has been confirmed very recently also in the strong-coupling regime by using conformal field theory techniques and the Bethe ansatz methods [8, 9]. Although these two methods are very powerful when applied to exactly solvable models, a more useful and familiar tool for a qualitative description of the Luttinger liquid is the conventional abelian bosonization method [4, 5, 6, 7]. The method allows us to write an interacting electron system as a Gaussian model of free bosonic phase fields introduced by Suzumura [4].

The question raised above is thus reduced to a problem of the tunneling through some potential barriers in a Luttinger liquid. Therefore we will study (1) the tunneling of electrons through a single barrier, (2) the resonant tunneling of spinless fermions through a double-barrier structure, and (3) the electronic transport in dirty conductors with many barriers. To attack them, we will adopt the Tomonaga-Luttinger model [10, 11, 12] with δ -function potentials and use the bosonization method.

In fact, the transport in Luttinger liquids has attracted great theoretical attention for about a decade. In particular, dirty Luttinger liquids with many impurities have been discussed in detail in a lot of papers [13, 14, 15, 16]. These studies showed that dirty Luttinger liquids exhibit the localization-delocalization transition at zero temperature when the interaction between electrons is changed. The usual Anderson localization of a 1D noninteracting system can be regarded as a special case of this interaction-induced localization-delocalization transition. The localization-delocalization transition in a dirty Luttinger liquid was first studied by a perturbation expansion with respect to the impurity potential by Chui and Bray [13] and then by Apel [14]. The transition was also investigated from the localized region by Suzumura and Fukuyama [15], who used the phase Hamiltonian representation and proposed to view the localization as a pinning process of phase fields by the impurity potential. In this thesis we will follow this idea to treat the tunneling through a few tunnel barriers in a Luttinger liquid.

It is a peculiar fact that until very recently the problem of a Luttinger liquid with a few defects has not been studied, although it seems simpler than the localization problem in a Luttinger liquid with many impurities. The single-barrier problem was first discussed by Kane and Fisher [17] and subsequently by the present author [18]; the resonant tunneling through a double barrier was also studied quite recently [19, 20, 21]. The papers by Kane and Fisher are complementary to and in part overlap the present thesis.

It is also worth noting that, as we will see in the following chapters, the tunneling in a Luttinger liquid is essentially equivalent to the well-known problem of the macroscopic quantum coherence in a dissipative system [22, 23, 24, 25], which in turn has a deep connection with many issues related to the infrared catastrophe, such as the Kondo effect [26]. Thus we can apply various techniques developed so far to our tunneling problem.

Although the Luttinger liquid has so far been just a theoretical toy model, it will become a subject of experimental study in the future. To see Luttinger-liquid behavior experimentally, one must prepare a 1D conductor; one candidate is a truly single-channel quantum wire. In a transport experiment the quantum wire of finite length L must be used and connected to three-dimensional (3D) leads. If both the resistance of the 3D leads and the contact resistance at the 1D-3D interfaces (though it is not known even theoretically what is happening at the interface of a Fermi liquid and a Luttinger liquid) are much less than that of the 1D wire, then one can probe the transport property of the Luttinger liquid at a temperature higher than $T_L = \hbar v_F / k_B L$. Therefore it is necessary to use a sufficiently long and clean wire to see the yet unseen Luttinger-liquid behavior which is expected to be observed at low temperature. This seems a rather difficult condition for experiments, and no experimental results suggesting Luttinger-liquid behavior have so far been observed. Though it does not exist at the present, such an ideal 1D wire will be available in the future. Then by fabricating one or two constrictions in the lead the tunneling transport in a Luttinger liquid can be studied experimentally.

A comment on the term "Luttinger liquid" might be in order here. It was first used by Haldane [3], who noticed that a wide class of 1D many-body systems has a low-energy excitation spectrum similar to the Luttinger model spectrum [11], and has since then become standard in the literature. The Luttinger model is closely related with the Tomonaga model, which was discussed by Tomonaga in 1950 [10]. The difference between these two models lies only in the high-energy cutoff: The Luttinger model deals with Dirac fermions whereas in the Tomonaga model the energy dispersion is cut off by a band width. In so far as the low-energy properties that we are interested in are concerned, both models are essentially

equivalent. In this sense, "Tomonaga-Luttinger liquid" might be a better term than the "Luttinger liquid." Nevertheless, the simple and common term "Luttinger liquid" will be used throughout this thesis.

The plan of this thesis will be as follows. In the rest of this chapter we review the abelian bosonization method and introduce the phase fields. We also review the localization-delocalization transition in a dirty Luttinger liquid. In Chap. 2 we explore the tunneling of electrons through a single barrier. It will be shown that in Luttinger liquids the barrier potential is renormalized to zero or infinity depending on the electron-electron interaction, and that at zero temperature the system can be classified into four phases, corresponding to either perfect transmission or perfect reflection of the charge and spin degrees of freedom. In the noninteracting case the potential is a marginal perturbation, which is consistent with the Landauer theory. In Chap. 3 we study the resonant tunneling of spinless fermions through a double-barrier structure. It will be shown that for weakly repulsive interaction the resonant tunneling is possible, but with anomalous temperature dependence of conductance peak height and width. In Chap. 4 we discuss the Anderson localization in 1D dirty quantum wires with emphasis on a crossover at finite temperature. The results are summarized in Chap. 5. Some complicated calculations are relegated to Appendices.

1.2 Tomonaga-Luttinger model

In this section we review briefly the bosonization method [4, 5, 6, 7, 12] for the Tomonaga-Luttinger model [10, 11], which is an exactly solvable model describing a 1D interacting electron system. A more complete discussion on the bosonization is found in Haldane's paper [3]. We take $\hbar = k_B = 1$ throughout this thesis.

The Fermi surface of a 1D electron system consists of two Fermi points, k_F and $-k_F$, around which we may linearize the energy dispersion of a free electron as

$$\epsilon_k = v_F(|k| - k_F), \quad (1.1)$$

where v_F is the Fermi velocity. Although this approximation is justified only near the Fermi points, we use the dispersion relation (1.1) for all momentum k . Thus we have two branches of energy dispersion as shown in Fig. 1.1. The negative-energy states ($k < k_F$ for branch 1 and $k > -k_F$ for 2) are all occupied at zero temperature if there is no interaction between electrons. This linearization of the dispersion is a crucial approximation, which makes the Tomonaga-Luttinger model exactly solvable. The error arising from the approximation should be small when we are dealing with low-energy processes only. Therefore we can expect that the results obtained from the model are reliable concerning the low-energy or long-distance properties of the system. Hence the kinetic energy part of the model Hamiltonian becomes

$$H_0 = v_F \sum_{k,s} (k - k_F) a_{1,k,s}^\dagger a_{1,k,s} + v_F \sum_{k,s} (-k - k_F) a_{2,k,s}^\dagger a_{2,k,s}, \quad (1.2)$$

where $a_{i,k,s}^\dagger$ ($a_{i,k,s}$) is a creation (annihilation) operator of an electron of branch i with momentum k and spin s ; $s = +1$ (-1) refers to up (down) spin. The creation and annihilation operators obey

$$\{a_{i,k,s}, a_{i',k',s'}\} = 0, \quad \{a_{i,k,s}^\dagger, a_{i',k',s'}^\dagger\} = 0, \quad \{a_{i,k,s}, a_{i',k',s'}\} = \delta_{i,i'} \delta_{k,k'} \delta_{s,s'}, \quad (1.3)$$

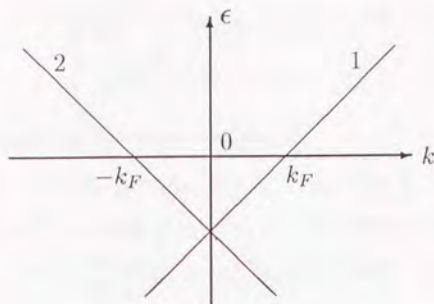


Figure 1.1: The linearized dispersion relation: $\epsilon = v_F(k - k_F)$ and $\epsilon = v_F(-k - k_F)$.

where $\{A, B\} \equiv AB + BA$.

The interaction part of the model Hamiltonian is given by

$$\begin{aligned}
 H_{\text{int}} = & \frac{1}{L} \sum_{k_1, s_1} \sum_{k_2, s_2} \sum_p (g_{2\parallel} \delta_{s_1, s_2} + g_{2\perp} \delta_{s_1, -s_2}) a_{1, k_1, s_1}^\dagger a_{1, k_1 - p, s_1} a_{2, k_2, s_2}^\dagger a_{2, k_2 + p, s_2} \\
 & + \frac{1}{L} \sum_{k_1, s_1} \sum_{k_2, s_2} \sum_{p > 0} (g_{4\parallel} \delta_{s_1, s_2} + g_{4\perp} \delta_{s_1, -s_2}) \\
 & \times (a_{1, k_1, s_1}^\dagger a_{1, k_1 - p, s_1} a_{1, k_2, s_2}^\dagger a_{1, k_2 + p, s_2} + a_{2, k_1, s_1}^\dagger a_{2, k_1 + p, s_1} a_{2, k_2, s_2}^\dagger a_{2, k_2 - p, s_2}), \quad (1.4)
 \end{aligned}$$

where L is the length of the system, $g_{2\parallel}$ and $g_{2\perp}$ are the matrix elements for the forward scattering, and $g_{4\parallel}$ and $g_{4\perp}$ are those for the scattering between electrons belonging to the same branch. We neglect both the backward scattering and umklapp scattering, simply assuming that they are irrelevant perturbations. It is important to note that the number of electrons of spin s is preserved for each branch; $[H_{\text{int}}, N_{is}] = 0$ where $N_{is} = \sum_k a_{i, k, s}^\dagger a_{i, k, s}$.

As explained in detail in a standard textbook [12], the total Hamiltonian, $H = H_0 + H_{\text{int}}$, can be conveniently expressed in terms of the charge and spin density operators as

$$\begin{aligned}
 H = & v_F(1 + \tilde{g}_{4\parallel} + \tilde{g}_{4\perp}) \sum_p |p| b_p^\dagger b_p + v_F(1 + \tilde{g}_{4\parallel} - \tilde{g}_{4\perp}) \sum_p |p| c_p^\dagger c_p \\
 & + v_F(\tilde{g}_{2\parallel} + \tilde{g}_{2\perp}) \sum_{p > 0} p (b_p^\dagger b_{-p}^\dagger + b_{-p} b_p) + v_F(\tilde{g}_{2\parallel} - \tilde{g}_{2\perp}) \sum_{p > 0} p (c_p^\dagger c_{-p}^\dagger + c_{-p} c_p), \quad (1.5)
 \end{aligned}$$

where

$$\tilde{g}_{2\parallel} \equiv \frac{g_{2\parallel}}{2\pi v_F}, \quad \tilde{g}_{2\perp} \equiv \frac{g_{2\perp}}{2\pi v_F}, \quad \tilde{g}_{4\parallel} \equiv \frac{g_{4\parallel}}{2\pi v_F}, \quad \tilde{g}_{4\perp} \equiv \frac{g_{4\perp}}{2\pi v_F}. \quad (1.6)$$

The annihilation operators b_p and c_p are proportional to the charge and spin density operators, respectively:

$$b_p = \begin{cases} \left(\frac{\pi}{pL}\right)^{1/2} \sum_{k, s} a_{1, k-p, s}^\dagger a_{1, k, s}, & p > 0 \\ \left(\frac{\pi}{|p|L}\right)^{1/2} \sum_{k, s} a_{2, k+|p|, s}^\dagger a_{2, k, s}, & p < 0, \end{cases} \quad (1.7)$$

$$c_p = \begin{cases} \left(\frac{\pi}{pL}\right)^{1/2} \sum_{k,s} s a_{1,k-p,s}^\dagger a_{1,k,s}, & p > 0 \\ \left(\frac{\pi}{|p|L}\right)^{1/2} \sum_{k,s} s a_{2,k+|p|,s}^\dagger a_{2,k,s}, & p < 0. \end{cases} \quad (1.8)$$

Note that b_p and c_p obey boson commutation relations:

$$[b_p, b_{p'}] = [c_p, c_{p'}] = [b_p, c_{p'}] = [b_p, c_p^\dagger] = 0, \quad [b_p, b_{p'}^\dagger] = [c_p, c_{p'}^\dagger] = \delta_{p,p'}. \quad (1.9)$$

Equation (1.5) can be easily diagonalized by using the Bogoliubov transformation, yielding

$$H = v_\rho \sum_p |p| \beta_p^\dagger \beta_p + v_\sigma \sum_p |p| \gamma_p^\dagger \gamma_p + \text{const.}, \quad (1.10)$$

where

$$\begin{aligned} v_\rho &= v_F \left[(1 + \tilde{g}_{4\parallel} + \tilde{g}_{4\perp})^2 - (\tilde{g}_{2\parallel} + \tilde{g}_{2\perp})^2 \right]^{1/2}, \\ b_p &= \beta_p \cosh \lambda_\rho - \beta_{-p}^\dagger \sinh \lambda_\rho, \\ \tanh(2\lambda_\rho) &= \frac{\tilde{g}_{2\parallel} + \tilde{g}_{2\perp}}{1 + \tilde{g}_{4\parallel} + \tilde{g}_{4\perp}}, \\ v_\sigma &= v_F \left[(1 + \tilde{g}_{4\parallel} - \tilde{g}_{4\perp})^2 - (\tilde{g}_{2\parallel} - \tilde{g}_{2\perp})^2 \right]^{1/2}, \\ c_p &= \gamma_p \cosh \lambda_\sigma - \gamma_{-p}^\dagger \sinh \lambda_\sigma, \\ \tanh(2\lambda_\sigma) &= \frac{\tilde{g}_{2\parallel} - \tilde{g}_{2\perp}}{1 + \tilde{g}_{4\parallel} - \tilde{g}_{4\perp}}. \end{aligned}$$

The operators β_p and γ_p , of course, obey the commutation relation,

$$[\beta_p, \beta_{p'}] = [\gamma_p, \gamma_{p'}] = [\beta_p, \gamma_{p'}] = [\beta_p, \gamma_p^\dagger] = 0, \quad [\beta_p, \beta_{p'}^\dagger] = [\gamma_p, \gamma_{p'}^\dagger] = \delta_{p,p'}. \quad (1.11)$$

Now we define phase fields by the following equations:

$$\begin{aligned} \theta_+(x) &\equiv i \sum_{k>0} \sqrt{\frac{\pi}{Lk}} e^{-\alpha k/2} \left[e^{-ikx} (b_k^\dagger + b_{-k}) - e^{ikx} (b_k + b_{-k}^\dagger) \right] \\ &= i \sqrt{\eta_\rho} \sum_{k>0} \sqrt{\frac{\pi}{Lk}} e^{-\alpha k/2} \left[e^{-ikx} (\beta_k^\dagger + \beta_{-k}) - e^{ikx} (\beta_k + \beta_{-k}^\dagger) \right], \end{aligned} \quad (1.12)$$

$$\begin{aligned} \theta_-(x) &\equiv i \sum_{k>0} \sqrt{\frac{\pi}{Lk}} e^{-\alpha k/2} \left[e^{-ikx} (b_k^\dagger - b_{-k}) - e^{ikx} (b_k - b_{-k}^\dagger) \right] \\ &= \frac{i}{\sqrt{\eta_\rho}} \sum_{k>0} \sqrt{\frac{\pi}{Lk}} e^{-\alpha k/2} \left[e^{-ikx} (\beta_k^\dagger - \beta_{-k}) - e^{ikx} (\beta_k - \beta_{-k}^\dagger) \right], \end{aligned} \quad (1.13)$$

$$\begin{aligned} \phi_+(x) &\equiv i \sum_{k>0} \sqrt{\frac{\pi}{Lk}} e^{-\alpha k/2} \left[e^{-ikx} (c_k^\dagger + c_{-k}) - e^{ikx} (c_k + c_{-k}^\dagger) \right] \\ &= i \sqrt{\eta_\sigma} \sum_{k>0} \sqrt{\frac{\pi}{Lk}} e^{-\alpha k/2} \left[e^{-ikx} (\gamma_k^\dagger + \gamma_{-k}) - e^{ikx} (\gamma_k + \gamma_{-k}^\dagger) \right], \end{aligned} \quad (1.14)$$

$$\begin{aligned} \phi_-(x) &\equiv i \sum_{k>0} \sqrt{\frac{\pi}{Lk}} e^{-\alpha k/2} \left[e^{-ikx} (c_k^\dagger - c_{-k}) - e^{ikx} (c_k - c_{-k}^\dagger) \right] \\ &= \frac{i}{\sqrt{\eta_\sigma}} \sum_{k>0} \sqrt{\frac{\pi}{Lk}} e^{-\alpha k/2} \left[e^{-ikx} (\gamma_k^\dagger - \gamma_{-k}) - e^{ikx} (\gamma_k - \gamma_{-k}^\dagger) \right], \end{aligned} \quad (1.15)$$

where α is a positive infinitesimal; later it will be taken as a finite number of the order of lattice spacing. The phase field $\theta_+(x)$ can be regarded as the phase of the charge density wave, whereas the phase $\theta_-(x)$ corresponds to the Josephson phase, i.e., the phase of a Cooper pair. The phase fields $\phi_+(x)$ and $\phi_-(x)$, on the other hand, are related to the spin degree of freedom. In the above equations we have defined η_ρ and η_σ by

$$\eta_\rho \equiv e^{-2\lambda_\rho} = \left(\frac{1 + (\tilde{g}_{4\parallel} + \tilde{g}_{4\perp}) - (\tilde{g}_{2\parallel} + \tilde{g}_{2\perp})}{1 + (\tilde{g}_{4\parallel} + \tilde{g}_{4\perp}) + (\tilde{g}_{2\parallel} + \tilde{g}_{2\perp})} \right)^{1/2}, \quad (1.16)$$

$$\eta_\sigma \equiv e^{-2\lambda_\sigma} = \left(\frac{1 + (\tilde{g}_{4\parallel} - \tilde{g}_{4\perp}) - (\tilde{g}_{2\parallel} - \tilde{g}_{2\perp})}{1 + (\tilde{g}_{4\parallel} - \tilde{g}_{4\perp}) + (\tilde{g}_{2\parallel} - \tilde{g}_{2\perp})} \right)^{1/2}. \quad (1.17)$$

As we will show below, various correlation functions decay algebraically at zero temperature, and their exponents are related to η_ρ and η_σ . In this sense η_ρ and η_σ are the most important parameters characterizing the system. Roughly speaking, for attractive interactions $\eta_{\rho(\sigma)}$ is larger than unity whereas for repulsive interactions it is smaller than unity. If the system has an SU(2) spin symmetry, then η_σ is fixed to be unity. In particular, for the noninteracting system, $\eta_\rho = \eta_\sigma = 1$.

A great advantage of the bosonization method comes from the fact that electron field operators can be written in terms of the phase fields or, equivalently, boson creation and annihilation operators, β_p and γ_p [27]:

$$\Psi_{1s}(x) = \frac{1}{\sqrt{2\pi\alpha}} \exp\left(ik_F x + \frac{i}{2} \{ \theta_+(x) + \theta_-(x) + s[\phi_+(x) + \phi_-(x)] \} + i\varphi_{1s} \right), \quad (1.18)$$

$$\Psi_{2s}(x) = \frac{1}{\sqrt{2\pi\alpha}} \exp\left(-ik_F x - \frac{i}{2} \{ \theta_+(x) - \theta_-(x) + s[\phi_+(x) - \phi_-(x)] \} + i\varphi_{2s} \right), \quad (1.19)$$

where φ_{is} is necessary for ensuring the anticommutation relations of Ψ_{is} with different i and s , and is given by

$$\begin{aligned} \varphi_{11} &= 0, \\ \varphi_{11} &= \pi \int dx \Psi_{11}^\dagger(x) \Psi_{11}(x), \\ \varphi_{21} &= \pi \sum_s \int dx \Psi_{1s}^\dagger(x) \Psi_{1s}(x), \\ \varphi_{21} &= \varphi_{21} + \pi \int dx \Psi_{21}^\dagger(x) \Psi_{21}(x). \end{aligned}$$

As noted below Eq. (1.4), φ_{is} is a preserved quantities and plays only a minor role of giving a factor ± 1 to Ψ_{is} . Thus we will not write φ_{is} explicitly in the following discussions.

Now that field operators are written in terms of boson operators, β_p and γ_p , with which the Hamiltonian is diagonalized, we can readily calculate various correlation functions. Define the following operators:

$$\begin{aligned} O_{\text{CDW}}(x) &\equiv \Psi_{21}^\dagger(x) \Psi_{11}(x) = \frac{1}{2\pi\alpha} \exp(i[2k_F x + \theta_+(x) + \phi_+(x)]), \\ O_{\text{SDW}}(x) &\equiv \Psi_{21}^\dagger(x) \Psi_{11}(x) = \frac{1}{2\pi\alpha} \exp(i[2k_F x + \theta_+(x) - \phi_-(x)]), \\ O_{\text{SS}}(x) &\equiv \Psi_{11}(x) \Psi_{21}(x) = \frac{1}{2\pi\alpha} \exp(i[\theta_-(x) + \phi_+(x)]), \\ O_{\text{TS}}(x) &\equiv \Psi_{11}(x) \Psi_{21}(x) = \frac{1}{2\pi\alpha} \exp(i[\theta_-(x) + \phi_-(x)]). \end{aligned}$$

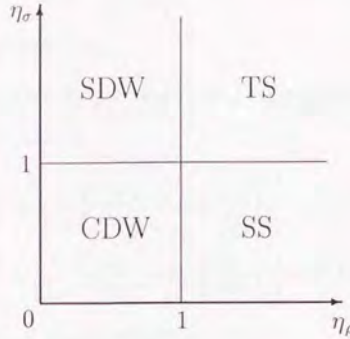


Figure 1.2: The phase diagram of the ground state for the spin-dependent Tomonaga-Luttinger model.

At zero temperature correlation functions for charge-density wave (CDW), spin-density wave (SDW), singlet superconductivity (SS), and triplet superconductivity (TS) are evaluated as

$$\begin{aligned} \langle O_{\text{CDW}}(x)O_{\text{CDW}}^\dagger(0) \rangle &= \frac{e^{2ik_F x}}{(2\pi\alpha)^2} \left(1 + \frac{x^2}{\alpha^2}\right)^{-\frac{1}{2}(\eta_\rho + \eta_\sigma)} \sim e^{2ik_F x} x^{-\eta_\rho - \eta_\sigma}, \\ \langle O_{\text{SDW}}(x)O_{\text{SDW}}^\dagger(0) \rangle &= \frac{e^{2ik_F x}}{(2\pi\alpha)^2} \left(1 + \frac{x^2}{\alpha^2}\right)^{-\frac{1}{2}(\eta_\rho + \eta_\sigma^{-1})} \sim e^{2ik_F x} x^{-\eta_\rho - \eta_\sigma^{-1}}, \\ \langle O_{\text{SS}}(x)O_{\text{SS}}^\dagger(0) \rangle &= \frac{1}{(2\pi\alpha)^2} \left(1 + \frac{x^2}{\alpha^2}\right)^{-\frac{1}{2}(\eta_\rho^{-1} + \eta_\sigma)} \sim x^{-\eta_\rho^{-1} - \eta_\sigma}, \\ \langle O_{\text{TS}}(x)O_{\text{TS}}^\dagger(0) \rangle &= \frac{1}{(2\pi\alpha)^2} \left(1 + \frac{x^2}{\alpha^2}\right)^{-\frac{1}{2}(\eta_\rho^{-1} + \eta_\sigma^{-1})} \sim x^{-\eta_\rho^{-1} - \eta_\sigma^{-1}}. \end{aligned}$$

We see that the correlation functions fall off algebraically for large x , which means that the system is just on the critical point at zero temperature. We show in Fig. 1.2 the phase diagram of the ground state which we infer from the most long-ranged correlation function.

Next we will express the Hamiltonian in terms of the phase fields only. We introduce the following operators:

$$P_+(x) = -\frac{1}{2\pi} \frac{d}{dx} \theta_-(x) = -\frac{1}{2\sqrt{\eta_\rho}} \sum_{k>0} \sqrt{\frac{k}{\pi L}} e^{-\alpha k/2} \left[e^{-ikx} (\beta_k^\dagger - \beta_{-k}) + e^{ikx} (\beta_k - \beta_{-k}^\dagger) \right], \quad (1.20)$$

$$P_-(x) = -\frac{1}{2\pi} \frac{d}{dx} \theta_+(x) = -\frac{\sqrt{\eta_\rho}}{2} \sum_{k>0} \sqrt{\frac{k}{\pi L}} e^{-\alpha k/2} \left[e^{-ikx} (\beta_k^\dagger + \beta_{-k}) + e^{ikx} (\beta_k + \beta_{-k}^\dagger) \right], \quad (1.21)$$

$$M_+(x) = -\frac{1}{2\pi} \frac{d}{dx} \phi_-(x) = -\frac{1}{2\sqrt{\eta_\sigma}} \sum_{k>0} \sqrt{\frac{k}{\pi L}} e^{-\alpha k/2} \left[e^{-ikx} (\gamma_k^\dagger - \gamma_{-k}) + e^{ikx} (\gamma_k - \gamma_{-k}^\dagger) \right], \quad (1.22)$$

$$M_-(x) = -\frac{1}{2\pi} \frac{d}{dx} \phi_+(x) = -\frac{\sqrt{\eta_\sigma}}{2} \sum_{k>0} \sqrt{\frac{k}{\pi L}} e^{-\alpha k/2} [e^{-ikx} (\gamma_k^\dagger + \gamma_{-k}) + e^{ikx} (\gamma_k + \gamma_{-k}^\dagger)]. \quad (1.23)$$

Then it immediately follows that

$$[\theta_+(x), P_+(x')] = [\theta_-(x), P_-(x')] = [\phi_+(x), M_+(x')] = [\phi_-(x), M_-(x')] = i\delta(x-x'). \quad (1.24)$$

From Eqs. (1.12)–(1.15) we get

$$\begin{aligned} \frac{1}{4\pi} \int dx \left[\frac{1}{\eta_\rho} \left(\frac{d\theta_+}{dx} \right)^2 + \eta_\rho \left(\frac{d\theta_-}{dx} \right)^2 \right] &= \sum_k |k| \left(\beta_k^\dagger \beta_k + \frac{1}{2} \right), \\ \frac{1}{4\pi} \int dx \left[\frac{1}{\eta_\sigma} \left(\frac{d\phi_+}{dx} \right)^2 + \eta_\sigma \left(\frac{d\phi_-}{dx} \right)^2 \right] &= \sum_k |k| \left(\gamma_k^\dagger \gamma_k + \frac{1}{2} \right). \end{aligned}$$

Hence the Hamiltonian H can be written as

$$H = v_\rho \int dx \left[\frac{1}{4\pi\eta_\rho} \left(\frac{d\theta_+}{dx} \right)^2 + \pi\eta_\rho P_+^2 \right] + v_\sigma \int dx \left[\frac{1}{4\pi\eta_\sigma} \left(\frac{d\phi_+}{dx} \right)^2 + \pi\eta_\sigma M_+^2 \right] \quad (1.25)$$

or

$$H = v_\rho \int dx \left[\frac{\eta_\rho}{4\pi} \left(\frac{d\theta_-}{dx} \right)^2 + \frac{\pi}{\eta_\rho} P_-^2 \right] + v_\sigma \int dx \left[\frac{\eta_\sigma}{4\pi} \left(\frac{d\phi_-}{dx} \right)^2 + \frac{\pi}{\eta_\sigma} M_-^2 \right]. \quad (1.26)$$

From the commutation relation (1.24) and the phase Hamiltonian, equations of motion for phase fields are obtained as

$$i \frac{\partial \theta_+}{\partial t} = [\theta_+, H] = 2\pi i v_\rho \eta_\rho P_+, \quad i \frac{\partial \phi_+}{\partial t} = [\phi_+, H] = 2\pi i v_\sigma \eta_\sigma M_+. \quad (1.27)$$

Thus Lagrangian of the system is

$$\begin{aligned} L &= \int dx \left(\frac{\partial \theta_+}{\partial t} P_+ + \frac{\partial \phi_+}{\partial t} M_+ \right) - H \\ &= \frac{1}{4\pi\eta_\rho} \int dx \left[\frac{1}{v_\rho} \left(\frac{\partial \theta_+}{\partial t} \right)^2 - v_\rho \left(\frac{\partial \theta_+}{\partial x} \right)^2 \right] + \frac{1}{4\pi\eta_\sigma} \int dx \left[\frac{1}{v_\sigma} \left(\frac{\partial \phi_+}{\partial t} \right)^2 - v_\sigma \left(\frac{\partial \phi_+}{\partial x} \right)^2 \right]. \end{aligned} \quad (1.28)$$

The imaginary-time action S is then written as

$$S = \frac{1}{4\pi\eta_\rho} \int d\tau \int dx \left[\frac{1}{v_\rho} \left(\frac{\partial \theta_+}{\partial \tau} \right)^2 + v_\rho \left(\frac{\partial \theta_+}{\partial x} \right)^2 \right] + \frac{1}{4\pi\eta_\sigma} \int d\tau \int dx \left[\frac{1}{v_\sigma} \left(\frac{\partial \phi_+}{\partial \tau} \right)^2 + v_\sigma \left(\frac{\partial \phi_+}{\partial x} \right)^2 \right], \quad (1.29)$$

where $\tau = it$. Our analysis of the tunneling through a single barrier (Chap. 2) will begin with this action. We will omit the subscript + of θ_+ and ϕ_+ in Chap. 2.

So far we have considered the spin-dependent Tomonaga-Luttinger model. In the rest of this section, we will discuss the spinless Tomonaga-Luttinger model.

The original total Hamiltonian for the spinless model is given by

$$H = v_F \sum_k (k - k_F) a_{1,k}^\dagger a_{1,k} + v_F \sum_k (-k - k_F) a_{2,k}^\dagger a_{2,k}$$

$$\begin{aligned}
& + \frac{1}{L} \sum_{k_1} \sum_{k_2} \sum_p g_2 a_{1,k_1}^\dagger a_{1,k_1-p} a_{2,k_2}^\dagger a_{2,k_2+p} \\
& + \frac{1}{L} \sum_{k_1} \sum_{k_2} \sum_{p>0} g_4 \left(a_{1,k_1}^\dagger a_{1,k_1-p} a_{1,k_2}^\dagger a_{1,k_2+p} + a_{2,k_1}^\dagger a_{2,k_1+p} a_{2,k_2}^\dagger a_{2,k_2-p} \right), \quad (1.30)
\end{aligned}$$

where $a_{i,k}$ ($a_{i,k}^\dagger$) is an annihilation (creation) operator of a fermion of branch i . As shown above for the electron system, the Hamiltonian (1.30) is written as

$$H = v_F(1 + \tilde{g}_4) \sum_p |p| b_p^\dagger b_p + v_F \tilde{g}_2 \sum_{p>0} p \left(b_p^\dagger b_{-p}^\dagger + b_{-p} b_p \right), \quad (1.31)$$

where $\tilde{g}_2 = g_2/2\pi v_F$, $\tilde{g}_4 = g_4/2\pi v_F$, and b_p is an annihilation operator of a boson,

$$b_p = \begin{cases} \sqrt{\frac{2\pi}{pL}} \sum_k a_{1,k-p}^\dagger a_{1,k}, & p > 0 \\ \sqrt{\frac{2\pi}{|p|L}} \sum_k a_{2,k+|p|}^\dagger a_{2,k}, & p < 0. \end{cases} \quad (1.32)$$

Equation (1.31) is diagonalized by the Bogoliubov transformation:

$$H = v \sum_p |p| \beta_p^\dagger \beta_p + \text{const.}, \quad v = v_F \left[(1 + \tilde{g}_4)^2 - (\tilde{g}_2)^2 \right]^{1/2}, \quad (1.33)$$

$$b_p = \beta_p \cosh \lambda - \beta_{-p}^\dagger \sinh \lambda, \quad \tanh(2\lambda) = \frac{\tilde{g}_2}{1 + \tilde{g}_4}.$$

The field operator of spinless fermions can also be expressed in terms of boson operators as

$$\Psi_1(x) = \frac{1}{\sqrt{2\pi\alpha}} \exp \left(ik_F x + \frac{i}{2} [\theta_+(x) + \theta_-(x)] \right), \quad (1.34)$$

$$\Psi_2(x) = \frac{1}{\sqrt{2\pi\alpha}} \exp \left(-ik_F x - \frac{i}{2} [\theta_+(x) - \theta_-(x)] + i\pi \int dx \Psi_1^\dagger(x) \Psi_1(x) \right), \quad (1.35)$$

where the phase fields are given by

$$\begin{aligned}
\theta_+(x) &= i \sum_{k>0} \sqrt{\frac{2\pi}{Lk}} e^{-\alpha k/2} \left[e^{-ikx} (b_k^\dagger + b_{-k}) - e^{ikx} (b_k + b_{-k}^\dagger) \right] \\
&= i\sqrt{\eta} \sum_{k>0} \sqrt{\frac{2\pi}{Lk}} e^{-\alpha k/2} \left[e^{-ikx} (\beta_k^\dagger + \beta_{-k}) - e^{ikx} (\beta_k + \beta_{-k}^\dagger) \right], \quad (1.36)
\end{aligned}$$

$$\begin{aligned}
\theta_-(x) &= i \sum_{k>0} \sqrt{\frac{2\pi}{Lk}} e^{-\alpha k/2} \left[e^{-ikx} (b_k^\dagger - b_{-k}) - e^{ikx} (b_k - b_{-k}^\dagger) \right] \\
&= \frac{i}{\sqrt{\eta}} \sum_{k>0} \sqrt{\frac{2\pi}{Lk}} e^{-\alpha k/2} \left[e^{-ikx} (\beta_k^\dagger - \beta_{-k}) - e^{ikx} (\beta_k - \beta_{-k}^\dagger) \right]. \quad (1.37)
\end{aligned}$$

The parameter η in the above equations is

$$\eta \equiv e^{-2\lambda} = \sqrt{\frac{1 + \tilde{g}_4 - \tilde{g}_2}{1 + \tilde{g}_4 + \tilde{g}_2}}. \quad (1.38)$$

Note that η is larger (smaller) than unity when g_2 is negative (positive), i.e., when the forward scattering is an attractive (repulsive) interaction.

Exponents of correlation functions are determined by η only. For example, we define two operators representing the correlation of density wave and superconductivity by $O_{DW}(x) \equiv \Psi_1^\dagger(x)\Psi_1(x) = \frac{1}{2\pi\alpha} \exp(i[2k_F x + \theta_+(x)])$ and $O_S(x) \equiv \Psi_1(x)\Psi_2(x) = \frac{1}{2\pi\alpha} \exp(i\theta_-(x))$. Then it is easy to see that at zero temperature the correlation functions for these two operators vary for large x as $\langle O_{DW}(x)O_{DW}^\dagger(0) \rangle \sim e^{2ik_F x - 2\eta}$ and $\langle O_S(x)O_S^\dagger(0) \rangle \sim x^{-2/\eta}$.

Now we define the following conjugate operators for $\theta_+(x)$ and $\theta_-(x)$:

$$P_+(x) = -\frac{1}{2} \sum_{k>0} \sqrt{\frac{k}{2\pi L}} e^{-\alpha k/2} \left[e^{-ikx} (b_k^\dagger - b_{-k}) - e^{ikx} (b_k + b_{-k}^\dagger) \right], \quad (1.39)$$

$$P_-(x) = -\frac{1}{2} \sum_{k>0} \sqrt{\frac{k}{2\pi L}} e^{-\alpha k/2} \left[e^{-ikx} (b_k^\dagger + b_{-k}) - e^{ikx} (b_k + b_{-k}^\dagger) \right]. \quad (1.40)$$

They obey $[\theta_+(x), P_+(x')] = [\theta_-(x), P_-(x')] = i\delta(x-x')$. Following the same path as in the derivation of Eq. (1.29), we can get the Euclidean action S expressed in terms of the phase field $\theta_+(x)$. The final result is

$$S = \frac{1}{8\pi\eta} \int d\tau \int dx \left[\frac{1}{v} \left(\frac{\partial \theta_+}{\partial \tau} \right)^2 + v \left(\frac{\partial \theta_+}{\partial x} \right)^2 \right]. \quad (1.41)$$

This action is the starting point of the theory of the resonant tunneling through a double-barrier structure which will be given in Chap. 3, where we will omit the subscript + of θ_+ .

1.3 Localization problem in dirty Luttinger liquids

Before going to detailed discussion on the tunneling through a few barriers, here we review existing theories on the effect of impurities in Luttinger liquids, i.e., theories on the localization-delocalization transition in dirty Luttinger liquids [13, 14, 15, 16].

The system we consider is the spin-dependent Tomonaga-Luttinger model with many impurities. The total Hamiltonian is given by $H_{\text{total}} = H + H_{\text{imp}}$, where H is the right-hand side of Eq. (1.25). The impurity potential causes backward scattering, and thus H_{imp} is written as

$$\begin{aligned} H_{\text{imp}} &= \int dx \sum_j V_0 \delta(x - R_j) \sum_s [\Psi_{1s}^\dagger(x) \Psi_{2s}(x) + \Psi_{2s}^\dagger(x) \Psi_{1s}(x)] \\ &= \frac{2V_0}{\pi\alpha} \sum_j \cos[2k_F R_j + \theta(R_j)] \cos \phi(R_j), \end{aligned} \quad (1.42)$$

where we have omitted the subscript + of θ_+ and ϕ_+ . It is seen that the impurity potential serves as a pinning potential for the phase fields. Here the analogy of this problem to the pinning of the charge density wave [28] is obvious as stressed by Suzumura and Fukuyama [15]. In the localization problem the quantum fluctuations represented by the τ -dependence of $\theta(\tau)$ and $\phi(\tau)$ is important, which tends to weaken the pinning effect.

Following Suzumura and Fukuyama [15], we will calculate the localization length by using the self-consistent harmonic approximation. We divide the phase fields into classical parts and fluctuating quantum variables as $\theta = \theta_{\text{cl}} + \hat{\theta}$ and $\phi = \phi_{\text{cl}} + \hat{\phi}$, and then expand the Hamiltonian with respect to $\hat{\theta}$ and $\hat{\phi}$ up to the second order. The terms linear in $\hat{\theta}$ and

$\hat{\phi}$ vanish due to the condition of minimization with respect to θ_{cl} and ϕ_{cl} . Then the total Hamiltonian is written as

$$\begin{aligned}
 H_{\text{total}} = & v_{\rho} \int dx \left[\frac{1}{4\pi\eta_{\rho}} \left(\frac{d\theta_{cl}}{dx} \right)^2 + \frac{1}{4\pi\eta_{\rho}} \left(\frac{d\hat{\theta}}{dx} \right)^2 + \pi\eta_{\rho} P^2 \right] \\
 & + v_{\sigma} \int dx \left[\frac{1}{4\pi\eta_{\sigma}} \left(\frac{d\phi_{cl}}{dx} \right)^2 + \frac{1}{4\pi\eta_{\sigma}} \left(\frac{d\hat{\phi}}{dx} \right)^2 + \pi\eta_{\sigma} M^2 \right] \\
 & + \int dx \sum_j \frac{2V_0}{\pi\alpha} \gamma \delta(x - R_j) \left[1 - \frac{1}{2} (\hat{\theta}(x)^2 - \langle \hat{\theta}^2 \rangle + \hat{\phi}(x)^2 - \langle \hat{\phi}^2 \rangle) \right] \cos[2k_F x + \theta_{cl}(x)] \cos \phi_{cl}(x),
 \end{aligned} \tag{1.43}$$

where

$$\gamma = \exp \left[-\frac{1}{2} (\langle \hat{\theta}^2 \rangle + \langle \hat{\phi}^2 \rangle) \right]. \tag{1.44}$$

We determine the averages $\langle \hat{\theta}^2 \rangle$ and $\langle \hat{\phi}^2 \rangle$ self-consistently with neglecting their spatial dependence.

The classical fields, θ_{cl} and ϕ_{cl} , are distorted by the impurity potential. The characteristic length, L_0 , of the distortion, which corresponds to the Fukuyama-Lee length [28] in the charge-density-wave pinning, is much longer than the average spacing of impurities since the impurity potential is assumed to be very weak. This is so-called weak-pinning regime. The length L_0 can be identified with the localization length. Then the classical part of the impurity (pinning) potential can be estimated as

$$\frac{1}{L_0} \sum_j \cos[2k_F R_j + \theta_{cl}(R_j)] \cos \phi_{cl}(R_j) = -\sqrt{\frac{n_i}{L_0}}, \tag{1.45}$$

where n_i is the density of impurities. The distortion also costs the elastic energy $\pi v_{\rho}/12\eta_{\rho}L_0^2$ per unit length [28]. Hence the total Hamiltonian is reduced to

$$\begin{aligned}
 H_{\text{total}} = & v_{\rho} \int dx \left[\frac{1}{4\pi\eta_{\rho}} \left(\frac{d\hat{\theta}}{dx} \right)^2 + \pi\eta_{\rho} P^2 + \frac{\pi}{12\eta_{\rho}L_0^2} \right] + v_{\sigma} \int dx \left[\frac{1}{4\pi\eta_{\sigma}} \left(\frac{d\hat{\phi}}{dx} \right)^2 + \pi\eta_{\sigma} M^2 \right] \\
 & - \frac{2V_0\gamma}{\pi\alpha} \sqrt{\frac{n_i}{L_0}} \int dx \left[1 - \frac{1}{2} (\hat{\theta}^2 - \langle \hat{\theta}^2 \rangle + \hat{\phi}^2 - \langle \hat{\phi}^2 \rangle) \right].
 \end{aligned} \tag{1.46}$$

The average $\langle \hat{\theta}^2 \rangle$ is calculated from the relation

$$\langle \hat{\theta}^2 \rangle = \sum_{\omega_n} \sum_k \frac{1}{Z_{\xi}} \frac{\delta^2 Z_{\xi}}{\delta \xi(k, \omega_n) \delta \xi(-k, -\omega_n)} \Big|_{\xi=0},$$

where

$$\begin{aligned}
 Z_{\xi} = & \int \mathcal{D}\hat{\theta} \exp \left\{ -\frac{1}{4\pi\eta_{\rho}v_{\rho}} \int_0^{\beta} d\tau \int dx \left[\left(\frac{d\hat{\theta}}{d\tau} \right)^2 + v_{\rho}^2 \left(\frac{d\hat{\theta}}{dx} \right)^2 + v_{\rho}^2 m_{\rho}^2 \hat{\theta}^2 \right] + \int_0^{\beta} d\tau \int dx \xi(x, \tau) \hat{\theta}(x, \tau) \right\} \\
 = & Z_{\xi}|_{\xi=0} \exp \left[\frac{\pi\eta_{\rho}v_{\rho}}{\beta L} \sum_{\omega_n} \sum_k \frac{\xi(k, \omega_n) \xi(-k, -\omega_n)}{\omega_n^2 + v_{\rho}^2 (k^2 + m_{\rho}^2)} \right]
 \end{aligned}$$

with

$$\begin{aligned}\hat{\theta}(x, \tau) &= \frac{1}{\beta L} \sum_{\omega_n} \sum_k e^{ikx - i\omega_n \tau} \hat{\theta}(k, \omega_n), \\ \xi(x, \tau) &= \frac{1}{\beta L} \sum_{\omega_n} \sum_k e^{ikx - i\omega_n \tau} \xi(k, \omega_n), \\ m_{\rho(\sigma)}^2 &= \frac{4\eta_{\rho(\sigma)} \gamma V_0}{\alpha v_{\rho(\sigma)}} \sqrt{\frac{n_i}{L_0}}.\end{aligned}$$

At zero temperature the average is obtained as

$$\langle \hat{\theta}^2 \rangle = \frac{\eta_{\rho} v_{\rho}}{2\pi} \int_{-1/\alpha}^{1/\alpha} dk \int_{-\infty}^{\infty} d\omega \frac{1}{\omega^2 + v_{\rho}^2(k^2 + m_{\rho}^2)} = \eta_{\rho} \ln \left(\frac{2}{\alpha m_{\rho}} \right), \quad (1.47)$$

and similarly

$$\langle \hat{\phi}^2 \rangle = \eta_{\sigma} \ln \left(\frac{2}{\alpha m_{\sigma}} \right). \quad (1.48)$$

Note that we have taken ultraviolet cutoff to be $1/\alpha$. Substituting these results into Eq. (1.44), we get

$$\gamma = \varepsilon_{\rho}^{-\frac{\eta_{\rho}}{4-\eta}} \varepsilon_{\sigma}^{-\frac{\eta_{\sigma}}{4-\eta}} \left(\frac{\alpha V_0}{v_F} \right)^{\frac{\eta}{4-\eta}} \left(\frac{n_i}{L_0} \right)^{\frac{\eta}{2(4-\eta)}}, \quad (1.49)$$

where $\varepsilon_{\rho} = (v_{\rho}/\eta_{\rho})/v_F$, $\varepsilon_{\sigma} = (v_{\sigma}/\eta_{\sigma})/v_F$, and $\eta = \eta_{\rho} + \eta_{\sigma}$.

At zero temperature the excess energy due to the distortion of the phase fields is

$$E = \frac{\pi v_{\rho} L}{12\eta_{\rho} L_0^2} - \frac{2\gamma V_0 L}{\pi \alpha} \sqrt{\frac{n_i}{L_0}} \left(1 + \frac{\langle \hat{\theta}^2 \rangle}{2} + \frac{\langle \hat{\phi}^2 \rangle}{2} \right) + \frac{1}{2} \sum_k \left[v_{\rho}(\sqrt{k^2 + m_{\rho}^2} - |k|) + v_{\sigma}(\sqrt{k^2 + m_{\sigma}^2} - |k|) \right], \quad (1.50)$$

where the third term represents the change in the zero-point fluctuation energy of the phase fields. The sum of the third term is evaluated, through the relation $\sum_k = \frac{L}{2\pi} \int_{-\alpha}^{\alpha} dk$, as

$$\begin{aligned}\frac{L}{2\pi} \int_0^{1/\alpha} dk v(\sqrt{k^2 + m^2} - k) &= \frac{vL}{4\pi} \left(k\sqrt{k^2 + m^2} + m^2 \ln |k + \sqrt{k^2 + m^2}| - k^2 \right) \Big|_0^{1/\alpha} \\ &= \frac{m^2 v L}{8\pi} \left[1 + 2 \ln \left(\frac{2}{\alpha m} \right) \right],\end{aligned}$$

and thus the excess energy per unit length reads

$$\frac{E}{L} = \frac{\pi v_{\rho}}{12\eta_{\rho} L_0^2} - \frac{2\gamma V_0}{\pi \alpha} \sqrt{\frac{n_i}{L_0}} \left(1 - \frac{\eta}{4} \right). \quad (1.51)$$

We determine the length L_0 from the minimization condition $\frac{d}{dL_0}(E/L) = 0$. From Eq. (1.51) we finally obtain [15]

$$n_i L_0 = \left(\frac{6}{\pi^2} \right)^{-\frac{4-\eta}{2(3-\eta)}} \varepsilon_{\rho}^{\frac{4-\eta_{\rho}}{2(3-\eta)}} \varepsilon_{\sigma}^{\frac{\eta_{\sigma}}{2(3-\eta)}} (\alpha n_i)^{\frac{2-\eta}{3-\eta}} \left(\frac{V_0}{v_F} \right)^{-\frac{2}{3-\eta}}. \quad (1.52)$$

From Eq. (1.52) we see that the localization length L_0 is finite for $\eta = \eta_{\rho} + \eta_{\sigma} < 3$, where the system is insulating. For $\eta_{\rho} + \eta_{\sigma} > 3$, L_0 is considered to be infinite, which means that the system is metallic. Hence the phase boundary of the localization-delocalization transition

is found to be $\eta_\rho + \eta_\sigma = 3$. The noninteracting system ($\eta_\rho = \eta_\sigma = 1$) is, of course, in the localized phase. It is also worth noting that the CDW phase in Fig. 1.2 is contained in the localized phase.

The above calculation is valid only for the localized phase. We next study the transition from the delocalized side using a simple renormalization group argument.

Using the replica trick to take the impurity average, we write the free energy of the system averaged over the impurity configuration as

$$\begin{aligned} \langle F \rangle_{\text{imp}} &= -\frac{1}{\beta} \lim_{n \rightarrow 0} \frac{\langle Z^n \rangle_{\text{imp}} - 1}{n}, \\ Z^n &= \int \prod_{j=1}^n \mathcal{D}\theta_j \mathcal{D}\phi_j \exp \left\{ -\frac{1}{4\pi\eta_\rho v_\rho} \int_0^\beta d\tau \int dx \sum_j \left[\left(\frac{\partial \theta_j}{\partial \tau} \right)^2 + v_\rho^2 \left(\frac{\partial \theta_j}{\partial x} \right)^2 \right] \right. \\ &\quad - \frac{1}{4\pi\eta_\sigma v_\sigma} \int_0^\beta d\tau \int dx \sum_j \left[\left(\frac{\partial \phi_j}{\partial \tau} \right)^2 + v_\sigma^2 \left(\frac{\partial \phi_j}{\partial x} \right)^2 \right] \\ &\quad \left. - \frac{1}{\pi\alpha} \int_0^\beta d\tau \int dx \sum_j \left(\xi e^{i(\theta_j + 2k_F x)} + \xi^* e^{-i(\theta_j + 2k_F x)} \right) \cos \phi_j \right\}, \end{aligned} \quad (1.53)$$

where j is the replica index, and ξ describes the random impurity potential with the distribution function

$$P = \exp \left(-\frac{1}{D} \int \xi^*(x) \xi(x) dx \right).$$

After averaging over the field ξ , $\langle Z^n \rangle_{\text{imp}}$ is obtained at zero temperature as

$$\begin{aligned} \langle Z^n \rangle_{\text{imp}} &= \int \prod_{j=1}^n \mathcal{D}\theta_j \mathcal{D}\phi_j \exp \left\{ -\frac{1}{16\pi^3 \eta_\rho v_\rho} \int d\omega \int dk (\omega^2 + v_\rho^2 k^2) \theta_j(k, \omega) \theta_j(-k, -\omega) \right. \\ &\quad - \frac{1}{16\pi^3 \eta_\sigma v_\sigma} \int d\omega \int dk (\omega^2 + v_\sigma^2 k^2) \phi_j(k, \omega) \phi_j(-k, -\omega) \\ &\quad \left. + \frac{D}{(\pi\alpha)^2} \sum_{j,k} \int d\tau_1 \int d\tau_2 \int dx e^{i[\theta_j(x, \tau_1) - \theta_k(x, \tau_2)]} \cos \phi_j(x, \tau_1) \cos \phi_k(x, \tau_2) \right\}, \end{aligned} \quad (1.54)$$

where

$$\begin{aligned} \theta_j(k, \omega) &= \int dk \int d\omega e^{-ikx + i\omega\tau} \theta_j(x, \tau), \\ \phi_j(k, \omega) &= \int dk \int d\omega e^{-ikx + i\omega\tau} \phi_j(x, \tau). \end{aligned}$$

In the above equations, the integrals over k and ω are performed in the region $0 \leq \bar{k}_\rho \leq \Lambda$ for θ_j , and $0 \leq \bar{k}_\sigma \leq \Lambda$ for ϕ_j , where $\bar{k}_\nu = \sqrt{k^2 + (\omega/v_\nu)^2}$. For $\tau_1 \approx \tau_2$ and $j = k$ the impurity term effectively yields the backward scattering. We are thus forced to consider the $g_{1\perp}$ term even when initially $g_{1\perp} = 0$ [16]. In the following discussion, however, we neglect this effect for simplicity.

We now perform the renormalization group transformation in the lowest order with respect to D . We first integrate out the fast modes of the phase fields, i.e., $\theta_j(k, \omega)$ with $\Lambda - d\Lambda < \bar{k}_\rho < \Lambda$ and $\phi_j(k, \omega)$ with $\Lambda - d\Lambda < \bar{k}_\sigma < \Lambda$. The first term of the cumulant expansion in powers of D is

$$\left\langle e^{i[\theta_j(x, \tau_1) - \theta_k(x, \tau_2)]} \cos \phi_j(x, \tau_1) \cos \phi_k(x, \tau_2) \right\rangle_{\text{fast}}$$

$$\begin{aligned}
&= e^{i\theta_{js}(x,\tau_1) - \theta_{ks}(x,\tau_2)} \cos \phi_{js}(x, \tau_1) \cos \phi_{ks}(x, \tau_2) \exp\left(-\sum_{\nu=\rho,\sigma} \frac{\eta_\nu v_\nu}{2\pi} \int_{\Lambda-d\Lambda < k_\nu < \Lambda} \frac{d\omega dk}{\omega^2 + v_\nu^2 k^2}\right) \\
&= \left(1 - (\eta_\rho + \eta_\sigma) \frac{d\Lambda}{\Lambda}\right) e^{i\theta_{js}(x,\tau_1) - \theta_{ks}(x,\tau_2)} \cos \phi_{js}(x, \tau_1) \cos \phi_{ks}(x, \tau_2), \quad (1.55)
\end{aligned}$$

where $\langle \rangle_{\text{fast}}$ denotes the average over the fast modes, and θ_{js} and ϕ_{js} represents slow modes. In the lowest order only the coupling constant D is renormalized. To accomplish the renormalization group transformation, we must rescale τ and x as $\tau \rightarrow \left(1 + \frac{d\Lambda}{\Lambda}\right) \tau$ and $x \rightarrow \left(1 + \frac{d\Lambda}{\Lambda}\right) x$. After the integration (1.55) and the rescaling, we obtain the coupling constant for the reduced cutoff $\Lambda - d\Lambda$:

$$D(\Lambda - d\Lambda) = D(\Lambda) \left(1 + \frac{d\Lambda}{\Lambda}\right)^3 \left[1 - (\eta_\rho + \eta_\sigma) \frac{d\Lambda}{\Lambda}\right] = D(\Lambda) \left[1 + (3 - \eta_\rho - \eta_\sigma) \frac{d\Lambda}{\Lambda}\right]. \quad (1.56)$$

or in differential form

$$\frac{dD}{dl} = (3 - \eta_\rho - \eta_\sigma) D, \quad (1.57)$$

where $dl = -d\Lambda/\Lambda$. Hence we recover the lowest-order scaling equation obtained earlier by a slightly different renormalization group argument [15, 16]. We see from Eq. (1.57) that the impurity potential is irrelevant when $\eta_\rho + \eta_\sigma > 3$, implying that the system is in the delocalized phase if $\eta_\rho + \eta_\sigma > 3$. Hence we get the same phase boundary $\eta_\rho + \eta_\sigma = 3$ as that obtained in the weak-pinning analysis.

So far we have reviewed the localization-delocalization transition in dirty Luttinger liquids only within the forward-scattering model. We note that the effect of the backward scattering and the umklapp scattering on the localization-delocalization transition has also been discussed in detail in Refs.[15, 16].

In the following chapters we will analyze tunneling in Luttinger liquids with a few tunnel barriers using the ideas developed in the study of the localization-delocalization transition in dirty Luttinger liquids: We adopt the phase Hamiltonian description and regard the barriers as a pinning potential for the phase fields. An essential difference is that our new system has local defects, in contrast to a dirty Luttinger liquid which is almost a uniform system after averaging over the impurity distribution.

Chapter 2

Tunneling through a Single Barrier

2.1 Introduction

In this chapter we investigate the tunneling of an electron through a single barrier in a one-dimensional electron system. If the electrons do not interact with each other, this is a quite easy problem. Suppose there is a potential, $V\delta(x)$, which simulates the tunnel barrier. Then we can easily show, by solving the Schrödinger equation with appropriate boundary conditions, that the transmission probability through the barrier is $[1 + (V/v_F)^2]^{-1}$ for an electron on the Fermi surface. The Landauer formula [29] tells that the conductance of the tunnel barrier at zero temperature is given by the transmission probability multiplied by e^2/π ($\hbar = 1$). In this way, if the electron-electron interaction can be disregarded, the conductance is easily calculated by solving an elementary scattering problem.

Now we switch on the electron-electron interaction. Unless a gap is generated in the excitation spectrum by some instabilities such as the Peierls instability, the system will become a Luttinger liquid. Having a Luttinger liquid, we ask ourselves the following question: How is the tunneling in Luttinger liquids different from that in the ordinary Fermi liquid, and how can we calculate the conductance without the Landauer formula? These are the subjects discussed in this chapter.

The problem of the tunneling through a single barrier in Luttinger liquids was first studied for *spinless* fermions by Kane and Fisher [17]. They derived an effective action for the phase field at the barrier site by integrating out the continuum degrees of freedom, and showed that the system is classified into two phases: insulating phase and perfectly conducting phase. They also pointed out that the current-voltage characteristic should show anomalous power-law behavior at zero temperature. On the other hand, Glazman *et al.* [30] studied the tunneling of the Wigner crystal through a pinning potential barrier [31], and derived a similar anomalous current-voltage characteristic.

In the following sections, we discuss the tunneling of an *electron* through a single barrier, generalizing the theory of Kane and Fisher to include the spin degrees of freedom. The model we analyze is the Tomonaga-Luttinger model with one δ -function potential. We calculate the conductance in both limits of strong and weak potential strength for low temperatures, and show that the tunneling in Luttinger liquids is entirely different from that in the Fermi liquids. It should be fair to comment that essentially the same results as those described in this chapter have been obtained independently by Kane and Fisher [20].

2.2 Effective action

We analyze the spin-dependent Tomonaga-Luttinger model [10, 11] with a scattering potential at $x = 0$. The partition function of the system at temperature T can be written in terms of phase fields, $\theta(x, \tau)$ and $\phi(x, \tau)$, as

$$Z = \int \mathcal{D}\theta \int \mathcal{D}\phi \exp\left(-\int_0^\beta d\tau [L_0(\tau) + L_1(\tau)]\right), \quad (2.1)$$

where $\beta = 1/T$, $\theta(x, \beta) = \theta(x, 0)$ and $\phi(x, \beta) = \phi(x, 0)$. $L_0(\tau)$ is the (imaginary-time) Lagrangian of a pure system given in Eq. (1.28):

$$L_0 = \frac{1}{4\pi} \int dx \left\{ \frac{1}{v_\rho \eta_\rho} (\partial_\tau \theta)^2 + \frac{v_\rho}{\eta_\rho} (\partial_x \theta)^2 + \frac{1}{v_\sigma \eta_\sigma} (\partial_\tau \phi)^2 + \frac{v_\sigma}{\eta_\sigma} (\partial_x \phi)^2 \right\}. \quad (2.2)$$

$L_1(\tau)$ represents the barrier potential and is given by

$$\begin{aligned} L_1 &= -V_0 \sum_s \left[\Psi_{1s}^\dagger(0, \tau) \Psi_{2s}(0, \tau) + \Psi_{2s}^\dagger(0, \tau) \Psi_{1s}(0, \tau) \right] \\ &= -\frac{2V_0}{\pi\alpha} \cos \theta(0, \tau) \cos \phi(0, \tau), \end{aligned} \quad (2.3)$$

where V_0 is the strength of the scattering potential, $\Psi_{1(2)s}$ is the field operator for an electron with velocity v_F ($-v_F$) and spin s , and α is a cutoff parameter of the order of the lattice spacing. We assume $V_0 > 0$, but in fact the results do not depend on the sign of V_0 ; in Sec. 2.3.2 we will see that the conductance depends on V_0^2 . The parameters η_ρ and η_σ have already been introduced in Eqs. (1.16) and (1.17).

We integrate out the phase fields except $\theta_0 = \theta(x=0)$ and $\phi_0 = \phi(x=0)$. Introducing auxiliary fields $\lambda_1(\tau)$ and $\lambda_2(\tau)$, we first rewrite the partition function as

$$\begin{aligned} Z &= \int \mathcal{D}\theta_0 \int \mathcal{D}\phi_0 \int \mathcal{D}\lambda_1 \int \mathcal{D}\lambda_2 \int \mathcal{D}\theta \int \mathcal{D}\phi \\ &\quad \times \exp\left(-\int_0^\beta d\tau \left\{ L_0(\tau) + L_1(\tau) + i\lambda_1(\tau)[\theta_0(\tau) - \theta(0, \tau)] + i\lambda_2(\tau)[\phi_0(\tau) - \phi(0, \tau)] \right\}\right), \end{aligned} \quad (2.4)$$

and then integrate out $\theta(x, \tau)$ and $\phi(x, \tau)$ to obtain

$$\begin{aligned} Z &= \int \mathcal{D}\theta_0 \int \mathcal{D}\phi_0 \int \mathcal{D}\lambda_1 \int \mathcal{D}\lambda_2 \exp\left(-\frac{\pi\eta_\rho v_\rho}{\beta} \sum_{\omega_n} \lambda_1(\omega_n) \lambda_1(-\omega_n) \int_{-\infty}^{\infty} \frac{dq}{2\pi} \frac{1}{\omega_n^2 + v_\rho^2 q^2} \right. \\ &\quad \left. -\frac{\pi\eta_\sigma v_\sigma}{\beta} \sum_{\omega_n} \lambda_2(\omega_n) \lambda_2(-\omega_n) \int_{-\infty}^{\infty} \frac{dq}{2\pi} \frac{1}{\omega_n^2 + v_\sigma^2 q^2} \right. \\ &\quad \left. + \frac{i}{\beta} \sum_{\omega_n} [\lambda_1(\omega_n) \theta_0(-\omega_n) + \lambda_2(\omega_n) \phi_0(-\omega_n)] \right. \\ &\quad \left. + \frac{2V_0}{\pi\alpha} \int_0^\beta d\tau \cos \theta_0(\tau) \cos \phi_0(\tau) \right), \end{aligned} \quad (2.5)$$

where $\omega_n = 2\pi n/\beta$ ($n = 0, \pm 1, \pm 2, \dots$) and we have neglected an unimportant numerical factor. Here the Fourier transforms are defined as

$$\theta_0(\omega_n) = \int_0^\beta d\tau \theta_0(\tau) e^{i\omega_n \tau}, \quad \phi_0(\omega_n) = \int_0^\beta d\tau \phi_0(\tau) e^{i\omega_n \tau},$$

$$\lambda_j(\omega) = \int_0^\beta d\tau \lambda_j(\tau) e^{i\omega_n \tau} \quad (j = 1, 2). \quad (2.6)$$

Integrating out λ_1 and λ_2 , we finally obtain

$$Z = \int \mathcal{D}\theta_0 \int \mathcal{D}\phi_0 \exp \left(-\frac{1}{2\pi\eta_\rho\beta} \sum_{\omega_n} |\omega_n| |\theta_0(\omega_n)|^2 - \frac{1}{2\pi\eta_\sigma\beta} \sum_{\omega_n} |\omega_n| |\phi_0(\omega_n)|^2 + \frac{2V_0}{\pi\alpha} \int_0^\beta d\tau \cos \theta_0(\tau) \cos \phi_0(\tau) \right). \quad (2.7)$$

Note that this partition function is similar to that of a quantum Brownian particle (coordinate (θ_0, ϕ_0)) moving in the periodic cosine potential (2.3) and coupled to a dissipative environment [22, 23, 24, 25]; in our model the low-lying charge and spin excitations cause the dissipation. Hence our 1D problem is now reduced to quantum mechanics of a particle, i.e., a 0D field theory. To avoid ultraviolet divergences, we introduce a high-frequency cutoff, $\Lambda \sim v_F/\alpha$, which may also serve as a mass of the particle $m \sim 1/\Lambda$ [25].

2.3 Weak barrier potential

In this section we consider the limit where the barrier potential is very weak. We thus perform RG transformations and calculate charge and spin conductances perturbatively with respect to V_0 .

2.3.1 Scaling equations

Following Fisher and Zwerger [25], we derive scaling equations for the barrier potential by recursively integrating out high-frequency modes. At zero temperature the partition function (2.7) is written as

$$Z = \int \mathcal{D}\theta_0 \int \mathcal{D}\phi_0 \exp(-S_0 - S_1) \quad (2.8)$$

where

$$\begin{aligned} S_0 &= \frac{1}{2\pi\eta_\rho} \int_{-\Lambda}^{\Lambda} \frac{d\omega}{2\pi} |\omega| |\theta_0(\omega)|^2 + \frac{1}{2\pi\eta_\sigma} \int_{-\Lambda}^{\Lambda} \frac{d\omega}{2\pi} |\omega| |\phi_0(\omega)|^2, \\ S_1 &= -\frac{2V_0}{\pi\alpha} \int d\tau \cos \theta_0(\tau) \cos \phi_0(\tau). \end{aligned} \quad (2.9)$$

We first divide the phase fields into slow and fast modes,

$$\theta_0(\tau) = \theta_{0s}(\tau) + \theta_{0f}(\tau), \quad \phi_0(\tau) = \phi_{0s}(\tau) + \phi_{0f}(\tau), \quad (2.10)$$

such that

$$\theta_0(\omega) \approx \begin{cases} \theta_{0s}(\omega), & |\omega| \leq \mu \\ \theta_{0f}(\omega), & \mu \leq |\omega| \leq \Lambda, \end{cases} \quad \phi_0(\omega) \approx \begin{cases} \phi_{0s}(\omega), & |\omega| \leq \mu \\ \phi_{0f}(\omega), & \mu \leq |\omega| \leq \Lambda. \end{cases} \quad (2.11)$$

Integrating out the fast modes θ_{0f} and ϕ_{0f} , we then get an effective action \tilde{S} for the slow modes in powers of V_0 :

$$\tilde{S} = \frac{1}{2\pi\eta_\rho} \int_{-\mu}^{\mu} \frac{d\omega}{2\pi} |\omega| |\theta_{0s}(\omega)|^2 + \frac{1}{2\pi\eta_\sigma} \int_{-\mu}^{\mu} \frac{d\omega}{2\pi} |\omega| |\phi_{0s}(\omega)|^2 + \langle S_1 \rangle - \frac{1}{2} (\langle S_1^2 \rangle - \langle S_1 \rangle^2) + O(V_0^3). \quad (2.12)$$

Here the averages are over the fast modes and given by

$$\langle S_1 \rangle = \frac{2V_0}{\pi\alpha} e^{-\frac{1}{2}[G_\theta(0)+G_\phi(0)]} \int d\tau \cos \theta_{0s} \cos \phi_{0s}, \quad (2.13)$$

$$\begin{aligned} \langle S_1^2 \rangle - \langle S_1 \rangle^2 &= \left(\frac{2V_0}{\pi\alpha} \right)^2 e^{-G_\theta(0)-G_\phi(0)} \int d\tau_1 \int d\tau_2 \\ &\times \left\{ \cos[\theta_{0s}(\tau_1) + \theta_{0s}(\tau_2)] \cos[\phi_{0s}(\tau_1) + \phi_{0s}(\tau_2)] (e^{-G_\theta(\tau_1-\tau_2)-G_\phi(\tau_1-\tau_2)} - 1) \right. \\ &\quad + \cos[\theta_{0s}(\tau_1) - \theta_{0s}(\tau_2)] \cos[\phi_{0s}(\tau_1) - \phi_{0s}(\tau_2)] (e^{G_\theta(\tau_1-\tau_2)+G_\phi(\tau_1-\tau_2)} - 1) \\ &\quad + \cos[\theta_{0s}(\tau_1) + \theta_{0s}(\tau_2)] \cos[\phi_{0s}(\tau_1) - \phi_{0s}(\tau_2)] (e^{-G_\theta(\tau_1-\tau_2)+G_\phi(\tau_1-\tau_2)} - 1) \\ &\quad \left. + \cos[\theta_{0s}(\tau_1) - \theta_{0s}(\tau_2)] \cos[\phi_{0s}(\tau_1) + \phi_{0s}(\tau_2)] (e^{G_\theta(\tau_1-\tau_2)-G_\phi(\tau_1-\tau_2)} - 1) \right\}, \end{aligned} \quad (2.14)$$

where the correlation functions for the fast modes are defined as

$$G_\theta(\tau) = \langle \theta_{0l}(\tau) \theta_{0l}(0) \rangle = \pi \eta_\rho \int_{-\Lambda}^{\Lambda} \frac{d\omega}{2\pi} \frac{e^{-i\omega\tau}}{|\omega|} W(\omega/\mu), \quad (2.15)$$

$$G_\phi(\tau) = \langle \phi_{0l}(\tau) \phi_{0l}(0) \rangle = \pi \eta_\sigma \int_{-\Lambda}^{\Lambda} \frac{d\omega}{2\pi} \frac{e^{-i\omega\tau}}{|\omega|} W(\omega/\mu), \quad (2.16)$$

with a smoothing function $W(x)$ satisfying $W(x) \rightarrow 0$ for $x \ll 1$ and $W(x) \approx 1$ for $x \gg 1$ [32]. For $\mu \ll \Lambda$ $G_\theta(0) = \eta_\rho \ln(\Lambda/\mu)$ and $G_\phi(0) = \eta_\sigma \ln(\Lambda/\mu)$, and thus Eq. (2.13) becomes

$$\langle S_1 \rangle = \frac{2V_0}{\pi\alpha} \left(\frac{\mu}{\Lambda} \right)^{\frac{1}{2}(\eta_\rho + \eta_\sigma)} \int d\tau \cos \theta_{0s}(\tau) \cos \phi_{0s}(\tau). \quad (2.17)$$

Since $G_\theta(\tau)$ and $G_\phi(\tau)$ are short-ranged and fall off exponentially for $\tau \gg 1/\mu$ [25], the second-order cumulant can be approximated as

$$\begin{aligned} \langle S_1^2 \rangle - \langle S_1 \rangle^2 &\approx \left(\frac{2V_0}{\pi\alpha} \right)^2 \left(\frac{\mu}{\Lambda} \right)^{\eta_\rho + \eta_\sigma} \int d\tau \left\{ a_1 \cos[2\theta_{0s}(\tau)] \cos[2\phi_{0s}] \right. \\ &\quad + a_2 \left[1 - \frac{1}{2} \left(\frac{d\theta_{0s}}{d\tau} \right)^2 - \frac{1}{2} \left(\frac{d\phi_{0s}}{d\tau} \right)^2 \right] \\ &\quad \left. + a_3 \cos[2\theta_{0s}(\tau)] + a_4 \cos[2\phi_{0s}(\tau)] \right\}, \end{aligned} \quad (2.18)$$

where

$$\begin{aligned} a_1 &= \int d\tau (e^{-G_\theta(\tau)-G_\phi(\tau)} - 1), & a_2 &= \int d\tau (e^{G_\theta(\tau)+G_\phi(\tau)} - 1), \\ a_3 &= \int d\tau (e^{-G_\theta(\tau)+G_\phi(\tau)} - 1), & a_4 &= \int d\tau (e^{G_\theta(\tau)-G_\phi(\tau)} - 1). \end{aligned} \quad (2.19)$$

Finally we must rescale the imaginary time as $\tau \rightarrow (\Lambda/\mu)\tau$ to complete the RG transformation. Note that it is not necessary to rescale θ_0 and ϕ_0 because the theory has underlying symmetries, $\theta_0(\tau) \rightarrow \theta_0(\tau) + 2\pi$ and $\phi_0(\tau) \rightarrow \phi_0(\tau) + 2\pi$ [25]. In addition, since the second term of the integrand in Eq. (2.18), $\int d\tau [(d\theta_{0s}/d\tau)^2 + (d\phi_{0s}/d\tau)^2]$, is irrelevant compared with $\int d\omega (|\omega| |\theta_{0s}(\omega)|^2 + |\omega| |\phi_{0s}(\omega)|^2)$, both η_ρ and η_σ are not renormalized. Hence the quantities

left to be renormalized are the barrier potential, $V_0 \cos \theta_0 \cos \phi_0$, and its descendants in the second order perturbation, i.e., $V_{2,0} \cos 2\theta_0$, $V_{0,2} \cos 2\phi_0$, and $V_{2,2} \cos 2\theta_0 \cos 2\phi_0$. We note that the potentials, $V_{2,0} \cos 2\theta_0$ and $V_{0,2} \cos 2\phi_0$, can also be written in terms of the fermion field operators at $x = 0$ as $\frac{1}{2}V_{2,0}(\Psi_{21}^\dagger \Psi_{11} \Psi_{21}^\dagger \Psi_{11} + H.c.)$ and $\frac{1}{2}V_{0,2}(\Psi_{21}^\dagger \Psi_{11} \Psi_{11}^\dagger \Psi_{21} + H.c.)$.

From Eq. (2.17) we get

$$V_0(\mu) = V_0(\Lambda) \left(\frac{\mu}{\Lambda} \right)^{\frac{1}{2}(\eta_\rho + \eta_\sigma) - 1}. \quad (2.20)$$

We obtain the differential scaling equation by differentiating $V_0(\mu)$ with respect to μ , keeping Λ and $V_0(\Lambda)$ fixed:

$$\frac{dV_0}{dl} = \left[1 - \frac{1}{2}(\eta_\rho + \eta_\sigma) \right] V_0(l) + O(V_0^3), \quad (2.21)$$

where $dl = -d\mu/\mu$. Thus if $\eta_\rho + \eta_\sigma > 2$ the potential scales to zero whereas for $\eta_\rho + \eta_\sigma < 2$ it grows as the cutoff μ is reduced.

The scaling equations for $V_{2,0}$ and $V_{0,2}$ can be derived in a similar way. Since $V_{2,0} \cos 2\theta_0$ and $V_{0,2} \cos 2\phi_0$ are generated by the second-order expansion as shown above, we should, from the beginning, include these two terms in the original action. Then after rescaling we get renormalized potentials as

$$V_{2,0}(\mu) = V_{2,0}(\Lambda) \left(\frac{\mu}{\Lambda} \right)^{2\eta_\rho - 1},$$

$$V_{0,2}(\mu) = V_{0,2}(\Lambda) \left(\frac{\mu}{\Lambda} \right)^{2\eta_\sigma - 1}.$$

Thus the differential RG equations are

$$\frac{dV_{2,0}}{dl} = (1 - 2\eta_\rho)V_{2,0}(l), \quad (2.22)$$

$$\frac{dV_{0,2}}{dl} = (1 - 2\eta_\sigma)V_{0,2}(l), \quad (2.23)$$

which show that $V_{2,0} \cos 2\theta_0$ ($V_{0,2} \cos 2\phi_0$) is relevant when $\eta_\rho < 1/2$ ($\eta_\sigma < 1/2$). These three RG equations, (2.21), (2.22), and (2.23), suffice for determining the phase diagram at zero temperature. Other higher-order terms, $V_{m,n} \cos m\theta_0 \cos n\phi_0$ ($m + n \geq 4$), generated by higher-order expansions are not important, since at least one of the above three pinning potentials is always relevant in parameter regions in which the higher-order terms become relevant, $m^2\eta_\rho + n^2\eta_\sigma < 2$.

From the RG equations we can deduce the phase diagram at $T = 0$ as shown in Fig. 2.1 where the phase boundaries are $\eta_\rho + \eta_\sigma = 2$, $\eta_\rho = 1/2$, and $\eta_\sigma = 1/2$. In region I, $V_0 \cos \theta_0 \cos \phi_0$ is relevant so that both θ_0 and ϕ_0 are pinned around the potential minima, which means that electrons are perfectly reflected by the barrier at $T = 0$ K. In region II, only $V_{0,2} \cos 2\phi_0$ is a relevant perturbation, and therefore spin phase, ϕ_0 , is pinned whereas charge phase, θ_0 , is not pinned. In region III, on the other hand, $V_{2,0} \cos 2\theta_0$ is relevant; the charge phase is pinned, while the spin phase is not pinned. The physical implications of these phenomena will be discussed in Sec. 2.4.1. Finally in region IV all the pinning potentials are irrelevant, so electrons can freely go through the barrier. It is interesting to note that the phase boundary $\eta_\rho + \eta_\sigma = 2$ obtained above is different from that of the Anderson localization transition studied before in the weak-pinning limit [15, 16]. This difference will be discussed in detail in Chap. 4.

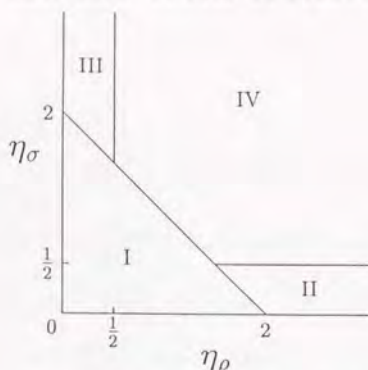


Figure 2.1: The phase diagram of the ground state in the $\eta_\rho - \eta_\sigma$ plane for the weak potential limit. The phase boundaries are $\eta_\rho + \eta_\sigma = 2$, $\eta_\rho = 1/2$, and $\eta_\sigma = 1/2$.

Regions II and III where only one of charge and spin phases is pinned are reminiscent of θ -glass and ϕ -glass in a dirty Luttinger liquid discussed by Suzumura and Fukuyama [15]. However, this similarity is superficial. The θ -glass (ϕ -glass) appears only when the backward (umklapp) scattering is present in addition to the impurity potential. On the other hand, in our single-barrier model only the forward scattering is considered away from the tunnel barrier. The $\cos 2\theta_0$ -term ($\cos 2\phi_0$ -term), which is relevant in the region III (II), is generated through renormalization from the barrier potential, $\frac{2V_0}{\pi\alpha} \cos 2\theta_0 \cos 2\phi_0$.

2.3.2 Conductance

Next we will calculate the charge (spin) conductance G_ρ (G_σ) in powers of V_0 by using the influence-functional formalism [33]. Since the method is described in detail in Ref. [25], where the mobility of a quantum Brownian particle is calculated, we simply apply their results to our problem. See Ref. [25] for details.

We assume that, when a voltage is applied to the system, a voltage difference V appears only at the potential barrier and there is no electric field in the leads. This is not exact treatment. As will be shown below, however, this approximation leads to reasonable results (each conductance has temperature-dependent correction terms which are consistent with the RG equations derived in the preceding section), and thus the approximation might be acceptable. Accordingly, we add an additional term, $eV\theta_0/\pi$, to L_1 in Eq. (2.3). The (charge) current J_ρ induced by the voltage difference is given by $J_\rho = -(e/\pi)(d\theta_0/dt)$ where t is a real time, and the charge conductance is defined by $G_\rho \equiv J_\rho/V$ with $V \rightarrow 0$. On the other hand, when there is a magnetic field difference H between the two sides of the potential barrier, another term, $\mu_B H (\phi_0/2\pi)$ (μ_B : Bohr magneton), must be included in L_1 , resulting in a spin current $J_\sigma = (1/2\pi)(d\phi_0/dt)$; the spin conductance is defined as $G_\sigma \equiv J_\sigma/H$ with $H \rightarrow 0$. In the absence of the potential $V_0 \cos \theta_0 \cos \phi_0$, G_ρ (G_σ) is $e^2 \eta_\rho / \pi$ ($\mu_B \eta_\sigma / (2\pi)$).

First we evaluate the charge conductance in powers of V_0 , assuming $V \neq 0$ but $H = 0$. Following the same path as in Ref. [25], we arrive at the following expression of the charge

current J_ρ :

$$\begin{aligned}
 J_\rho &= \frac{e}{\pi} \lim_{t \rightarrow \infty} \frac{1}{t} \langle \theta(t) \rangle, \\
 \langle \theta(t) \rangle &= \int_{-\infty}^{\infty} d\theta \int_{-\infty}^{\infty} d\phi \theta P(\theta, \phi, t), \\
 P(\theta, \phi, t) &= \int_{-\infty}^{\infty} d\theta_0 \int_{-\infty}^{\infty} d\phi_0 \int_{-\infty}^{\infty} d\theta'_0 \int_{-\infty}^{\infty} d\phi'_0 \langle \theta_0, \phi_0 | \hat{\rho}(0) | \theta'_0, \phi'_0 \rangle J(\theta, \phi, \theta, \phi, t; \theta_0, \phi_0, \theta'_0, \phi'_0, 0), \\
 J(\theta, \phi, \theta', \phi', t; \theta_0, \phi_0, \theta'_0, \phi'_0, 0) &= \lim_{M_\theta, M_\phi \rightarrow 0} \int_{\theta_0}^{\theta} \mathcal{D}\theta \int_{\phi_0}^{\phi} \mathcal{D}\phi \int_{\theta'_0}^{\theta'} \mathcal{D}\theta' \int_{\phi'_0}^{\phi'} \mathcal{D}\phi' \exp(iS[\theta, \phi] - iS[\theta', \phi'] + i\Phi[\theta, \phi, \theta', \phi']), \\
 S[\theta, \phi] &= \int_0^t dt \left[\frac{M_\theta}{2} \left(\frac{d\theta}{dt} \right)^2 + \frac{M_\phi}{2} \left(\frac{d\phi}{dt} \right)^2 + \frac{2V_0}{\pi\alpha} \cos\theta \cos\phi + \frac{1}{\pi} eV\theta \right], \\
 i\Phi[\theta, \phi, \theta', \phi'] &= \frac{i}{\pi\eta_\rho} \int_0^t dt' \theta_1(t') \frac{d\theta_2(t')}{dt'} - \frac{i}{\pi\eta_\rho} \theta_1(t) \theta_2(t) \\
 &\quad + \frac{i}{\pi\eta_\sigma} \int_0^t dt' \phi_1(t') \frac{d\phi_2(t')}{dt'} - \frac{i}{\pi\eta_\sigma} \phi_1(t) \phi_2(t) - S_2[\theta_2, \phi_2], \\
 S_2[\theta_2, \phi_2] &= \frac{1}{\pi\eta_\rho} \int_0^t dt' \int_0^{t'} ds \theta_2(t') \alpha_R(t' - s) \theta_2(s) + \frac{1}{\pi\eta_\sigma} \int_0^t dt' \int_0^{t'} ds \phi_2(t') \alpha_R(t' - s) \phi_2(s), \\
 \alpha_R(t) &= \int_0^\infty \frac{d\omega}{\pi} \omega \cos(\omega t) \coth\left(\frac{\beta\omega}{2}\right), \\
 \theta_1 &= \frac{1}{2}(\theta + \theta'), \quad \theta_2 = \theta - \theta', \quad \phi_1 = \frac{1}{2}(\phi + \phi'), \quad \phi_2 = \phi - \phi'.
 \end{aligned}$$

$\hat{\rho}(0)$ is the density matrix at $t = 0$, when the system is assumed to be in equilibrium. After some manipulations one gets

$$\begin{aligned}
 J_\rho &= \frac{e^2}{\pi} \eta_\rho V \\
 &\quad - e\eta_\rho \lim_{t \rightarrow \infty} \frac{1}{t} \sum_{n>0} \sum_{n'>0} \sum_{\{e_{1j}, s_{1j}\}} \sum_{\{e_{2j}, s_{2j}\}} \left(\frac{iV_0}{2\pi\alpha} \right)^n \left(-\frac{iV_0}{2\pi\alpha} \right)^{n'} \\
 &\quad \times \int_0^t dt_1 \int_0^{t_1} dt_2 \cdots \int_0^{t_{n-1}} dt_n \int_0^t dt'_1 \int_0^{t'_1} dt'_2 \cdots \int_0^{t'_{n'-1}} dt'_n \int_0^t dt' \frac{1}{2} [\rho(t') + \rho'(t')] \\
 &\quad \times \exp\left(i \int_0^t dt_0 \left\{ \frac{1}{\pi} eV \tilde{\theta}(t_0) - \frac{1}{2} \tilde{\theta}(t_0) [\rho(t_0) + \rho'(t_0)] \right. \right. \\
 &\quad \quad \left. \left. - \frac{1}{2} \tilde{\phi}(t_0) [\sigma(t_0) + \sigma'(t_0)] \right\} - S_2[\tilde{\theta}, \tilde{\phi}] \right), \quad (2.24)
 \end{aligned}$$

where

$$\begin{aligned}
 \rho(t') &= \sum_{j=1}^n e_{1j} \delta(t' - t_j), & \rho'(t') &= \sum_{j=1}^{n'} e_{2j} \delta(t' - t'_j), & (e_{ij} &= \pm 1) \\
 \sigma(t') &= \sum_{j=1}^n s_{1j} \delta(t' - t_j), & \sigma'(t') &= \sum_{j=1}^{n'} s_{2j} \delta(t' - t'_j), & (s_{ij} &= \pm 1) \\
 \tilde{\theta}(t') &= \pi\eta_\rho \left(\sum_{j=1}^n e_{1j} \Theta(t' - t_j) - \sum_{j=1}^{n'} e_{2j} \Theta(t' - t'_j) \right), \\
 \tilde{\phi}(t') &= \pi\eta_\sigma \left(\sum_{j=1}^n s_{1j} \Theta(t' - t_j) - \sum_{j=1}^{n'} s_{2j} \Theta(t' - t'_j) \right),
 \end{aligned}$$

and $\Theta(t')$ is the step function. The summations in Eq. (2.24) are performed under the charge and spin neutrality conditions,

$$\sum_{j=1}^n \epsilon_{1j} = \sum_{j=1}^{n'} \epsilon_{2j}, \quad \sum_{j=1}^n s_{1j} = \sum_{j=1}^{n'} s_{2j}, \quad (2.25)$$

which imply that $n + n'$ must be even. In the lowest order ($n = n' = 1$), Eq. (2.24) is evaluated as

$$\begin{aligned} J_\rho &= \frac{e^2}{\pi} \eta_\rho V \\ &\quad - e \eta_\rho \left(\frac{V_0}{\pi \alpha} \right)^2 \tanh \left(\frac{1}{2} \eta_\rho \beta e V \right) \\ &\quad \times \int_{-\infty}^{\infty} dt \cos(\eta_\rho e V t) \exp \left[-(\eta_\rho + \eta_\sigma) \int_0^\infty d\omega \frac{e^{-\omega/\Lambda}}{\omega} \left((1 - \cos \omega t) \coth \frac{\beta \omega}{2} + i \sin \omega t \right) \right], \end{aligned} \quad (2.26)$$

where we have adopted an exponential cutoff, $\exp(-\omega/\Lambda)$. The charge conductance G_ρ is then obtained as

$$G_\rho = \frac{e^2 \eta_\rho}{\pi} \left[1 - \frac{\sqrt{\pi} \eta_\rho}{2} \frac{\Gamma((\eta_\rho + \eta_\sigma)/2)}{\Gamma((\eta_\rho + \eta_\sigma + 1)/2)} \left(\frac{V_0}{\alpha \Lambda} \right)^2 \left(\frac{\pi T}{\Lambda} \right)^{\eta_\rho + \eta_\sigma - 2} \right], \quad (2.27)$$

where $\Gamma(x)$ is the Γ function (see Appendix A.1 for details). The next leading term in the expansion can also be obtained from Eq. (2.24). Here we evaluate it by a simpler method: we replace the barrier potential $(2V_0/\pi\alpha) \cos \theta_0 \cos \phi_0$ by $(2V_{2,0}/\pi\alpha) \cos 2\theta_0$, and calculate the charge conductance in the lowest order. By so doing, together with Eq. (2.27), we get G_ρ up to the order $(V_0/\alpha\Lambda)^4$ as

$$G_\rho = \frac{e^2 \eta_\rho}{\pi} \left[1 - c_0 \left(\frac{V_0}{\alpha \Lambda} \right)^2 \left(\frac{\pi T}{\Lambda} \right)^{\eta_\rho + \eta_\sigma - 2} - c_1 \left(\frac{V_{2,0}}{\alpha \Lambda} \right)^2 \left(\frac{\pi T}{\Lambda} \right)^{4\eta_\rho - 2} \right], \quad (2.28)$$

where c_0 and c_1 are dimensionless constants which depend on η_ρ , η_σ , and the cutoff procedure. Note that $V_{2,0}$ is of order $V_0^2/\alpha\Lambda$.

The current-voltage characteristic of the single barrier is obtained from Eq. (2.26). At zero temperature it becomes

$$\begin{aligned} J_\rho &= \frac{e^2}{\pi} \eta_\rho V - e \eta_\rho \left(\frac{V_0}{\pi \alpha} \right)^2 \int_{-\infty}^{\infty} dt \cos(\eta_\rho e V t) \exp \left(-(\eta_\rho + \eta_\sigma) \int_0^\infty d\omega \frac{e^{-\omega/\Lambda}}{\omega} (1 - e^{-i\omega t}) \right) \\ &\quad - e \eta_\rho \left(\frac{V_{2,0}}{\pi \alpha} \right)^2 \int_{-\infty}^{\infty} dt \cos(2\eta_\rho e V t) \exp \left(-4\eta_\rho \int_0^\infty d\omega \frac{e^{-\omega/\Lambda}}{\omega} (1 - e^{-i\omega t}) \right) \\ &= \frac{e^2}{\pi} \eta_\rho V - \frac{\pi e \eta_\rho}{\Lambda \Gamma(\eta_\rho + \eta_\sigma)} \left(\frac{V_0}{\pi \alpha} \right)^2 \left(\frac{\eta_\rho e V}{\Lambda} \right)^{\eta_\rho + \eta_\sigma - 1} - \frac{\pi e \eta_\rho}{\Lambda \Gamma(4\eta_\rho)} \left(\frac{V_{2,0}}{\pi \alpha} \right)^2 \left(\frac{2\eta_\rho e V}{\Lambda} \right)^{4\eta_\rho - 1}, \end{aligned} \quad (2.29)$$

where we have included the contribution from $V_{2,0} \cos 2\theta_0$ and neglected unimportant exponential factors such as $\exp(-\eta_\rho e V/\Lambda)$ (see Appendix A.2). For temperatures $T \ll eV$ the current-voltage relation deviates from Ohm's law, as described in Eq. (2.29). If $eV \ll T \ll \Lambda$, on the other hand, the current-voltage characteristic obeys Ohm's law, $J_\rho = G_\rho V$, where G_ρ is given by Eq. (2.28).

The spin conductance G_σ can also be evaluated in a similar manner by taking $H \neq 0$ and $V = 0$. Here we show only the final expression which is valid up to the order $(V_0/\alpha\Lambda)^4$:

$$G_\sigma = \frac{\mu_B \eta_\sigma}{2\pi} \left[1 - c'_0 \left(\frac{V_0}{\alpha\Lambda} \right)^2 \left(\frac{\pi T}{\Lambda} \right)^{\eta_\rho + \eta_\sigma - 2} - c'_1 \left(\frac{V_{0,2}}{\alpha\Lambda} \right)^2 \left(\frac{\pi T}{\Lambda} \right)^{4\eta_\sigma - 2} \right], \quad (2.30)$$

where c'_0 and c'_1 are dimensionless numbers.

The temperature dependence of G_ρ and G_σ is naturally understood from the scaling equations (2.21), (2.22), and (2.23). For example, integrating the RG equation (2.21) from $\mu = \Lambda$ to $\mu = T$ yields the renormalized potential, $(2V_0/\pi\alpha)(T/\Lambda)^{\frac{1}{2}(\eta_\rho + \eta_\sigma) - 1}$. Then, the reduction of the conductances due to the potential scattering is proportional to the square of the renormalized one, giving the power-law dependence of $T^{\eta_\rho + \eta_\sigma - 2}$ in Eqs. (2.28) and (2.30). The same reasoning can be applied also to the reductions due to $V_{2,0} \cos 2\theta_0$ and $V_{0,2} \cos 2\phi_0$.

The above perturbative calculations are valid if the reductions of the conductances due to the potential scattering are much smaller than the 0th-order term, $e^2 \eta_\rho / \pi$ or $\mu_B \eta_\sigma / 2\pi$. Thus Eqs. (2.28) and (2.29) are valid down to $T = 0$ K in regions II and IV of Fig. 2.1, where $G_\rho(T = 0 \text{ K}) = e^2 \eta_\rho / \pi$. In the other regions (I and III), however, the expansion is valid only for high temperatures. At low temperatures expansions with respect to the tunneling matrix elements become appropriate, giving $G_\rho(T = 0 \text{ K}) = 0$. Similarly, the expansion of G_σ (2.30) is justified only in regions III and IV down to $T = 0$ K, and $G_\sigma(T = 0 \text{ K}) = \mu_B \eta_\sigma / 2\pi$. In regions I and II, on the other hand, the expansion fails at low temperatures, which suggests $G_\sigma(T = 0 \text{ K}) = 0$. In summary, at low temperatures the perturbative calculations are justified in the regions where the pinning potential is irrelevant and the relevant phase field is not pinned. Finally we note that for the noninteracting case ($\eta_\rho = \eta_\sigma = 1$) the leading-order corrections proportional to $(V_0/\alpha\Lambda)^2$ in Eqs. (2.28) and (2.30) are independent of T , which is consistent with what the Landauer formula tells: the conductance can take any value from 0 to e^2/π at zero temperature.

2.4 Strong barrier potential

In this section we consider the opposite limit in which the barrier potential is very strong, $V_0/\alpha\Lambda \gg 1$. In this limit the electron transport can be viewed as the tunneling from a potential minimum to an adjacent minimum, and tunneling matrix elements are natural expansion parameters. The cosine potential (2.3) has minima at $(\theta_0, \phi_0) = ((m+n)\pi, (m-n)\pi)$ and maxima at $(\theta_0, \phi_0) = ((m+n+1)\pi, (m-n)\pi)$, where m and n are integers (Fig. 2.2). Thus a particle initially at $(\theta_0, \phi_0) = (0, 0)$ can tunnel to $(\pm\pi, \pm\pi)$ through a lower tunnel barrier and to $(\pm 2\pi, 0)$ and $(0, \pm 2\pi)$ through a higher barrier. Physically these processes correspond to the tunneling of one electron or hole $((\pm\pi, \pm\pi))$, the singlet pair of two electrons or holes $((\pm 2\pi, 0))$, and the triplet electron-hole pair $((0, \pm 2\pi))$, respectively.

2.4.1 Duality mapping and scaling equations

Generalizing the duality argument by Schmid [23] and using the dilute instanton gas approximation (DIGA), we show below that the partition function in the strong potential limit is mapped to that in the weak potential limit discussed in the preceding section.

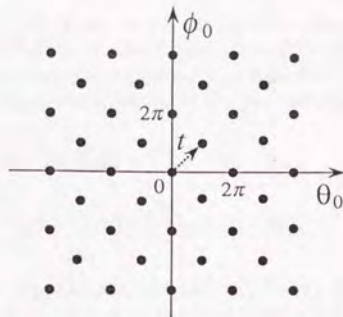


Figure 2.2: Minima of the pinning potential $-(2V_0/\pi\alpha) \cos \theta_0 \cos \phi_0$. The matrix element for the $(0, 0) \rightarrow (\pi, \pi)$ tunneling is t .

Remembering that the high-frequency cutoff Λ serves as the mass m of the Brownian particle, we may write the partition function (2.7) as

$$Z = \int \mathcal{D}\theta_0 \int \mathcal{D}\phi_0 \exp(-S_0 - S_1) \quad (2.31)$$

$$S_0 = \int_0^\beta d\tau \left\{ \frac{1}{2}m \left[\left(\frac{d\theta_0}{d\tau} \right)^2 + \left(\frac{d\phi_0}{d\tau} \right)^2 \right] + \frac{2V_0}{\pi\alpha} (1 - \cos \theta_0 \cos \phi_0) \right\} \quad (2.32)$$

$$S_1 = \frac{1}{2\pi\eta_\rho} \sum_{\omega_n} |\omega_n| |\theta_0(\omega_n)|^2 + \frac{1}{2\pi\eta_\sigma} \sum_{\omega_n} |\omega_n| |\phi_0(\omega_n)|^2. \quad (2.33)$$

Note that for simplicity we have assumed that the mass is isotropic in the (θ_0, ϕ_0) plane. We evaluate the partition function in the semiclassical limit, in which the functional integral is dominated by the stationary path of $S_0 + S_1$. It is important to notice that S_0 describes the physics in the short timescale, i.e., tunneling of an electron (instanton), whereas S_1 describes the physics in the long timescale, i.e., interaction between instantons. We, therefore, first construct the stationary paths of S_0 , denoted by $\bar{\theta}_0$ and $\bar{\phi}_0$, and then we substitute them into S_1 . $\bar{\theta}_0(\tau)$ and $\bar{\phi}_0(\tau)$ are determined from

$$\frac{\delta S_0}{\delta \bar{\theta}_0} = -m \frac{d^2 \bar{\theta}_0}{d\tau^2} + \frac{2V_0}{\pi\alpha} \sin \bar{\theta}_0 \cos \bar{\phi}_0 = 0, \quad (2.34)$$

$$\frac{\delta S_0}{\delta \bar{\phi}_0} = -m \frac{d^2 \bar{\phi}_0}{d\tau^2} + \frac{2V_0}{\pi\alpha} \cos \bar{\theta}_0 \sin \bar{\phi}_0 = 0, \quad (2.35)$$

or equivalently,

$$\frac{d^2}{d\tau^2} (\bar{\theta}_0 + \bar{\phi}_0) = \frac{2V_0}{\pi\alpha m} \sin(\bar{\theta}_0 + \bar{\phi}_0), \quad (2.36)$$

$$\frac{d^2}{d\tau^2} (\bar{\theta}_0 - \bar{\phi}_0) = \frac{2V_0}{\pi\alpha m} \sin(\bar{\theta}_0 - \bar{\phi}_0). \quad (2.37)$$

A solution of $d^2 X/d\tau^2 = (2V_0/\pi\alpha m) \sin X$ describing one instanton at $x = 0$ is given by

$$X(\tau) = 2 \arccos \left(-\tanh[\tau(2V_0/\pi\alpha m)^{1/2}] \right), \quad (2.38)$$

which satisfies $X(-\infty) = 0$ and $X(\infty) = 2\pi$. From this we see that the width of the instanton is of order $(\pi\alpha m/2V_0)^{1/2}$. In the DIGA, we neglect the overlaps of instantons assuming that β is much larger than the width and that fugacity of instantons is very small. Thus we write $\bar{\theta}_0$ and $\bar{\phi}_0$ as linear combinations of the one-instanton solution $X(\tau)$:

$$\bar{\theta}_0(\tau) + \bar{\phi}_0(\tau) = \sum_{j=1}^{n_1} e_{1j} X(\tau - \tau_{1j}), \quad (2.39)$$

$$\bar{\theta}_0(\tau) - \bar{\phi}_0(\tau) = \sum_{j=1}^{n_2} e_{2j} X(\tau - \tau_{2j}), \quad (2.40)$$

where $e_{ij} = 1$ (instanton) or -1 (anti-instanton) and τ_{ij} 's specify the locations of instantons or anti-instantons. It follows from $\bar{\theta}_0(0) = \bar{\theta}_0(\beta)$ and $\bar{\phi}_0(0) = \bar{\phi}_0(\beta)$ that $\sum_j e_{1j} = \sum_j e_{2j} = 0$ (neutrality condition). We may write the Fourier transform of $\bar{\theta}_0(\tau)$ and $\bar{\phi}_0(\tau)$ as

$$\bar{\theta}_0(\omega_n) = \int_0^\beta d\tau \bar{\theta}_0(\tau) e^{i\omega_n \tau} = \frac{i\pi}{\omega_n} \sum_{j=1}^{n_1} e_{1j} \exp(i\omega_n \tau_{1j}) + \frac{i\pi}{\omega_n} \sum_{j=1}^{n_2} e_{2j} \exp(i\omega_n \tau_{2j}), \quad (2.41)$$

$$\bar{\phi}_0(\omega_n) = \int_0^\beta d\tau \bar{\phi}_0(\tau) e^{i\omega_n \tau} = \frac{i\pi}{\omega_n} \sum_{j=1}^{n_1} e_{1j} \exp(i\omega_n \tau_{1j}) - \frac{i\pi}{\omega_n} \sum_{j=1}^{n_2} e_{2j} \exp(i\omega_n \tau_{2j}), \quad (2.42)$$

where we have used an approximation,

$$\int_0^\beta d\tau e^{i\omega_n \tau} \frac{d}{d\tau} X(\tau - \tau_{ij}) \approx e^{i\omega_n \tau_{ij}} \int_{-\infty}^{\infty} d\tau \frac{dX(\tau)}{d\tau} = 2\pi e^{i\omega_n \tau_{ij}}. \quad (2.43)$$

By substituting Eqs. (2.41) and (2.42) into Eq. (2.33), the partition function can be calculated, within the DIGA, as

$$\begin{aligned} Z = & \sum_{n_1=0}^{\infty} \sum_{n_2=0}^{\infty} \sum_{\{e_{1j}\}} \sum_{\{e_{2j}\}} \frac{1}{n_1! n_2!} \int_0^\beta d\tau_{11} \cdots \int_0^\beta d\tau_{1n_1} \int_0^\beta d\tau_{21} \cdots \int_0^\beta d\tau_{2n_2} \\ & \times y_0^{n_1+n_2} \exp \left(-\frac{\pi}{2\eta_\rho \beta} \sum_{\omega_n} \frac{1}{|\omega_n|} \left| \sum_{j=1}^{n_1} e_{1j} \exp(i\omega_n \tau_{1j}) + \sum_{j=1}^{n_2} e_{2j} \exp(i\omega_n \tau_{2j}) \right|^2 \right. \\ & \left. - \frac{\pi}{2\eta_\sigma \beta} \sum_{\omega_n} \frac{1}{|\omega_n|} \left| \sum_{j=1}^{n_1} e_{1j} \exp(i\omega_n \tau_{1j}) - \sum_{j=1}^{n_2} e_{2j} \exp(i\omega_n \tau_{2j}) \right|^2 \right), \quad (2.44) \end{aligned}$$

where $\sum_{\{e_{j\pm}\}}$ represents summation over possible configurations of e_{ij} 's under the neutrality conditions, and y_0 is the instanton fugacity, i.e., tunneling matrix element t corresponding to $(\theta_0, \phi_0) = (0, 0) \rightarrow (\pm\pi, \pm\pi)$. Equation (2.44) can be simplified by introducing dual fields $\bar{\theta}_0$ and $\bar{\phi}_0$ as

$$\begin{aligned} Z \propto & \sum_{n_1=0}^{\infty} \sum_{n_2=0}^{\infty} \sum_{\{e_{1j}\}} \sum_{\{e_{2j}\}} \frac{1}{n_1! n_2!} \int_0^\beta d\tau_{11} \cdots \int_0^\beta d\tau_{1n_1} \int_0^\beta d\tau_{21} \cdots \int_0^\beta d\tau_{2n_2} \int \mathcal{D}\bar{\theta}_0 \int \mathcal{D}\bar{\phi}_0 \\ & \times y_0^{n_1+n_2} \exp \left(-\frac{\eta_\rho}{2\pi\beta} \sum_{\omega_n} |\omega_n| |\bar{\theta}_0(\omega_n)|^2 - \frac{\eta_\sigma}{2\pi\beta} \sum_{\omega_n} |\omega_n| |\bar{\phi}_0(\omega_n)|^2 \right. \\ & \left. + i \sum_{j=1}^{n_1} e_{1j} [\bar{\theta}_0(\tau_{1j}) + \bar{\phi}_0(\tau_{1j})] + i \sum_{j=1}^{n_2} e_{2j} [\bar{\theta}_0(\tau_{2j}) - \bar{\phi}_0(\tau_{2j})] \right) \end{aligned}$$

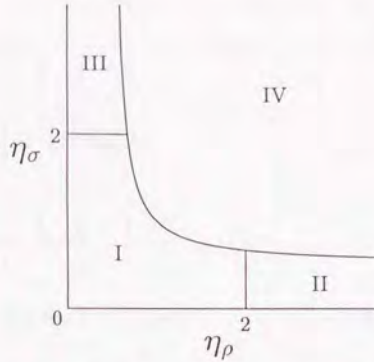


Figure 2.3: The phase diagram of the ground state for the strong potential limit. The phase boundaries are $\frac{1}{\eta_\rho} + \frac{1}{\eta_\sigma} = 2$, $\eta_\rho = 2$, and $\eta_\sigma = 2$. The charge conductance G_ρ is 0 in regions I and III, and $e^2\eta_\rho/\pi$ in regions II and IV at zero temperature. The spin conductance G_σ is 0 in regions I and II, and $\mu_B\eta_\sigma/2\pi$ in regions III and IV at zero temperature.

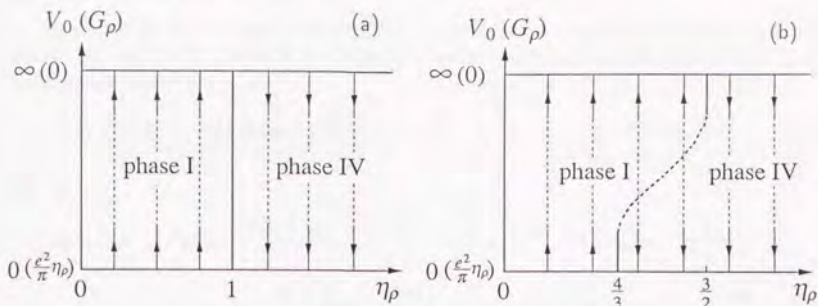
$$\begin{aligned}
 &= \int \mathcal{D}\tilde{\theta}_0 \int \mathcal{D}\tilde{\phi}_0 \exp\left(-\frac{\eta_\rho}{2\pi\beta} \sum_{\omega_n} |\omega_n| |\tilde{\theta}_0(\omega_n)|^2 - \frac{\eta_\sigma}{2\pi\beta} \sum_{\omega_n} |\omega_n| |\tilde{\phi}_0(\omega_n)|^2 \right. \\
 &\quad \left. + 2y_0 \int_0^\beta d\tau \cos[\tilde{\theta}_0(\tau) + \tilde{\phi}_0(\tau)] + 2y_0 \int_0^\beta d\tau \cos[\tilde{\theta}_0(\tau) - \tilde{\phi}_0(\tau)]\right) \\
 &= \int \mathcal{D}\tilde{\theta}_0 \int \mathcal{D}\tilde{\phi}_0 \exp\left(-\frac{\eta_\rho}{2\pi\beta} \sum_{\omega_n} |\omega_n| |\tilde{\theta}_0(\omega_n)|^2 - \frac{\eta_\sigma}{2\pi\beta} \sum_{\omega_n} |\omega_n| |\tilde{\phi}_0(\omega_n)|^2 \right. \\
 &\quad \left. + 4y_0 \int_0^\beta d\tau \cos \tilde{\theta}_0(\tau) \cos \tilde{\phi}_0(\tau)\right). \tag{2.45}
 \end{aligned}$$

We see that Eq. (2.45) is identical to the original partition function (2.7) if we replace $1/\eta_{\rho(\sigma)}$, $V_0/\pi\alpha$, θ_0 , and ϕ_0 by $\eta_{\rho(\sigma)}$, $2y_0$, $\tilde{\theta}_0$, and $\tilde{\phi}_0$, respectively. It is of interest to note that $\tilde{\theta}_0$ and $\tilde{\phi}_0$ correspond to $\theta_-(x=0)$ and $\phi_-(x=0)$ introduced in Chap. 1. Thus $\tilde{\theta}_0$ represents the Josephson phase whereas $\tilde{\theta}_0$ corresponds to the charge. $\tilde{\phi}_0$ is also the conjugate variable of ϕ_0 in the same sense.

Since the partition function in the strong potential limit is found to be identical to that in the weak potential limit, we can readily write down the scaling equations applying the analysis in the preceding section. As is shown in Sec. 2.3.1, the second-order cumulant expansion of $y_0 \cos \tilde{\theta}_0 \cos \tilde{\phi}_0$ yields $y_{2,0} \cos 2\tilde{\theta}_0$ and $y_{0,2} \cos 2\tilde{\phi}_0$. By analogy with the fact that $y_0 \cos \tilde{\theta}_0 \cos \tilde{\phi}_0$ represents the tunneling from $(\theta_0, \phi_0) = (0, 0)$ to $(\pm\pi, \pm\pi)$, $y_{2,0} \cos 2\tilde{\theta}_0$ and $y_{0,2} \cos 2\tilde{\phi}_0$ correspond to tunnelings from $(0, 0)$ to $(\pm 2\pi, 0)$ and to $(0, \pm 2\pi)$, respectively. We note here that if $(d\theta_0/d\tau)^2$ and $(d\phi_0/d\tau)^2$ in Eq. (2.32) do not have the same coefficient m , then the effective action in Eq. (2.45) will have $y_{2,0} \cos 2\theta_0$, $y_{0,2} \cos 2\phi_0$, etc.

From Eqs. (2.21), (2.22), and (2.23), we obtain

$$\frac{dy_0}{dt} = \left[1 - \frac{1}{2} \left(\frac{1}{\eta_\rho} + \frac{1}{\eta_\sigma} \right) \right] y_0(t), \tag{2.46}$$

Figure 2.4: The RG flow diagram for $\eta_\rho = \eta_\sigma$ (a) and $\eta_\rho = 2\eta_\sigma$ (b).

$$\frac{dy_{2,0}}{dl} = \left(1 - \frac{2}{\eta_\rho}\right) y_{2,0}(l), \quad (2.47)$$

$$\frac{dy_{0,2}}{dl} = \left(1 - \frac{2}{\eta_\sigma}\right) y_{0,2}(l), \quad (2.48)$$

from which we deduce the phase diagram at $T = 0$ K (Fig. 2.3). The ground state is classified into four regions, and phase boundaries are $\frac{1}{\eta_\rho} + \frac{1}{\eta_\sigma} = 2$, $\eta_\rho = 2$, and $\eta_\sigma = 2$. In region I all the fugacities (tunneling matrix elements) scale to zero, which means that no tunneling occurs at $T = 0$ K. In region II (III) only $y_{2,0}$ ($y_{0,2}$) scales to a larger value, which means that only the singlet electron pair (triplet electron-hole pair) can tunnel although the individual electron is perfectly reflected by the barrier at $T = 0$ K. This corresponds to the fact that in this region II (III) the singlet superconductivity (spin density wave) instability is the most enhanced one for the 1D system without impurities (see Fig. 1.2). Lastly, in region IV y_0 scales to be larger so that the barrier transmits electrons perfectly at $T = 0$ K. The phase diagram is qualitatively the same as that in the weak potential limit (Fig. 2.1). Quantitatively, however, the phase boundaries change as V_0 increases from Fig. 2.1 to Fig. 2.3 in contrast to the spinless model [17]; the pinning regions (I, II, and III) expand as the potential barrier becomes higher.

From Figs. 2.1 and 2.3 we can deduce the RG flows (Fig. 2.4). Here the essential point is that η_ρ and η_σ are not renormalized so that the RG flows are all vertical [25]. When $\eta_\rho = \eta_\sigma$ (Fig. 2.4(a)), the phase boundary is vertical at $\eta_\rho = \eta_\sigma = 1$, and the RG flows are reminiscent of those of a quantum Brownian particle in a cosine potential [24, 25] as well as of the spinless Fermion model [17]. The same flow diagram is obtained for the case of $\eta_\sigma = 1$, i.e., the case where the system has an $SU(2)$ spin symmetry. The noninteracting Fermi liquid ($\eta_\rho = \eta_\sigma = 1$) is just on the vertical phase boundary, where the barrier potential is a marginal perturbation. In general, however, the phase boundary is not vertical and looks like an unstable fixed line. In Fig. 2.4(b) we show the RG flows along the line $\eta_\rho = 2\eta_\sigma$.

2.4.2 Conductance

In this section we calculate the charge and spin conductances perturbatively in powers of the tunneling matrix element t from the golden rule.

As shown by Caldeira and Leggett [22], the dissipation suffered by the particle of coordinate (θ_0, ϕ_0) in the partition function (2.7) can be expressed as the linear-coupling with harmonic oscillators:

$$Z \propto \int \prod_j \mathcal{D}x_{1j} \int \prod_k \mathcal{D}x_{2k} \int \mathcal{D}\theta_0 \int \mathcal{D}\phi_0 \exp\left(-\int_0^\beta d\tau L(\{x_{1j}\}, \{x_{2k}\}; \theta_0, \phi_0)\right), \quad (2.49)$$

where

$$\begin{aligned} L(\{x_{1j}\}, \{x_{2k}\}; \theta_0, \phi_0) = & \sum_j \left(\frac{1}{2} m_{1j} \left(\frac{dx_{1j}}{d\tau} \right)^2 + \frac{1}{2} m_{1j} \omega_{1j}^2 x_{1j}^2 + g_{1j} x_{1j} \theta_0 + \frac{g_{1j}^2}{2m_{1j}\omega_{1j}^2} \theta_0^2 \right) \\ & + \sum_k \left(\frac{1}{2} m_{2k} \left(\frac{dx_{2k}}{d\tau} \right)^2 + \frac{1}{2} m_{2k} \omega_{2k}^2 x_{2k}^2 + g_{2k} x_{2k} \phi_0 + \frac{g_{2k}^2}{2m_{2k}\omega_{2k}^2} \phi_0^2 \right) \\ & + \frac{2V_0}{\pi\alpha} (1 - \cos \theta_0 \cos \phi_0) \end{aligned} \quad (2.50)$$

with spectral functions for the harmonic oscillators $\{x_{1j}\}$ and $\{x_{2k}\}$,

$$J_1(\omega) = \sum_j \frac{\pi g_{1j}^2}{2m_{1j}\omega_{1j}} \delta(\omega - \omega_{1j}) = \frac{\omega}{\pi\eta_\rho} \Theta(\omega), \quad (2.51)$$

$$J_2(\omega) = \sum_k \frac{\pi g_{2k}^2}{2m_{2k}\omega_{2k}} \delta(\omega - \omega_{2k}) = \frac{\omega}{\pi\eta_\sigma} \Theta(\omega). \quad (2.52)$$

The tunneling probability through the potential barrier is calculated from the overlap between the initial state and the final state. The probability of the tunneling from $(\theta_0, \phi_0) = (0, 0)$ to (π, π) is thus given by

$$\begin{aligned} P_{(0,0) \rightarrow (\pi,\pi)} &= 2\pi t^2 \sum_{i,f} |\langle f|i \rangle|^2 e^{-\beta E_i} \delta(E_f - E_i - eV) / \sum_i e^{-\beta E_i} \\ &= t^2 \int_{-\infty}^{\infty} dt_0 \langle e^{-iH_f t_0} e^{iH_i t_0} \rangle_i e^{ieV t_0}, \end{aligned} \quad (2.53)$$

where V is the applied voltage and $|i\rangle$ ($|f\rangle$) represents eigenstates of H_i (H_f) with energy E_i (E_f). The initial- and final-state Hamiltonian are obtained from $L(\{x_{1j}\}, \{x_{2k}\}; \theta_0, \phi_0)$ by setting $(\theta_0, \phi_0) = (0, 0)$ and (π, π) , respectively:

$$H_i = \sum_j \omega_{1j} \left(a_j^\dagger a_j + \frac{1}{2} \right) + \sum_k \omega_{2k} \left(b_k^\dagger b_k + \frac{1}{2} \right), \quad (2.54)$$

$$\begin{aligned} H_f = & \sum_j \left[\omega_{1j} \left(a_j^\dagger a_j + \frac{1}{2} \right) + \frac{\pi g_{1j}}{\sqrt{2m_{1j}\omega_{1j}}} (a_j + a_j^\dagger) + \frac{\pi^2 g_{1j}^2}{2m_{1j}\omega_{1j}^2} \right] \\ & + \sum_k \left[\omega_{2k} \left(b_k^\dagger b_k + \frac{1}{2} \right) + \frac{\pi g_{2k}}{\sqrt{2m_{2k}\omega_{2k}}} (b_k + b_k^\dagger) + \frac{\pi^2 g_{2k}^2}{2m_{2k}\omega_{2k}^2} \right], \end{aligned} \quad (2.55)$$

where a_j and b_k (a_j^\dagger and b_k^\dagger) are the annihilation (creation) operator for the mode j and k , respectively. The thermal average in Eq. (2.53) is performed with respect to H_i as $\langle X \rangle_i = \text{Tr}(X e^{-\beta H_i}) / \text{Tr}(e^{-\beta H_i})$. The above two Hamiltonians are related to each other by $H_f = U^\dagger H_i U$, where the unitary operator U is given by

$$U = \exp \left[\sum_j \frac{\pi g_{1j}}{\sqrt{2m_{1j}\omega_{1j}^3}} (a_j^\dagger - a_j) + \sum_k \frac{\pi g_{2k}}{\sqrt{2m_{2k}\omega_{2k}^3}} (b_k^\dagger - b_k) \right]. \quad (2.56)$$

With the help of this relation, Eq. (2.53) is evaluated as

$$P_{(0,0) \rightarrow (\pi,\pi)} = t^2 \int_{-\infty}^{\infty} dt_0 \exp \left[ieVt_0 - \pi \int_0^{\infty} \frac{d\omega}{\omega^2} [J_1(\omega) + J_2(\omega)] \left((1 - \cos \omega t_0) \coth \frac{\beta\omega}{2} + i \sin \omega t_0 \right) \right]. \quad (2.57)$$

In the same way, the probability of the reverse process, $(\theta_0, \phi_0) = (\pi, \pi) \rightarrow (0, 0)$, is obtained as

$$\begin{aligned} P_{(\pi,\pi) \rightarrow (0,0)} &= t^2 \int_{-\infty}^{\infty} dt_0 \langle e^{-iHt_0} e^{iHt_0} \rangle_f e^{-ieVt_0} \\ &= e^{-\beta eV} P_{(0,0) \rightarrow (\pi,\pi)}, \end{aligned} \quad (2.58)$$

where the last line represents the detailed balance. The difference between $P_{(0,0) \rightarrow (\pi,\pi)}$ and $P_{(\pi,\pi) \rightarrow (0,0)}$ amounts to the net charge current J_ρ :

$$\begin{aligned} J_\rho &= 2e (P_{(0,0) \rightarrow (\pi,\pi)} - P_{(\pi,\pi) \rightarrow (0,0)}) \\ &= 2et^2 (1 - e^{-\beta eV}) \int_{-\infty}^{\infty} dt_0 \exp \left[ieVt_0 - \left(\frac{1}{\eta_\rho} + \frac{1}{\eta_\sigma} \right) \int_0^{\infty} \frac{d\omega}{\omega} \left((1 - \cos \omega t_0) \coth \frac{\beta\omega}{2} + i \sin \omega t_0 \right) \right], \end{aligned} \quad (2.59)$$

where the prefactor 2 comes from the spin degeneracy. Note that the integral in Eq. (2.59) is similar to the second term in Eq. (2.26), in agreement with the duality mapping $\eta_{\rho(\sigma)} \rightarrow 1/\eta_{\rho(\sigma)}$. Hence, in the lowest order, the charge conductance G_ρ is given by

$$G_\rho = 2e^2 t^2 \beta \int_{-\infty}^{\infty} dt_0 \exp \left[- \left(\frac{1}{\eta_\rho} + \frac{1}{\eta_\sigma} \right) \int_0^{\infty} d\omega \frac{e^{-\omega/\Lambda}}{\omega} \left((1 - \cos \omega t_0) \coth \frac{\beta\omega}{2} + i \sin \omega t_0 \right) \right], \quad (2.60)$$

where we have introduced an exponential cutoff $e^{-\omega/\Lambda}$ to avoid ultraviolet divergences. At low temperatures Eq. (2.60) is estimated as

$$G_\rho = d_1 e^2 \left(\frac{t}{\Lambda} \right)^2 \left(\frac{\pi T}{\Lambda} \right)^{\frac{1}{\eta_\rho} + \frac{1}{\eta_\sigma} - 2}, \quad (2.61)$$

where d_1 is given by $2\pi^{3/2} \Gamma(\frac{1}{2\eta_\rho} + \frac{1}{2\eta_\sigma}) / \Gamma(\frac{1}{2\eta_\rho} + \frac{1}{2\eta_\sigma} + \frac{1}{2})$. The next-order term of the charge conductance is due to the tunneling from $(\theta_0, \phi_0) = (0, 0)$ to $(2\pi, 0)$, whose tunneling matrix element, t_2 , is of order t^2/Λ . The probability for this tunneling process is then obtained as

$$P_{(0,0) \rightarrow (2\pi,0)} = t_2^2 \int_{-\infty}^{\infty} dt_0 \exp \left[2ieVt_0 - 4\pi \int_0^{\infty} \frac{d\omega}{\omega^2} J_1(\omega) \left((1 - \cos \omega t_0) \coth \frac{\beta\omega}{2} + i \sin \omega t_0 \right) \right]. \quad (2.62)$$

The probability for the reverse process is obtained from the detailed balance relation, $P_{(2\pi,0) \rightarrow (0,0)} = e^{-2\beta eV} P_{(0,0) \rightarrow (2\pi,0)}$. Thus the charge conductance due to these tunneling processes is

$$2e^2 t_2^2 \beta \int_0^{\infty} dt_0 \exp \left[- \frac{4}{\eta_\rho} \int_0^{\infty} d\omega \frac{e^{-\omega/\Lambda}}{\omega} \left((1 - \cos \omega t_0) \coth \frac{\beta\omega}{2} + i \sin \omega t_0 \right) \right]. \quad (2.63)$$

From Eqs. (2.61) and (2.63), we get the charge conductance, up to the order of $(t/\Lambda)^4$, as

$$G_\rho = d_1 e^2 \left(\frac{t}{\Lambda} \right)^2 \left(\frac{\pi T}{\Lambda} \right)^{\frac{1}{\eta_\rho} + \frac{1}{\eta_\sigma} - 2} + d_2 e^2 \left(\frac{t_2}{\Lambda} \right)^2 \left(\frac{\pi T}{\Lambda} \right)^{\frac{4}{\eta_\rho} - 2}, \quad (2.64)$$

where d_2 is a dimensionless number of order unity.

The current-voltage characteristic at zero temperature is also obtained from Eqs. (2.59) and (2.62) as

$$\begin{aligned}
 J_\rho &= 2et^2 \int_{-\infty}^{\infty} dt_0 \exp \left[ieVt_0 - \left(\frac{1}{\eta_\rho} + \frac{1}{\eta_\sigma} \right) \int_0^\infty d\omega \frac{e^{-\omega/\Lambda}}{\omega} (1 - e^{-i\omega t_0}) \right] \\
 &\quad + et_2^2 \int_{-\infty}^{\infty} dt_0 \exp \left[2ieVt_0 - \frac{4}{\eta_\rho} \int_0^\infty d\omega \frac{e^{-\omega/\Lambda}}{\omega} (1 - e^{-i\omega t_0}) \right] \\
 &= \frac{4et^2}{\Lambda \Gamma \left(\frac{1}{\eta_\rho} + \frac{1}{\eta_\sigma} \right)} \left(\frac{eV}{\Lambda} \right)^{\frac{1}{\eta_\rho} + \frac{1}{\eta_\sigma} - 1} + \frac{2et_2^2}{\Lambda \Gamma \left(\frac{1}{\eta_\rho} \right)} \left(\frac{2eV}{\Lambda} \right)^{\frac{4}{\eta_\rho} - 1}, \quad (2.65)
 \end{aligned}$$

where we have neglected unimportant exponential factors. Equation (2.65) shows that the tunneling is suppressed in the charge-pinning regions I and III: $J_\rho \propto V^g$ ($g > 1$). This result is reminiscent of recent theories on the effect of electromagnetic environment on the Coulomb blockade in a single tunnel junction [34, 35]. In our model the many-body correlations suppress the tunneling. In regions II and IV, on the other hand, Eq. (2.65) tells that the tunneling is enhanced to give $J_\rho \propto V^g$ with $g < 1$. However, this is not the case; the enhancement suggests that the expansion in powers of t is not valid, and rather the expansion in powers of V_0 described in Sec. 2.3.2 becomes appropriate.

We can also evaluate the spin conductance G_σ in the same way. The lowest-order conductance is obtained again from $P_{(0,0) \rightarrow (\pi,\pi)}$ and $P_{(\pi,\pi) \rightarrow (0,0)}$, but the relation between the two probabilities is now given by $P_{(\pi,\pi) \rightarrow (0,0)} = e^{-\beta\mu_B H/2} P_{(\pi,\pi) \rightarrow (0,0)}$, where H is the magnetic field difference across the barrier. The next-order term is obtained by examining the tunneling from $(\theta_0, \phi_0) = (0, 0)$ to $(0, 2\pi)$. Hence the spin conductance is calculated up to the order of $(t/\Lambda)^4$ as

$$G_\sigma = d_1' \mu_B \left(\frac{t}{\Lambda} \right)^2 \left(\frac{\pi T}{\Lambda} \right)^{\frac{1}{\eta_\rho} + \frac{1}{\eta_\sigma} - 2} + d_2' \mu_B \left(\frac{t_2}{\Lambda} \right)^2 \left(\frac{\pi T}{\Lambda} \right)^{\frac{4}{\eta_\rho} - 2}, \quad (2.66)$$

where d_1' and d_2' are dimensionless numbers.

Equations (2.64) and (2.66) are correct low-temperature expansions for the conductances in the parameter regions where the corresponding phase field is pinned at zero temperature: the expansion is valid in regions I and III of Fig. 2.3 for G_ρ and in I and II for G_σ . In the other regions, II and IV for G_ρ and III and IV for G_σ , as the temperature is lowered, the tunneling probabilities scale to infinity while the potential V_0 scales to zero. Thus in this case the perturbative calculations in powers of V_0 become appropriate for low temperatures.

2.5 Summary

In this chapter we have studied the tunneling through a potential barrier in the spin-dependent Tomonaga-Luttinger model. Our findings are summarized below.

- The effective action for θ_0 and ϕ_0 is obtained. It is reminiscent of the Caldeira-Leggett model of the macroscopic quantum tunneling. The dissipation is due to the low-lying charge density and spin density excitations in the Luttinger liquids.
- The zero-temperature phase diagram is classified into four regions (Figs. 2.1 and 2.3) in terms of $G_\rho(T=0)$ and $G_\sigma(T=0)$. In contrast to the spinless case, the phase boundaries change as the strength of the barrier is varied.

- The noninteracting Fermi liquid always locates on a phase boundary. Thus the barrier potential is a marginal perturbation. This result is consistent with the standard Landauer approach.
- The charge conductance and spin conductance are calculated perturbatively in both limits of weak barrier and strong barrier. They have anomalous power-law dependence on temperature arising from infrared divergences.

Chapter 3

Resonant Tunneling

3.1 Introduction

In the previous chapter, we discussed the tunneling through a single barrier in a Luttinger liquid. Taking a step forward, we will introduce one more barrier in the Luttinger liquid; the aim of this chapter is then to discuss effects of the electron correlation on the resonant tunneling through a double barrier. The model we employ is the 1D *spinless* Tomonaga-Luttinger model with two δ -function potentials at $x = -R/2$ and $R/2$. A similar model has been studied recently by Kane and Fisher [19], who considered mainly the low-temperature limit and discussed the zero-temperature phase diagram. On the other hand, the analysis given below covers both the low- and high-temperature regime, and emphasis will be put on a crossover between the two regimes [21].

Our analysis is largely motivated by recent experimental and theoretical studies [36, 37, 38, 39] which have revealed that the resonant transport through a quantum dot of nanometer scale is affected by the Coulomb blockade [1]. Also important is the discreteness of the energy levels in a semiconductor quantum dot. It is known that the conductance of the dot shows a periodic variation as a function of gate voltage which controls the electron density in the dot. The period of the conductance oscillations is determined by the charging energy U , whereas the temperature dependence of the peak height changes around the temperature comparable to the energy spacing of the discrete levels, $\Delta\epsilon$ [38, 39]. Typically, U and $\Delta\epsilon$ are estimated as $U \sim 0.5$ meV and $\Delta\epsilon \sim 0.05$ meV.

Although the electron-electron interaction has already been included, as g parameters, in the Tomonaga-Luttinger model, the long-range part of the Coulomb interaction may not be fully treated in the model; the bosonized Hamiltonian of the Tomonaga-Luttinger model does not have any term corresponding to the charging energy. To reconcile this, we introduce a charging-energy term *by hand* in an effective action. With this effective action we calculate the conductance for spinless fermions and discuss the crossover in the temperature dependence of the conductance. We note that, since our fermion is spinless, the Kondo effect does not occur in our model.

Before going to detailed analysis of the resonant tunneling in Luttinger liquids, it must be instructive to review first the resonant tunneling of noninteracting spinless fermions. To be specific, we consider a tight-binding model described by the following Hamiltonian (Fig. 3.1(a)),

$$H_V = -W \sum_n (c_{n+1}^\dagger c_n + c_n^\dagger c_{n+1}) + V (c_0^\dagger c_0 + c_N^\dagger c_N) - \epsilon_0 \sum_{n=1}^{N-1} c_n^\dagger c_n, \quad (3.1)$$

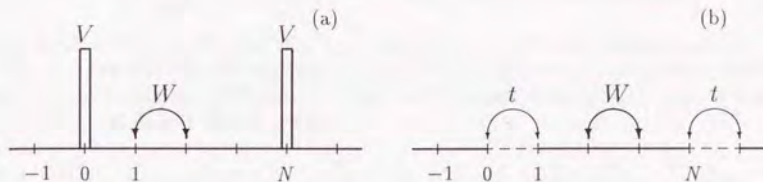


Figure 3.1: The tight-binding model with (a) two on-site potential barriers and (b) two weak links.

where c_n is an annihilation operator of a spinless fermion at site n , W is a hopping matrix element ($W > 0$), V is a potential simulating the tunnel barrier, and ε_0 is site-energy difference controlled by the gate voltage. We assume that the chemical potential μ is zero. By solving the Schrödinger equation, the transmission probability through the barriers is obtained approximately as

$$T_V(\varepsilon_0) = \frac{1}{1 + \frac{V^2}{8W^2} \left(4 + \frac{V^2}{W^2}\right) \left[1 + \cos(2k_F R + \frac{2R}{v_F} \varepsilon_0 - \delta)\right]}, \quad (3.2)$$

where $R = Na$, $\tan \delta = 4VW/(4W^2 + V^2)$, and $v_F = 2aW$ with a being the lattice constant. From the Landauer formula [29], the conductance at temperature T is given by

$$G = \frac{e^2}{2\pi} \int T_V(\varepsilon_0 - E) \left(-\frac{df(E)}{dE}\right), \quad (3.3)$$

where $f(E)$ is the Fermi distribution function. Substituting Eq. (3.2) into Eq. (3.3), we get the conductance for $V \ll W$ as

$$\begin{aligned} \frac{G}{e^2/2\pi} &= \int dE \frac{\beta}{4 \cosh^2 \frac{\beta E}{2}} \left\{ 1 + \frac{V^2}{8W^2} \left(4 + \frac{V^2}{W^2}\right) \left[1 + \cos\left(2k_F R + \frac{2R}{v_F}(\varepsilon_0 - E)\right)\right] \right\}^{-1} \\ &= 1 - \frac{V^2}{2W^2} \left(1 + \cos \varphi_0 \frac{2\pi RT}{v_F \sinh \frac{2\pi RT}{v_F}}\right) \\ &\quad + \frac{V^4}{8W^4} \left(2 + 3 \cos \varphi_0 \frac{2\pi RT}{v_F \sinh \frac{2\pi RT}{v_F}} + \cos 2\varphi_0 \frac{4\pi RT}{v_F \sinh \frac{4\pi RT}{v_F}}\right) + O((V/W)^6), \end{aligned} \quad (3.4)$$

where $\varphi_0 \equiv 2k_F R + (2R\varepsilon_0/v_F)$. At low temperatures ($T \ll v_F/R$), this reduces to

$$\begin{aligned} \frac{G}{e^2/2\pi} &= 1 - \frac{V^2}{2W^2} \left\{ 1 + \cos \varphi_0 \left[1 - \frac{2}{3} \left(\frac{\pi RT}{v_F}\right)^2 + \dots\right] \right\} \\ &\quad + \frac{V^4}{8W^4} \left\{ 2 + 3 \cos \varphi_0 \left[1 - \frac{2}{3} \left(\frac{\pi RT}{v_F}\right)^2 + \dots\right] + \cos 2\varphi_0 \left[1 - \frac{8}{3} \left(\frac{\pi RT}{v_F}\right)^2 + \dots\right] \right\}. \end{aligned} \quad (3.5)$$

At high temperatures ($T \gg v_F/R$), on the other hand, it becomes

$$\frac{G}{e^2/2\pi} = 1 - \frac{V^2}{2W^2} \left(1 + \frac{\pi RT}{v_F} e^{-2\pi RT/v_F} \cos \varphi_0\right)$$

$$+ \frac{V^4}{8W^4} \left(2 + \frac{3\pi RT}{v_F} e^{-2\pi RT/v_F} \cos \varphi_0 + \frac{2\pi RT}{v_F} e^{-4\pi RT/v_F} \cos 2\varphi_0 \right). \quad (3.6)$$

In Sec. 3.3.2 we will see that a similar expansion of G is possible for Luttinger liquids.

The above model describes how the transport is disturbed by two weak potential barriers. Next we consider another model in which there are two weak links but no potential barriers (Fig. 3.1(b)); the Hamiltonian is given by

$$H_t = -W \sum_{n \neq 0, N} (c_{n+1}^\dagger c_n + c_n^\dagger c_{n+1}) - t (c_1^\dagger c_0 + c_0^\dagger c_1 + c_{N+1}^\dagger c_N + c_N^\dagger c_{N+1}) - \varepsilon_0 \sum_{n=1}^{N-1} c_n^\dagger c_n. \quad (3.7)$$

We assume that t is much smaller than W ($0 < t \ll W$). Of course, in the limit $V \gg W$, the on-site-barrier model discussed above is essentially equivalent to this weak-link model. After some calculations we find that the transmission probability is approximately given by

$$T_t = \frac{8t^4}{W^4} \frac{1}{1 - \cos(2k_F R + \frac{2R\varepsilon_0}{v_F}) + 2\frac{t^4}{W^4} [3 + \cos(2k_F R + \frac{2R\varepsilon_0}{v_F})]}. \quad (3.8)$$

Since $t/W \ll 1$, T_t is much smaller than unity except on resonance. Thus we expand the denominator in Eq. (3.8) around the resonance point ($\varepsilon \equiv \varepsilon_0 + k_F v_F = 0$). Expanding the cosine as $\cos(2k_F R + \frac{2R\varepsilon_0}{v_F}) \approx 1 - 2(R\varepsilon/v_F)^2$, we get

$$T_t = \frac{\Gamma_0^2}{\varepsilon^2 + \Gamma_0^2}, \quad (3.9)$$

where

$$\Gamma_0 \equiv 2 \frac{v_F}{R} \frac{t^2}{W^2}. \quad (3.10)$$

This quantity can be interpreted as an escape rate out of a resonance level formed in between the two weak links. With the transmission probability, $T_{\text{single}} = (2t/W)^2$, through a single weak link, Γ_0 is rewritten as νT_{single} where $\nu = v_F/2R$ is an attempt frequency [40]. Note that Γ_0 is a T -independent quantity; it will be shown in Sec. 3.4.2 that in Luttinger liquids the escape rate is renormalized to be dependent on T . From the Landauer formula we obtain the conductance at temperature T as

$$G = \frac{e^2}{2\pi} \int dE \frac{\Gamma_0^2}{\varepsilon^2 + \Gamma_0^2} \left(-\frac{df(E)}{dE} \right). \quad (3.11)$$

In Sec. 3.4.2, we will encounter an expression similar to Eq. (3.11) for the conductance of the resonant tunneling in Luttinger liquids. Note that just on resonance the conductance at $T = 0$ K becomes $e^2/2\pi$ for any V_0 and t . This is a peculiar feature of the resonant tunneling through the symmetric double-barrier structure. In the following sections, we will see that this feature is related to the fact that on resonance the barrier potential is irrelevant for the noninteracting system.

The above discussion is concerned with symmetric barriers only. It is easy to generalize Eq. (3.11) for the case where the hopping matrix elements at the weak links are different: $t_L \neq t_R$. In this case the conductance is given by

$$G = \frac{e^2}{2\pi} \int dE \frac{\Gamma_L \Gamma_R}{\varepsilon_0^2 + \frac{1}{4}(\Gamma_L + \Gamma_R)^2} \left(-\frac{df(E)}{dE} \right), \quad (3.12)$$

where $\Gamma_{L(R)} = 2(v_F/R)(t_{L(R)}/W)^2$. Thus the conductance is less than $e^2/2\pi$ at $T = 0$ K even on resonance.

3.2 Effective action

As a model for an interacting spinless fermion system, we analyze the spinless Tomonaga-Luttinger model with two barriers at $x = -R/2$ and $R/2$. Using the bosonization method explained in Sec. 1.2, we write the partition function at temperature $T = 1/\beta$ as

$$Z = \int \mathcal{D}\theta \exp \left(-\frac{1}{8\pi\eta} \int_0^\beta d\tau \int dx \left[\frac{1}{v} (\partial_\tau \theta(x, \tau))^2 + v (\partial_x \theta(x, \tau))^2 \right] + \frac{1}{\pi\alpha} \int_0^\beta d\tau \left\{ V_L \cos[\theta(-R/2, \tau) - k_F R] + V_R \cos[\theta(R/2, \tau) + k_F R] \right\} \right),$$

where α is a cutoff of the order of the lattice constant. v and η are defined by Eqs. (1.33) and (1.38). To avoid ultraviolet divergences, we also introduce a high-frequency cutoff, $\Lambda \sim v/\alpha$, which is of the order of the band width. We assume that the barrier structure is symmetric: $|V_L| = |V_R| = V_0$. Without loss of generality we can take $V_L = V_R = V_0$. The effect of asymmetry will be briefly discussed later.

The effective action for $\theta(R/2)$ and $\theta(-R/2)$ is obtained by integrating out the phase field $\theta(x)$ except $\theta(R/2)$ and $\theta(-R/2)$. The method is essentially the same as what is used in Sec. 2.2. We first introduce auxiliary fields, $\lambda_1(\tau)$ and $\lambda_2(\tau)$ to ensure that $\theta_1(\tau) = \theta(-R/2, \tau)$ and $\theta_2(\tau) = \theta(R/2, \tau)$, and then integrate out $\theta(x)$:

$$\begin{aligned} Z &= \int \mathcal{D}\theta \int \mathcal{D}\theta_1 \int \mathcal{D}\theta_2 \int \mathcal{D}\lambda_1 \int \mathcal{D}\lambda_2 \\ &\quad \times \exp \left(-\frac{1}{8\pi\eta} \int_0^\beta d\tau \int dx \left[\frac{1}{v} (\partial_\tau \theta)^2 + v (\partial_x \theta)^2 \right] \right. \\ &\quad \left. + i \int_0^\beta d\tau \lambda_1 [\theta_1 - \theta(-R/2)] + i \int_0^\beta d\tau \lambda_2 [\theta_2 - \theta(R/2)] \right. \\ &\quad \left. + \frac{V_0}{\pi\alpha} \int_0^\beta d\tau [\cos(\theta_1 - k_F R) + \cos(\theta_2 + k_F R)] \right) \\ &\propto \int \mathcal{D}\theta_1 \int \mathcal{D}\theta_2 \int \mathcal{D}\lambda_1 \int \mathcal{D}\lambda_2 \\ &\quad \times \exp \left(-\frac{2\eta v}{\beta} \sum_{\omega_n} |\bar{\lambda}(\omega_n)|^2 \int dk \frac{\cos^2(kR/2)}{\omega_n^2 + v^2 k^2} + \frac{2i}{\beta} \sum_{\omega_n} \bar{\lambda}(-\omega_n) \bar{\theta}(\omega_n) \right. \\ &\quad \left. - \frac{\eta v}{2\beta} \sum_{\omega_n} |\bar{\lambda}(\omega_n)|^2 \int dk \frac{\sin^2(kR/2)}{\omega_n^2 + v^2 k^2} + \frac{i}{2\beta} \sum_{\omega_n} \bar{\lambda}(-\omega_n) \bar{\theta}(\omega_n) \right. \\ &\quad \left. + \frac{2V_0}{\pi\alpha} \int_0^\beta d\tau \cos \bar{\theta}(\tau) \cos \left[\frac{1}{2} \bar{\theta}(\tau) + k_F R \right] \right), \end{aligned}$$

where

$$\begin{aligned} \bar{\theta} &= \frac{1}{2}(\theta_1 + \theta_2), & \hat{\theta} &= \theta_2 - \theta_1, \\ \bar{\lambda} &= \frac{1}{2}(\lambda_1 + \lambda_2), & \bar{\lambda} &= \lambda_2 - \lambda_1. \end{aligned}$$

Integrating out $\bar{\lambda}$ and $\bar{\lambda}$, we finally get the effective action for $\bar{\theta}$ and $\hat{\theta}$ as

$$S_{\text{eff}} = \frac{1}{2\pi\eta\beta} \sum_{\omega_n} \frac{|\omega_n|}{1 + \exp(-|\omega_n|/\Delta\epsilon)} |\bar{\theta}(\omega_n)|^2 + \frac{1}{8\pi\eta\beta} \sum_{\omega_n} \frac{|\omega_n|}{1 - \exp(-|\omega_n|/\Delta\epsilon)} |\hat{\theta}(\omega_n)|^2$$

$$\begin{aligned}
& + \frac{U}{(2\pi)^2} \int_0^\beta d\tau (\tilde{\theta}(\tau))^2 - \frac{eV}{2\pi} \int_0^\beta d\tau \tilde{\theta}(\tau) - \frac{eV_g}{2\pi} \int_0^\beta d\tau \tilde{\theta}(\tau) \\
& - \frac{2V_0}{\pi\alpha} \int_0^\beta d\tau \cos \tilde{\theta}(\tau) \cos \left[\frac{1}{2} \tilde{\theta}(\tau) + k_F R \right], \quad (3.13)
\end{aligned}$$

where $\Delta\epsilon = v/R$. The average phase $\bar{\theta}$ is related to the current J through the two barriers by $J = -(e/2\pi)(d\bar{\theta}/dt)$, while the phase difference $\hat{\theta}$ is related to the excess charge Q accumulated in the confined region between two barriers by $Q = -e\hat{\theta}/2\pi$. Therefore, whether electrons can tunnel through the barriers is directly related to whether $\bar{\theta}$ is pinned or not pinned by the pinning potential, $(2V_0/\pi\alpha) \cos \bar{\theta} \cos[\frac{1}{2}\hat{\theta} + k_F R]$.

In order to take account of the long-range part of the Coulomb interaction which is not fully incorporated in the bosonization method, we have introduced in Eq. (3.13) the charging energy $Q^2/2C = U (\hat{\theta}/2\pi)^2$ where C is the capacitance; the repulsive energy $U = e^2/2C$ is assumed to be larger than $\Delta\epsilon$.

We have also included in Eq. (3.13) the energy coming from difference of the chemical potential across the barriers:

$$-\frac{1}{2\pi} \left[\int_{-\infty}^{-R/2} \mu_L \partial_x \theta dx + \int_{-R/2}^{R/2} \mu_I \partial_x \theta dx + \int_{R/2}^{\infty} \mu_R \partial_x \theta dx \right] = -\frac{1}{2\pi} e(V\bar{\theta} + V_g \hat{\theta}), \quad (3.14)$$

where μ_I stands for an average of the electrostatic energy in between two barriers, $V = (\mu_R - \mu_L)/e$ is the voltage difference between the right- and left-hand sides of the barrier region, and the gate voltage $V_g = [\mu_I - \frac{1}{2}(\mu_R + \mu_L)]/e$. By varying V_g we can tune the average value of the massive field $\bar{\theta}$ and the excess charge Q . The resonance is achieved by controlling V_g . As is evident from Eq. (3.14), we have assumed that the chemical potential, μ_L and μ_R , and the electrostatic energy, μ_I , are constant in each of three regions ($x < -\frac{R}{2}$, $-\frac{R}{2} < x < \frac{R}{2}$, and $x > \frac{R}{2}$). Strictly speaking, this assumption is not correct and should be considered as an approximation. In principle, the chemical potential can be defined only for the reservoirs connected to the left and right leads, and the electric field in the leads must be determined self-consistently. However, this approach is not easy to carry out. We have thus adopted the above-mentioned approximation, which will be shown to reproduce correct linear conductance for the noninteracting case [compare Eqs. (A.8), (A.9), and (3.45) with Eqs. (3.5), (3.6), and (3.11)].

As can be easily seen in Eq. (3.13), the charge fluctuation $\hat{\theta}$ in the confined region has a mass gap, $\frac{1}{8\pi^2}(U + \frac{\pi}{\eta}\Delta\epsilon)$, while the average phase $\bar{\theta}$ remains massless and suffers the dissipation [22, 23] whose strength crosses over from $1/2\pi\eta$ for $|\omega_n| \gg \Delta\epsilon$ to $1/4\pi\eta$ for $|\omega_n| \ll \Delta\epsilon$. This decrease in the dissipation as the temperature is lowered across $\Delta\epsilon$ results in the nonmonotonic temperature dependence of the peak height of the conductance resonances as described below.

3.3 Weak barrier potential

We first examine the weak potential limit $V_0 \ll \alpha\Lambda$, where a naive picture holds that electron propagation is slightly disturbed by barrier potentials.

3.3.1 Scaling equations

In this section we derive scaling equations perturbatively in powers of V_0 . The results given below are essentially the same as those obtained by Kane and Fisher [19].

Since the $\tilde{\theta}$ field has the mass gap, we can safely integrate it out perturbatively in powers of V_0 to get the cumulant expansion of the barrier potential:

$$\begin{aligned}
& \left\langle \left\langle \frac{2V_0}{\pi\alpha} \int_0^\beta d\tau \cos \tilde{\theta}(\tau) \cos \left[\frac{1}{2} \tilde{\theta}(\tau) + k_F R \right] \right\rangle \right\rangle \\
& \equiv \ln \left\langle \exp \left(\frac{2V_0}{\pi\alpha} \int_0^\beta d\tau \cos \tilde{\theta}(\tau) \cos \left[\frac{1}{2} \tilde{\theta}(\tau) + k_F R \right] \right) \right\rangle_{\tilde{\theta}} \\
& = \frac{2V_0}{\pi\alpha} \int_0^\beta d\tau \cos \tilde{\theta}(\tau) \left\langle \cos \left[\frac{1}{2} \tilde{\theta}(\tau) + k_F R \right] \right\rangle_{\tilde{\theta}} \\
& \quad + \frac{1}{2} \left(\frac{2V_0}{\pi\alpha} \right)^2 \int_0^\beta d\tau_1 \int_0^\beta d\tau_2 \cos \tilde{\theta}(\tau_1) \cos \tilde{\theta}(\tau_2) \left\{ \left\langle \cos \left[\frac{1}{2} \tilde{\theta}(\tau_1) + k_F R \right] \cos \left[\frac{1}{2} \tilde{\theta}(\tau_2) + k_F R \right] \right\rangle_{\tilde{\theta}} \right. \\
& \quad \left. - \left\langle \cos \left[\frac{1}{2} \tilde{\theta}(\tau_1) + k_F R \right] \right\rangle_{\tilde{\theta}} \left\langle \cos \left[\frac{1}{2} \tilde{\theta}(\tau_2) + k_F R \right] \right\rangle_{\tilde{\theta}} \right\} \\
& \quad + \dots, \tag{3.15}
\end{aligned}$$

where $\langle A \rangle_{\tilde{\theta}}$ represents the thermal average of A with respect to $\tilde{\theta}$. It is easy to show that

$$\left\langle \cos \left[\frac{1}{2} \tilde{\theta}(\tau) + k_F R \right] \right\rangle_{\tilde{\theta}} = \exp[-\gamma(0)] \cos \frac{\varphi}{2} \tag{3.16}$$

$$\begin{aligned}
& \left\langle \cos \left[\frac{1}{2} \tilde{\theta}(\tau_1) + k_F R \right] \cos \left[\frac{1}{2} \tilde{\theta}(\tau_2) + k_F R \right] \right\rangle_{\tilde{\theta}} - \left\langle \cos \left[\frac{1}{2} \tilde{\theta}(\tau_1) + k_F R \right] \right\rangle_{\tilde{\theta}} \left\langle \cos \left[\frac{1}{2} \tilde{\theta}(\tau_2) + k_F R \right] \right\rangle_{\tilde{\theta}} \\
& = \frac{1}{2} e^{-2\gamma(0)+2\gamma(\tau_1-\tau_2)} + \frac{1}{2} e^{-2\gamma(0)-2\gamma(\tau_1-\tau_2)} \cos \varphi - e^{-2\gamma(0)} \cos^2 \frac{\varphi}{2}, \tag{3.17}
\end{aligned}$$

where

$$\varphi = \frac{2\pi e V_g}{\pi \Delta \epsilon + 2U} + 2k_F R, \tag{3.18}$$

$$\gamma(\tau) = \frac{\pi^2}{4\beta} \sum_{\omega_n} \cos \omega_n \tau \left(U + \frac{\pi}{2\eta} \frac{|\omega_n|}{1 - \exp(-|\omega_n|/\Delta \epsilon)} \right)^{-1}. \tag{3.19}$$

Since the right-hand side of Eq. (3.17) is a short-ranged function of $|\tau_1 - \tau_2|$, we may approximate Eq. (3.15) as

$$\begin{aligned}
& \left\langle \left\langle \frac{2V_0}{\pi\alpha} \int_0^\beta d\tau \cos \tilde{\theta}(\tau) \cos \left[\frac{1}{2} \tilde{\theta}(\tau) + k_F R \right] \right\rangle \right\rangle \\
& \approx \frac{2V_0}{\pi\alpha} e^{-\gamma(0)} \cos \frac{\varphi}{2} \int_0^\beta d\tau \cos \tilde{\theta}(\tau) \\
& \quad + \tau_0 \left(\frac{V_0}{\pi\alpha} \right)^2 (1 - e^{-2\gamma(0)}) (1 - e^{-2\gamma(0)} \cos \varphi) \int_0^\beta d\tau \cos^2 \tilde{\theta}(\tau) + \dots,
\end{aligned}$$

where τ_0 is a constant of order $(U + \frac{\pi}{2\eta} \Delta \epsilon)^{-1}$. Thus the zero-temperature effective action for $\tilde{\theta}$ may be written approximately as

$$\begin{aligned}
\tilde{S}_{\text{eff}} = & \frac{1}{4\pi^2 \eta} \int_{-\Lambda}^{\Lambda} d\omega \frac{|\omega|}{1 + \exp(-|\omega|/\Delta \epsilon)} |\tilde{\theta}(\omega)|^2 - \frac{eV}{2\pi} \int_0^\infty d\tau \tilde{\theta}(\tau) \\
& - \sum_{n=1}^{\infty} \frac{V_n}{\pi\alpha} \int_0^\infty d\tau \cos n\tilde{\theta}(\tau). \tag{3.20}
\end{aligned}$$

Now we perform the RG transformation of Eq. (3.20). For $\Delta \epsilon \ll |\omega| \ll \Lambda$, $\exp(-|\omega|/\Delta \epsilon)$ of the first term may be neglected. Then Eq. (3.20) becomes mathematically the same as the

effective action discussed in Chap. 2; the model is equivalent to the quantum mechanics of a particle moving in the cosine potential with dissipation. Repeating the same RG calculations, we can easily obtain the lowest-order scaling equations for the pinning potentials, V_1 , V_2 , ..., as

$$\begin{aligned}\frac{dV_1}{dl} &= \left(1 - \frac{1}{2}\eta\right)V_1, \\ \frac{dV_2}{dl} &= (1 - 2\eta)V_2, \\ \frac{dV_n}{dl} &= \left(1 - \frac{n^2}{2}\eta\right)V_n.\end{aligned}\quad (3.21)$$

For $|\omega| \ll \Delta\epsilon$, on the other hand, $\exp(-|\omega/\Delta\epsilon|)$ may be replaced by unity. Also in this case we can perform a similar RG calculation to obtain the scaling equations:

$$\begin{aligned}\frac{dV_1}{dl} &= (1 - \eta)V_1, \\ \frac{dV_2}{dl} &= (1 - 4\eta)V_2, \\ \frac{dV_n}{dl} &= (1 - n^2\eta)V_n.\end{aligned}\quad (3.22)$$

We see from these scaling equations that V_n is relevant if $\eta < 1/n^2$ ($\eta < 2/n^2$) for $|\omega| \ll \Delta\epsilon$ ($|\omega| \gg \Delta\epsilon$). Since V_1 is proportional to $\cos(\varphi/2)$, it vanishes when $\varphi = 2\pi(2m+1)$ (m : integer). Furthermore it is easily shown that all the odd-order cumulants, V_{2m+1} 's, also vanish for $\varphi = 2\pi(2m+1)$. The vanishing of V_1 exactly corresponds to the resonance. However, even on resonance V_2 does not vanish. Therefore on resonance V_2 is the most relevant perturbation whereas away from resonance V_1 is the most relevant one. Summarizing these arguments, we find that for $|\omega| \ll \Delta\epsilon$ the pinning potential is relevant when $\eta < 1$ (1/4) off (on) resonance. That is, at low temperatures ($T \ll \Delta\epsilon$), electrons cannot tunnel through the barriers if $\eta < 1$ ($\eta < 1/4$) away from (just on) resonance.

3.3.2 Conductance

Now we calculate the conductance G in powers of V_0 as a function of the temperature T and the gate voltage V_g .

According to the linear-response theory, the conductance is related to the current-current correlation function. Since the current is in turn related to $\bar{\theta}$ by $J = -(e/2\pi)(d\bar{\theta}/dt)$, the conductance can be obtained from the correlation function of $\bar{\theta}$:

$$G = -\frac{i}{\beta} \left(\frac{e}{2\pi}\right)^2 \lim_{\omega \rightarrow +0} \omega Q^R(\omega), \quad (3.23)$$

where the retarded correlation function $Q^R(\omega)$ is defined by

$$\begin{aligned}Q^R(\omega) &\equiv Q(\omega_n) \Big|_{i\omega_n \rightarrow \omega + i0^+}, \\ Q(\omega_n) &\equiv \langle \bar{\theta}(\omega_n) \bar{\theta}(-\omega_n) \rangle = \frac{\int \mathcal{D}\bar{\theta} \int \mathcal{D}\hat{\theta} \bar{\theta}(\omega_n) \bar{\theta}(-\omega_n) \exp(-S_{\text{eff}})}{\int \mathcal{D}\bar{\theta} \int \mathcal{D}\hat{\theta} \exp(-S_{\text{eff}})}.\end{aligned}$$

By using the relation

$$\begin{aligned} & \exp\left(\frac{2V_0}{\pi\alpha} \int_0^\beta d\tau \cos\bar{\theta}(\tau) \cos\left(\frac{1}{2}\bar{\theta}(\tau) + k_F R\right)\right) \\ &= \sum_{m=0}^{\infty} \sum_{\{e_j\}} \sum_{\{s_j\}} \frac{1}{m!} \left(\frac{V_0}{2\pi\alpha}\right)^m \int_0^\beta d\tau_1 \cdots \int_0^\beta d\tau_m \exp\left(\frac{i}{\beta} \sum_{\omega_n} \sum_{j=1}^m e^{-i\omega_n \tau_j} \left[e_j \bar{\theta}(\omega_n) + \frac{s_j}{2} \bar{\theta}(\omega_n)\right] + ik_F R \sum_{j=1}^m s_j\right), \end{aligned}$$

the two-point correlation function $Q(\omega_n)$ is calculated as

$$\begin{aligned} Q(\omega_n) &= \frac{\pi\eta\beta}{|\omega'_n|} (1 + e^{-|\omega_n|/\Delta\epsilon}) \\ &\quad - \frac{\pi^2\eta^2}{\omega_n^2} (1 + e^{-|\omega_n|/\Delta\epsilon})^2 \sum_{m=1}^{\infty} \sum_{\{e_j\}} \sum_{\{s_j\}} \frac{1}{(2m)!} \left(\frac{V_0}{2\pi\alpha}\right)^{2m} \int_0^\beta d\tau_1 \cdots \int_0^\beta d\tau_{2m} \\ &\quad \times \sum_{j=1}^{2m} \sum_{k=1}^{2m} e_j e_k e^{i\omega_n(\tau_j - \tau_k)} Z_{2m}(\{e_j\}, \{s_j\}) \\ &\quad \times \left\{ 1 + \sum_{m=1}^{\infty} \sum_{\{e_j\}} \sum_{\{s_j\}} \frac{1}{(2m)!} \left(\frac{V_0}{2\pi\alpha}\right)^{2m} \int_0^\beta d\tau_1 \cdots \int_0^\beta d\tau_{2m} Z_{2m}(\{e_j\}, \{s_j\}) \right\}^{-1}, \end{aligned} \quad (3.24)$$

where $e_j = \pm 1$, $s_k = \pm 1$. The summation over possible configurations of e_j 's, $\sum_{\{e_j\}}$, is performed under the neutrality condition, $\sum_j e_j = 0$. As for $\sum_{\{s_k\}}$, there is no such restriction because $\bar{\theta}$ has a mass gap. The function Z_{2m} in Eq. (3.24) is given by

$$\begin{aligned} Z_{2m}(\{e_j\}, \{s_j\}) &= \exp\left(-\frac{\pi\eta}{2\beta} \sum_{\omega'_n} \frac{1 + e^{-|\omega'_n|/\Delta\epsilon}}{|\omega'_n|} \sum_{j=1}^{2m} \sum_{k=1}^{2m} e_j e_k e^{i\omega'_n(\tau_j - \tau_k)} + \frac{i\varphi}{2} \sum_{j=1}^{2m} s_j\right) \\ &\quad - \frac{\pi\eta}{2\beta} \sum_{\omega'_n} \left(\frac{|\omega'_n|}{1 - e^{-|\omega'_n|/\Delta\epsilon}} + \frac{2\eta U}{\pi}\right)^{-1} \sum_{j=1}^{2m} \sum_{k=1}^{2m} s_j s_k e^{i\omega'_n(\tau_j - \tau_k)}. \end{aligned}$$

From Eqs. (3.23) and (3.24) we see that $Q(\omega_n)$ and thus G are expanded in even powers of V_0 as $Q(\omega_n) = Q_0(\omega_n) + Q_2(\omega_n) + \dots$ and $G = G_0 + G_2 + \dots$, where $Q_{2n}(\omega_n)$ and G_{2n} are proportional to V_0^{2n} . The 0th order term of G is given by $G_0 = \epsilon^2\eta/2\pi$. The calculation of the higher-order terms is straightforward but so complicated that here we give only the results (see for details Appendix A.3):

$$\begin{aligned} G &= \frac{\epsilon^2\eta}{2\pi} - a_1\epsilon^2 \left(\frac{V_0}{\alpha\Lambda}\right)^2 \left(\frac{2\eta U}{\Delta\epsilon}\right)^\eta \left(\frac{\pi T}{\Lambda}\right)^{2\eta-2} (1 + \cos\varphi) \\ &\quad - b_1\epsilon^2 \left(\frac{V_0}{\alpha\Lambda}\right)^4 \left(\frac{\Lambda}{U}\right)^2 \left(\frac{\pi T}{\Lambda}\right)^{4\eta-2} \left(\frac{\pi T}{\Delta\epsilon}\right)^{4\eta} \left[1 + \left(\frac{2\eta U}{\pi\Lambda}\right)^{2\eta} \cos\varphi\right]^2 + \dots \end{aligned} \quad (3.25)$$

for $T \ll \Delta\epsilon \ll U$ and

$$\begin{aligned} G &= \frac{\epsilon^2\eta}{2\pi} - a_2\epsilon^2 \left(\frac{V_0}{\alpha\Lambda}\right)^2 \left(\frac{2\eta U}{\pi\Lambda}\right)^\eta \left(\frac{\pi T}{\Lambda}\right)^{\eta-2} (1 + \cos\varphi) \\ &\quad - b_2\epsilon^2 \left(\frac{V_0}{\alpha\Lambda}\right)^4 \left(\frac{\Lambda}{U}\right)^2 \left(\frac{\pi T}{\Lambda}\right)^{4\eta-2} \left[1 + \left(\frac{2\eta U}{\pi\Lambda}\right)^{2\eta} \cos\varphi\right]^2 + \dots \end{aligned} \quad (3.26)$$

for $\Delta\epsilon \ll T \ll U$, where a_i and b_i are dimensionless numbers of order 1. We note that these expressions contain only the most important contributions in each order of V_0 . For example,

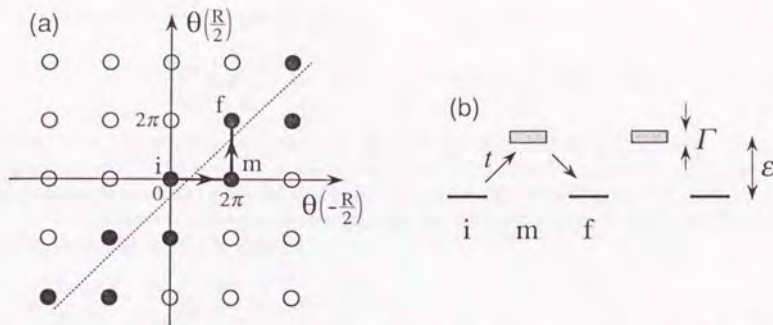


Figure 3.2: (a) Illustration of possible configurations of the phase fields for $T \ll U$; the dashed line is $\hat{\theta} = 2\pi e V_g / (\frac{\pi}{\eta} \Delta \epsilon + 2U)$. (b) Schematic of the tight-binding model.

we have not written terms proportional to $V_0^2 T^{2\eta} \times T^2$ in Eq. (3.25), which may dominate the 4th-order term proportional to $V_0^4 T^{4\eta-2}$; however, such terms are harmless since 2η is positive, and thus we may neglect them.

Just on resonance the second terms in Eqs. (3.25) and (3.26) vanish ($\cos \varphi = -1$). Since at low temperatures $G - \frac{e^2 \eta}{2\pi}$ is proportional to $T^{2(\eta-1)}$ away from resonance and to $T^{2(4\eta-1)}$ on resonance, the expansion is valid down to $T = 0$ if $\eta > 1$ and $\eta > \frac{1}{4}$, for respective cases. Otherwise, the above expansion is justified only above the temperature \tilde{T} at which the temperature-dependent correction becomes comparable to the first term $e^2 \eta / 2\pi$. Below \tilde{T} the conductance G will scale to zero as $T \rightarrow 0$.

3.4 Strong barrier potential

Next we will consider the strong potential limit $V_0 \gg \alpha \Lambda$. The electron transport in this limit can be viewed as the tunneling between minima of the cosine potential. For simplicity we assume $k_F R \equiv 0 \pmod{2\pi}$ and $-U - \frac{\pi}{2\eta} \Delta \epsilon \leq e V_g \leq 0$. Then the potential minima are $(\hat{\theta}, \hat{\theta}) = (2\pi l, 2\pi m)$ with l and m being integers (Fig. 3.2(a)). Since the $\hat{\theta}$ field has a mass gap, at low temperatures ($T \ll \frac{1}{8\pi^2} (2U + \frac{\pi}{\eta} \Delta \epsilon)$) configurations of the phase fields may be restricted to the filled circles neighboring the dashed line, $\hat{\theta} = 2\pi e V_g / (\frac{\pi}{\eta} \Delta \epsilon + 2U)$, in Fig. 3.2(a). Thus the problem reduces to a 1D tight-binding model with a hopping matrix element t and an off-resonance energy $\epsilon = e V_g + U + \frac{\pi}{2\eta} \Delta \epsilon$ (Fig. 3.2(b)).

3.4.1 Scaling equations and phase diagram

Scaling equations for $|\omega| \ll \Delta \epsilon$ have been derived by Kane and Fisher [19]. Generalizing their arguments, we derive scaling equations for $|\omega| \gg \Delta \epsilon$ as well as for $|\omega| \ll \Delta \epsilon$. In the following we assume $k_B T \ll \Delta \epsilon$.

In the limit where the barrier potential is very strong, the path integral can be evaluated within the dilute-instanton-gas approximation as in Sec. 2.4.1. We neglect width of

instantons and write $\bar{\theta}(\tau)$ and $\hat{\theta}(\tau)$ as

$$\bar{\theta}(\tau) = \pi \sum_{j=1}^{2n} e_j \Theta(\tau - \tau_j), \quad \hat{\theta}(\tau) = 2\pi \sum_{j=1}^{2n} s_j \Theta(\tau - \tau_j), \quad (3.27)$$

where $2n$ is the number of instantons, $\Theta(x)$ is the step function, τ_j 's specify location of instantons ($0 \leq \tau_1 < \tau_2 < \dots < \tau_{2n} \leq \beta$), $e_j = 1$ or -1 , and $s_j = (-1)^j$. $\sum_{\{e_j\}}$ represents summation over all the possible configurations under the neutrality condition $\sum_j e_j = 0$.

In the dilute-instanton-gas approximation, the partition function is expanded in powers of the tunneling matrix element t :

$$\begin{aligned} Z = & \sum_{n=0}^{\infty} \sum_{\{e_j\}} t^{2n} \int_0^{\beta} d\tau_{2n} \int_0^{\tau_{2n}} d\tau_{2n-1} \dots \int_0^{\tau_2} d\tau_1 \\ & \times \exp \left(-\frac{\pi}{2\eta\beta} \sum_{\omega_n} \sum_{j,k=1}^{2n} e_j e_k \frac{e^{i\omega_n(\tau_j - \tau_k)}}{|\omega_n| [1 + \exp(-|\omega_n|/\Delta\epsilon)]} \right. \\ & \left. - \frac{\pi}{2\eta\beta} \sum_{\omega_n} \sum_{j,k=1}^{2n} s_j s_k \frac{e^{i\omega_n(\tau_j - \tau_k)}}{|\omega_n| [1 - \exp(-|\omega_n|/\Delta\epsilon)]} - (U + \epsilon V_g) \sum_{j=1}^{2n} s_j \tau_j \right). \end{aligned} \quad (3.28)$$

Since the propagators for $\bar{\theta}$ and $\hat{\theta}$ may be approximated as

$$\begin{aligned} \frac{|\omega_n|}{1 - \exp(-|\omega_n|/\Delta\epsilon)} & \approx \begin{cases} \Delta\epsilon + \frac{1}{2}|\omega_n|, & |\omega_n| \ll \Delta\epsilon \\ |\omega_n|, & |\omega_n| \gg \Delta\epsilon, \end{cases} \\ \frac{|\omega_n|}{1 + \exp(-|\omega_n|/\Delta\epsilon)} & \approx \begin{cases} \frac{1}{2}|\omega_n|, & |\omega_n| \ll \Delta\epsilon \\ |\omega_n|, & |\omega_n| \gg \Delta\epsilon, \end{cases} \end{aligned}$$

we can write the partition function (3.28) as

$$Z = \sum_n \sum_{\{e_j\}} t^{2n} \int_0^{\beta} d\tau_{2n} \int_0^{\tau_{2n}} d\tau_{2n-1} \dots \int_0^{\tau_2} d\tau_1 \exp \left(\frac{1}{2\eta} \sum_{j < k} (e_j e_k + s_j s_k) f(\tau_j - \tau_k; \tau_c) - \epsilon \sum_j s_j \tau_j \right), \quad (3.29)$$

where τ_c is a short-distance cutoff ($\tau_c = 1/\Lambda$) and

$$f(\tau; \tau_c) = \begin{cases} \ln(|\tau|/\tau_c^2 \Delta\epsilon), & |\tau| \gg \frac{1}{\Delta\epsilon} \\ 2 \ln(|\tau|/\tau_c), & \tau_c \ll |\tau| \ll \frac{1}{\Delta\epsilon}. \end{cases} \quad (3.30)$$

The distance between instantons, $\tau_{j+1} - \tau_j$, is always assumed to be larger than τ_c .

In this way the partition function of the double-barrier model is mapped to a classical 1D Coulomb gas model. In this Coulomb gas model, particles (instantons) have two kinds of charge, e_j and s_j , and the strength of the Coulomb interaction depends on distance between two particles (Eq. (3.30)). To derive scaling equations, we apply the real-space renormalization-group method of Anderson, Yuval, and Hamann [41].

It is obvious that ϵ is a relevant perturbation. When $\beta\epsilon \gg 1$, two particles at $\tau = \tau_{2j-1}$ and τ_{2j} are bound with each other because of the exponential factor, $\exp(-\epsilon \sum_j (-1)^j \tau_j)$. These closely bound particles can be regarded as a single object. Neglecting every pair of

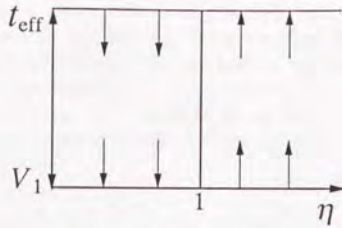


Figure 3.3: Off-resonance flow diagram. This diagram is equivalent to that of the tunneling of spinless fermions through a *single* barrier.

particles whose charges have different sign, i.e., $e_{2j-1} = -e_{2j}$, we can write the partition function as

$$Z = \sum_n \sum_{\{\tilde{e}_j\}} \left(\frac{t^2}{\varepsilon}\right)^{2n} \exp\left(\frac{2}{\eta} \sum_{j>k} \tilde{e}_j \tilde{e}_k f(\tau_j - \tau_k; \tau_c)\right), \quad (3.31)$$

where $\tilde{e}_j = \frac{1}{2}(e_{2j-1} + e_{2j}) = \pm 1$ and $\sum_j \tilde{e}_j = 0$. Equation (3.31) is equal to the partition function of the single-barrier model discussed in Chap. 2 with an effective tunneling matrix element $t_{\text{eff}} = t^2/\varepsilon$, which describes tunneling through two barriers via a virtual state. Thus, the scaling equation for t_{eff} is readily obtained as

$$\frac{dt_{\text{eff}}}{dl} = \begin{cases} (1 - \frac{1}{\eta})t_{\text{eff}}, & \mu < \Delta\varepsilon \\ (1 - \frac{2}{\eta})t_{\text{eff}}, & \mu > \Delta\varepsilon, \end{cases} \quad (3.32)$$

where μ is a reduced cutoff and $dl = -d\mu/\mu$. From Eq. (3.32) we see that, away from resonance and at low energy, the tunneling is relevant for $\eta > 1$ but irrelevant for $\eta < 1$. This is consistent with the result obtained in Sec. 3.3.1. Thus we conclude that, when the resonance is not achieved, the tunneling through a double barrier is essentially the same as the tunneling through a single barrier. The RG flows are shown in Fig. 3.3.

We now consider the on-resonance case where we may set $\varepsilon = 0$. Scaling equations can be obtained by integrating out pairs of an instanton and an anti-instanton ($e_j = -e_{j+1}$) separated by a distance between τ_c and $\tau_c + d\tau_c$. In this procedure we may discard closely spaced instanton-instanton pairs ($e_j = e_{j+1}$), since introducing such pairs is energetically unfavorable. Although the renormalization-group method invented by Anderson *et al.* is a standard technique, the derivation of scaling equations is described below for completeness by extending Kane and Fisher's argument [19, 20].

At the starting point of the renormalization τ_c is equal to $1/\Lambda$. Since the probability that two or more successive close pairs appear is very small, we may write the partition function as

$$Z = \sum_n \sum_{\{e_j\}} t^{2n} \int_0^\beta d\tau_{2n} \int_0^{\tau_{2n}} d\tau_{2n-1} \cdots \int_0^{\tau_2} d\tau_1 \exp\left(\frac{1}{2\eta} \sum_{j>k} (e_j e_k + K s_j s_k) f(\tau_j - \tau_k; \tau_c)\right) \\ \times \left\{ 1 + t^2 \sum_{l=1}^{2n-1} \sum_{e'=\pm 1} \int d\tau' \int d\tau'' \exp\left(\frac{1}{2\eta} \sum_{m=1}^{2n} (e_m e' + K s_m s') [f(\tau_m - \tau'; \tau_c) - f(\tau_m - \tau''; \tau_c)]\right) \right\}, \quad (3.33)$$

where $\tau_l < \tau' - \tau_c - d\tau_c < \tau'' < \tau' - \tau_c < \tau' < \tau_{l+1}$ and K is initially equal to 1 but will be renormalized later. In deriving Eq. (3.33) we have used the fact that the pair we will integrate out is composed of an instanton and an anti-instanton (thus $e' = -e''$ and $s' = (-1)^l = -s''$). Since the density of instantons and anti-instantons is thought to be very small, we may assume that $|\tau_m - \tau'|$ is much larger (smaller) than $1/\Delta\epsilon$, then both $|\tau_m - \tau_l|$ and $|\tau_m - \tau_{l+1}|$ are also much larger (smaller) than $1/\Delta\epsilon$. Thus the integration over τ' and τ'' can be calculated as follows:

$$\begin{aligned}
& t^2 \sum_{l=1}^{2n-1} \sum_{e'=\pm 1} \int d\tau' \int d\tau'' \exp\left(\frac{1}{2\eta} \sum_{m=1}^{2n} (\epsilon_m e' + K s_m s') [f(\tau_m - \tau'; \tau_c) - f(\tau_m - \tau''; \tau_c)]\right) \\
&= t^2 \sum_{l=1}^{2n-1} \sum_{e'=\pm 1} \int d\tau' \int d\tau'' \exp\left(\frac{1}{2\eta} \sum_{m=1}^{2n} (\epsilon_m e' + K s_m s') q_m \ln \frac{\tau_m - \tau'}{\tau_m - \tau' + \tau_c}\right) \\
&\approx t^2 \sum_l \sum_{e'=\pm 1} \int d\tau' \int d\tau'' \left[1 - \frac{1}{2\eta} \sum_m q_m (\epsilon_m e' + K s_m s') \frac{\tau_c}{\tau_m - \tau'}\right] \\
&\approx 2t^2 \beta d\tau_c - \frac{4}{\eta} t^2 K \tau_c d\tau_c \sum_{l>m} s_l s_m f(\tau_l - \tau_m; \tau_c), \tag{3.34}
\end{aligned}$$

where q_m is defined by

$$q_m \equiv \begin{cases} 2, & |\tau' - \tau_m| \ll 1/\Delta\epsilon \\ 1, & |\tau' - \tau_m| \gg 1/\Delta\epsilon. \end{cases}$$

Note that there is no term involving $e_l e_m$ due to the summation over e' . From Eqs. (3.33) and (3.34), the renormalized partition function is obtained as

$$\begin{aligned}
Z_{\tau_c + d\tau_c} &= \sum_n \sum_{\{e_j\}} t^{2n} \int d\tau_{2n} \cdots \int d\tau_1 \exp\left(\frac{1}{2\eta} \sum_{j>k} (\epsilon_j e_k + K s_j s_k) f(\tau_j - \tau_k; \tau_c)\right) \\
&\quad \times \left[1 + 2t^2 \beta d\tau_c - \frac{4}{\eta} t^2 K \tau_c d\tau_c \sum_{l>m} s_l s_m f(\tau_l - \tau_m; \tau_c)\right] \\
&\approx e^{2t^2 \beta d\tau_c} \sum_n \sum_{\{e_j\}} t^{2n} \left(\frac{\tau_c + d\tau_c}{\tau_c}\right)^{-\frac{n}{\eta}(1+K)} \\
&\quad \times \int d\tau_{2n} \cdots \int d\tau_1 \exp\left(\frac{1}{2\eta} \sum_{j>k} [\epsilon_j e_k + K s_j s_k (1 - 8t^2 \tau_c d\tau_c)] f(\tau_j - \tau_k; \tau_c + d\tau_c)\right), \tag{3.35}
\end{aligned}$$

where we have used the relation $\sum_{j>k} \epsilon_j e_k = \sum_{j>k} s_j s_k = -n$. This renormalized partition function has the same functional form as the original one. Hence we get scaling equations for dimensionless quantities, $\tilde{t} \equiv t\tau_c$ and K :

$$\frac{d\tilde{t}}{d \ln \tau_c} = \left(1 - \frac{1+K}{2\eta}\right) \tilde{t}, \tag{3.36}$$

$$\frac{dK}{d \ln \tau_c} = -8\tilde{t}^2 K. \tag{3.37}$$

These are the recursion relations for $\tau_c \ll 1/\Delta\epsilon$. The renormalization of K occurs because $\tilde{\theta}$ is restricted to 0 and -2π , i.e., the sign of s_j must alternate. On the other hand, the charge

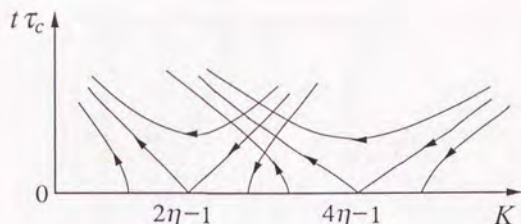


Figure 3.4: On-resonance flow diagram. The RG flows near $K = 2\eta - 1$ are for $\tau_c \ll 1/\Delta\epsilon$, and the flows near $K = 4\eta - 1$ are for $\tau_c \gg 1/\Delta\epsilon$.

e_j corresponding to $\bar{\theta}$ can change freely as long as the neutrality condition is satisfied. This is why e_j 's are not renormalized.

We now turn to the scaling equations for $\tau_c \gg 1/\Delta\epsilon$. The derivation proceeds almost in the same way up to integrating over τ' and τ'' (Eq. (3.34)). However, for $\tau_c \gg 1/\Delta\epsilon$ the function f reads $f(\tau; \tau_c) = \ln(|\tau|/\tau_c)$. Accordingly, in place of Eq. (3.35), the partition function becomes

$$Z_{\tau_c+d\tau_c} = e^{2t^2\beta d\tau_c} \sum_n \sum_{\{e_j\}} t^{2n} \left(\frac{\tau_c + d\tau_c}{\tau_c} \right)^{-\frac{n}{2\eta}(1+K)} \\ \times \int d\tau_{2n} \cdots \int d\tau_1 \exp \left(\frac{1}{2\eta} \sum_{j>k} [e_j e_k + K s_j s_k (1 - 8t^2 \tau_c d\tau_c)] f(\tau_j - \tau_k; \tau_c + d\tau_c) \right).$$

Therefore the scaling equations are obtained as

$$\frac{d\tilde{t}}{d \ln \tau_c} = \left(1 - \frac{1+K}{4\eta} \right) \tilde{t}, \quad (3.38)$$

$$\frac{dK}{d \ln \tau_c} = -8\tilde{t}^2 K. \quad (3.39)$$

The scaling equation for K is unchanged.

The scaling equations (3.36)–(3.39) are integrated to give

$$8\eta\tilde{t}^2 - K + (2\eta - 1) \ln K = \text{const.}$$

for $\tau_c \ll 1/\Delta\epsilon$, and

$$16\eta\tilde{t}^2 - K + (4\eta - 1) \ln K = \text{const.}$$

for $\tau_c \gg 1/\Delta\epsilon$. Hence we arrive at a flow diagram shown in Fig. 3.4. In this figure we draw flows for both $\tau_c \ll 1/\Delta\epsilon$ and for $\tau_c \gg 1/\Delta\epsilon$. These flows should connect smoothly around $\tau_c \approx 1/\Delta\epsilon$, though in Fig. 3.4 the RG flows are drawn as they intersect. At the starting point of the scaling ($\tau_c = 1/\Delta$), \tilde{t} is very small and K equals 1. Under the RG transformation both \tilde{t} and K change along scaling flows. For $\eta > \frac{1}{2}$ it is clear that \tilde{t} grows large, so the resonant tunneling is enhanced at small energy scale. We deduce that this growing RG flows join to the flows in the weak-potential limit discussed in Sec. 3.2.1. Thus at zero temperature spinless fermions will transmit perfectly on resonance regardless of the strength of the tunnel barriers. For $\eta < \frac{1}{2}$, on the other hand, we see that \tilde{t} flows to zero, which is also consistent

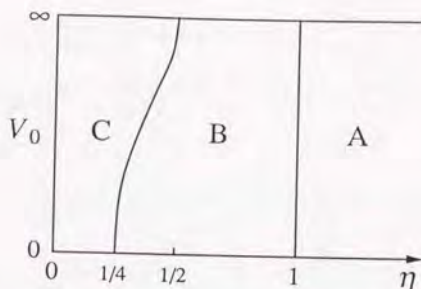


Figure 3.5: Zero-temperature phase diagram for spinless fermions.

with the flows in the weak-barrier limit. Therefore in this case the tunneling is completely blocked at zero temperature. If $\frac{1}{2} < \eta < 1$, then the starting point $K = 1$ lies in between $2\eta - 1$ and $4\eta - 1$, and thus under the RG transformation \tilde{l} first decreases, then turns to increase, and eventually grows very large. From this we conclude that for $\eta > \frac{1}{2}$ \tilde{l} is relevant at low energy scales, and fermions can tunnel through barriers freely.

The above argument assumes that the initial value of \tilde{l} is much smaller than unity. As we increase this initial value, however, a separatrix is crossed above which the RG flows go to large \tilde{l} . This was pointed out by Kane and Fisher [19], who concluded that for $\frac{1}{4} < \eta < \frac{1}{2}$ there is a Kosterlitz-Thouless phase transition between the perfect transmission and the perfect reflection through the double barrier.

Combining the off-resonance (Fig. 3.3) and the on-resonance flow diagram (Fig. 3.4), we arrive at the following schematic phase diagram at $T = 0$ (Fig. 3.5), which was first proposed by Kane and Fisher [19]. There are three phases A, B, and C separated by two lines $\eta = 1$ and $\eta = \eta^*(V_0)$, where $\eta^*(V_0)$ continuously changes from $\eta^*(0) = \frac{1}{4}$ to $\eta^*(\infty) = \frac{1}{2}$. In the A phase ($\eta > 1$) the barrier potentials are irrelevant perturbations, and the conductance at $T = 0$ is always $\frac{e^2\eta}{2\pi}$ irrespective to V_g . In this phase the perturbative calculation in powers of $V_0/\alpha\Lambda$ works well. In the C phase ($0 < \eta < \eta^*$), on the other hand, the potentials are relevant and the conductance is always zero at $T = 0$. Lastly, in the B phase ($\eta^* < \eta < 1$), the conductance at $T = 0$ is $\frac{e^2\eta}{2\pi}$ precisely on resonance and zero otherwise. The noninteracting Fermi liquid locates on the phase boundary between A and B so that the conductance is exactly $e^2/2\pi$ on resonance but takes a finite value in between $e^2/2\pi$ and 0 off resonance. This agrees with the result of the standard Landauer approach explained briefly in Sec. 3.1.

3.4.2 Conductance

In this section we calculate the conductance as a function of T and ε . Introducing a heat bath consisting of harmonic oscillators linearly coupled with the phases $\bar{\theta}$ and $\bar{\theta}$, we can construct an equivalent model to Eq. (3.13) as Caldeira and Leggett did in the theory of the macroscopic quantum tunneling [22]. The effective Hamiltonian for this equivalent model is given by

$$H(\bar{\theta}, \bar{\theta}) = \sum_{\alpha} \left(\frac{P_{\alpha}^2}{2M_{\alpha}} + \frac{1}{2} M_{\alpha} \Omega_{\alpha}^2 X_{\alpha}^2 + \bar{\lambda}_{\alpha} \bar{\theta} X_{\alpha} + \frac{\bar{\lambda}_{\alpha}^2 \bar{\theta}^2}{2M_{\alpha} \Omega_{\alpha}^2} \right)$$

$$\begin{aligned}
& + \sum_{\beta} \left(\frac{p_{\beta}^2}{2m_{\beta}} + \frac{1}{2} m_{\beta} \omega_{\beta}^2 x_{\beta}^2 + \bar{\lambda}_{\beta} \bar{\theta} x_{\beta} + \frac{\bar{\lambda}_{\beta}^2 \bar{\theta}^2}{2m_{\beta} \omega_{\beta}^2} \right) \\
& + \frac{1}{8\pi^2} \left(2U + \frac{\pi}{\eta} \Delta\epsilon \right) \bar{\theta}^2 - \frac{eV}{2\pi} \bar{\theta} - \frac{eV_g}{2\pi} \bar{\theta} + \frac{2V_0}{\pi\alpha} \left(1 - \cos \bar{\theta} \cos \frac{\bar{\theta}}{2} \right) \quad (3.40)
\end{aligned}$$

with spectral functions,

$$\bar{J}(\omega) \equiv \sum_{\alpha} \frac{\pi \bar{\lambda}_{\alpha}^2}{2M_{\alpha} \Omega_{\alpha}} \delta(\omega - \Omega_{\alpha}) = \frac{\omega}{\pi\eta} \left[\frac{1}{2} + \pi\Delta\epsilon \sum_{n=1}^{\infty} \delta(\omega - \pi\Delta\epsilon(2n-1)) \right], \quad (3.41)$$

$$\bar{J}(\omega) \equiv \sum_{\beta} \frac{\pi \bar{\lambda}_{\beta}^2}{2m_{\beta} \omega_{\beta}} \delta(\omega - \omega_{\beta}) = \frac{\omega}{4\pi\eta} \left[\frac{1}{2} + \pi\Delta\epsilon \sum_{n=1}^{\infty} \delta(\omega - 2\pi n\Delta\epsilon) \right]. \quad (3.42)$$

The equivalence is demonstrated in Appendix A.4.

The tunneling conductance G is calculated from the probabilities of the second-order hopping (tunneling) process between i site and f site. The transition probability from i site to f site via m site and that for the reverse process are given by

$$\begin{aligned}
P(i \rightarrow m \rightarrow f) &= 2\pi t^4 \sum_{i,f} e^{-\beta E_i} \left| \sum_m \frac{\langle f|m\rangle \langle m|i\rangle}{E_m - E_i + i\Gamma} \right|^2 \delta(E_f - E_i) / \sum_i e^{-\beta E_i}, \\
P(f \rightarrow m \rightarrow i) &= 2\pi t^4 \sum_{i,f} e^{-\beta E_f} \left| \sum_m \frac{\langle i|m\rangle \langle m|f\rangle}{E_m - E_f + i\Gamma} \right|^2 \delta(E_i - E_f) / \sum_f e^{-\beta E_f}.
\end{aligned}$$

Note that these two probabilities are related with each other by the detailed balance relation: $P(f \rightarrow m \rightarrow i) = e^{-\beta eV} P(i \rightarrow m \rightarrow f)$. The life-time effect of the intermediate state m is taken into account by inserting the finite imaginary number $i\Gamma$ in the denominator; Γ is the width of a resonance level formed in between two barriers and is calculated as the escape rate from the m site to the i site or f site:

$$\begin{aligned}
\Gamma &= 2t^2 \int_{-\infty}^{\infty} dt_0 \langle e^{-iH_m t_0} e^{iH_i t_0} \rangle_i \Big|_{V=0} \\
&\approx \begin{cases} 2\pi B(\frac{1}{2\eta}, \frac{1}{2}) \Delta\epsilon \left(\frac{t}{\Lambda} \right)^2 \left(\frac{\pi^2 \Delta\epsilon T}{\Lambda^2} \right)^{\frac{1}{\eta}-1}, & T \ll \Delta\epsilon \\ 2\pi B(\frac{1}{\eta}, \frac{1}{2}) T \left(\frac{t}{\Lambda} \right)^2 \left(\frac{\pi T}{\Lambda} \right)^{\frac{2}{\eta}-2}, & \Delta\epsilon \ll T \ll U, \end{cases} \quad (3.43)
\end{aligned}$$

where $B(a, b)$ is the beta function. Note that if we set $\eta = 1$ and $\Lambda = \pi W$ for $T \ll \Delta\epsilon$, Eq. (3.43) reproduces the level width for the noninteracting case (Eq. (3.10)).

The conductance G is calculated from the difference between $P(i \rightarrow m \rightarrow f)$ and $P(f \rightarrow m \rightarrow i)$:

$$\begin{aligned}
G &= \lim_{V \rightarrow 0} \frac{e}{V} \{ P(i \rightarrow m \rightarrow f) - P(f \rightarrow m \rightarrow i) \} \\
&= \beta e^2 P(i \rightarrow m \rightarrow f) \Big|_{V=0} \\
&= \beta e^2 t^4 \int_{-\infty}^{\infty} dt_0 \int_0^{\infty} dt_2 \left\langle e^{iH_i(t_0-t_1+t_2)} e^{iH_m t_1} e^{-iH_f t_0} e^{-iH_m t_2} \right\rangle_i e^{-\Gamma(t_1+t_2)} \Big|_{V=0}, \quad (3.44)
\end{aligned}$$

where $\langle Q \rangle_i = \text{Tr} Q e^{-\beta H_i} / \text{Tr} e^{-\beta H_i}$. The three Hamiltonians H_i , H_m , and H_f are those for the harmonic oscillators with shifted origins: $H_i = H(0, 0)$, $H_m = H(\pi, -2\pi)$, and

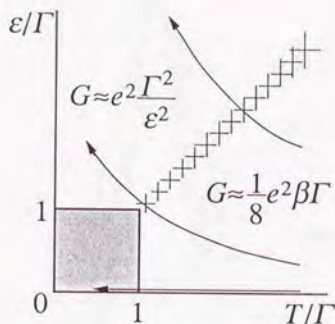


Figure 3.6: Asymptotic form of G . The RG flows for $\frac{1}{2} < \eta < 1$ and $T \ll \Delta\epsilon$ are also depicted. In the shaded region ($T < \Gamma$ and $\epsilon < \Gamma$) the expansion in powers of t fails.

$H_f = H(2\pi, 0)$. After some manipulations Eq. (3.44) can be transformed to

$$G = \frac{e^2 \beta}{8\pi} \int_{-\infty}^{\infty} dE \frac{\Gamma^2}{(E - \epsilon)^2 + \Gamma^2} \left| \frac{\Gamma(\frac{1}{2\eta} + i\frac{\beta E}{2\pi})}{\Gamma(\frac{1}{2\eta})} \right|^4, \quad (3.45)$$

where $\Gamma(x)$ is the gamma function. The derivation of Eqs. (3.43) and (3.45) is described in Appendix A.5. Note that for the noninteracting case ($\eta = 1$) Eq. (3.45) reproduces the correct result, Eq. (3.11), for any temperature. For general interacting systems (Luttinger liquids), however, Eq. (3.45) can be justified only when $T \gg \epsilon, \Gamma$ or $\epsilon \gg T, \Gamma$. In other words, Eq. (3.45) is valid as long as the conductance is much smaller than $e^2 \eta / 2\pi$.

When the temperature T is much higher than ϵ and Γ , Eq. (3.45) is approximated as

$$G \approx \frac{e^2}{8} \beta \Gamma \left| \frac{\Gamma(\frac{1}{2\eta} + i\frac{\beta \epsilon}{2\pi})}{\Gamma(\frac{1}{2\eta})} \right|^4, \quad (3.46)$$

which is proportional to $e^2 (\beta \epsilon)^{\frac{2}{\eta} - 2} e^{-\beta \epsilon} \beta \Gamma$ for $\beta \epsilon \gg 1$. In this case the tunneling can be thought of as a thermally activated sequential tunneling via a real transition to the intermediate state m . In the other case where ϵ is much larger than T and Γ , Eq. (3.45) is approximated as

$$G \approx e^2 \frac{\Gamma^2}{\epsilon^2}. \quad (3.47)$$

This conductance originates from a tunneling via a virtual transition to the intermediate state. Figure 3.6 summarizes Eqs. (3.46) and (3.47). Also shown are the RG flows for $\frac{1}{2} < \eta < 1$ and $T \ll \Delta\epsilon$. In the shaded region the perturbation expansion in powers of t fails, and we should rather take $V_0/\alpha\Lambda$ as a small expansion parameter.

The line shape of the resonance peaks, i.e., ϵ dependence of G , is now ready for discussion for $T \gg \Gamma$, which is most relevant to experiments. In this temperature range the ϵ dependence is given by Eq. (3.46) for $\epsilon \leq T$ and by Eq. (3.47) for $\epsilon \gg T$ (far away from resonance). We plot $|\Gamma(\frac{1}{2\eta} + i\frac{\beta \epsilon}{2\pi})/\Gamma(\frac{1}{2\eta})|^4$ in Fig. 3.7. We can see from this figure that for

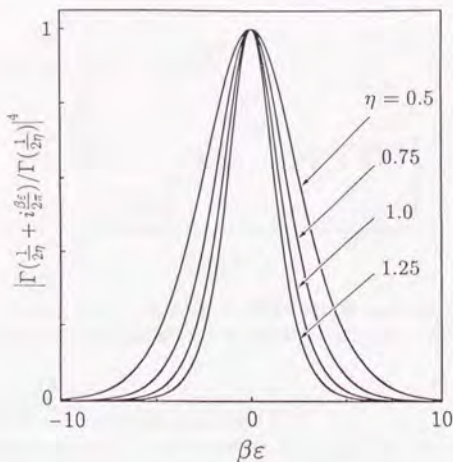


Figure 3.7: The line shape of the conductance G for $T \gg \Gamma$: $|\Gamma(\frac{1}{2\eta} + i\frac{\beta\epsilon}{2\pi})/\Gamma(\frac{1}{2\eta})|^4$ as a function of ϵ . For $\eta = 1$ it is equal to $-\frac{4}{\beta}f'(\epsilon) = \text{sech}^2\frac{\beta\epsilon}{2}$.

$T \gg \Gamma$ the line shape is very similar to that for the noninteracting Fermi liquid, $-f'(\epsilon)$, when the temperature in $f(\epsilon)$ is properly adjusted. Therefore the temperature obtained from the experimental data by applying the noninteracting electron formula (3.11) is higher (lower) than the true temperature when the interaction is repulsive (attractive). The line shape in the low-temperature regime ($T \ll \Gamma$) will be briefly discussed later.

The T dependence of the resonance peak height or width, on the other hand, is quite different from the Fermi liquid due to the renormalization of Γ . In contrast to the noninteracting case ($\eta = 1$ and $U = 0$), Γ in Eq. (3.43) in general depends on T . Note that the interaction is taken into account through U as well as η different from 1. From Eq. (3.43) both Γ and Γ/T depend on T and behave as $\Gamma \sim T^{\frac{2}{\eta}-1}$, $\Gamma/T \sim T^{\frac{2}{\eta}-2}$ for $T \gg \Delta\epsilon$, and $\Gamma \sim T^{\frac{1}{\eta}-1}$, $\Gamma/T \sim T^{\frac{1}{\eta}-2}$ for $T \ll \Delta\epsilon$. When $\eta < \frac{1}{2}$, both Γ and Γ/T monotonically decrease as T is lowered. When $\frac{1}{2} < \eta < 1$, Γ keeps decreasing while Γ/T decreases for $T \geq \Delta\epsilon$ but turns to increase below $\Delta\epsilon$. When $1 < \eta < 2$, Γ decreases for $T \geq \Delta\epsilon$ and turns to increase below $\Delta\epsilon$ while Γ/T increases monotonically with decreasing temperature. When $\eta > 2$, both Γ and Γ/T always increase. Thus, Γ or Γ/T is a nonmonotonic function of T for $\frac{1}{2} < \eta < 2$. For $T \leq \Gamma$ the temperature dependence of Γ is directly observable as the width of the resonance peak, while for $T \geq \Gamma$ it is reflected not in the width $\sim T$, but in the peak height $\sim e^2\Gamma/T$. For moderate repulsive interaction ($\frac{1}{2} < \eta < 1$), which we consider to be the most relevant case to experiments, the typical T dependence of the conductance line shape is summarized in Fig. 3.8. Starting with the temperature $T(> \Gamma$ and $> \Delta\epsilon$), as the temperature is lowered, we find that the peak height and the width decrease first as $T^{\frac{2}{\eta}-2}$ and T , respectively. Around $T \approx \Delta\epsilon$, however, the peak height has a minimum and turns to increase as $T^{\frac{1}{\eta}-2}$ below $\Delta\epsilon$, while the width continues to decrease as T . When the temperature is lowered further to some temperature $T^*(< \Delta\epsilon)$, Γ will become comparable with T , i.e., the peak height $\sim e^2$. Below this temperature T^* , the peak height saturates

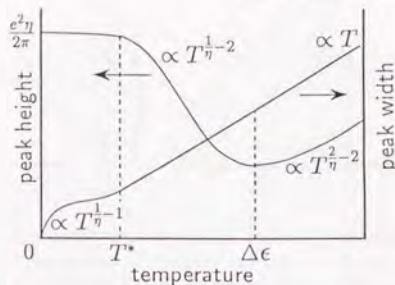


Figure 3.8: The temperature dependence of the height and the width of the conductance peak for $\frac{1}{2} < \eta < 1$. The peak height has a minimum around $T \approx \Delta\epsilon$. The width eventually vanishes as $T \rightarrow 0$.

toward $e^2\eta/2\pi$ while the width decreases as $T^{\frac{1}{\eta}-1}$.

Now we comment on the low-temperature line shape of the conductance resonances in the B phase. At low temperature and just on resonance the perturbative treatment with respect to $V_0/\alpha\Lambda$ is valid, and the peak value of the conductance is given by Eq. (3.26) with $\cos\varphi = -1$; $G \approx e^2\eta/2\pi$. Far away from resonance, on the other hand, the perturbative calculation in powers of t becomes appropriate, and the conductance is obtained from Eq. (3.45) as $G \approx e^2\Gamma^2/\epsilon^2$. It is not easy to calculate the conductance for the intermediate regime between the two limits (just on resonance and far away from resonance), since one must sum up all the contributions from the higher-order tunneling processes. Very recently Kane and Fisher [19] have argued by using the renormalization group that $G \approx \epsilon^2(c\epsilon/T^{1-\eta})^{-\frac{2}{\eta}}$ in this regime, where c is a dimensionful constant. Therefore one can expect that as ϵ is increased, the conductance decreases, from the maximum value of order $e^2\eta/2\pi$, first as $\epsilon^{-\frac{2}{\eta}}$ and then as ϵ^{-2} . Thus there must be a characteristic crossover energy around which the exponent changes from $-\frac{2}{\eta}$ to -2 . In our theory this energy scale is implicitly assumed to be of order Γ .

Finally we briefly comment on the validity of the results obtained in this section. In calculating G we have correctly taken into account the renormalization of Γ but neglected that of K . Since dK/dl is proportional to t^2 (3.37), our method is equivalent to the RG analysis in the lowest order of t .

3.5 Asymmetric Barriers

Up to now we have discussed the tunneling through a symmetric double-barrier structure. In this section we briefly discuss the effect of asymmetry of barrier structures. In asymmetric structures ($|V_L| \neq |V_R|$), the true resonance cannot be achieved. This is most easily seen in the weak potential limit. In this limit, the first-order cumulant, V_1 , of the double-barrier potential is proportional to $(V_L + V_R) \cos\bar{\theta} \cos\frac{\varphi}{2} + (V_L - V_R) \sin\bar{\theta} \sin\frac{\varphi}{2}$, which cannot vanish for any φ unless $|V_L| = |V_R|$. As the temperature is lowered, V_1 becomes larger for repulsive electron-electron interactions. Therefore the low-temperature behavior of the system is described more appropriately in the opposite limit of strong barrier potential. In this limit also, it is impossible to reach the true resonance. This can be shown by using scal-

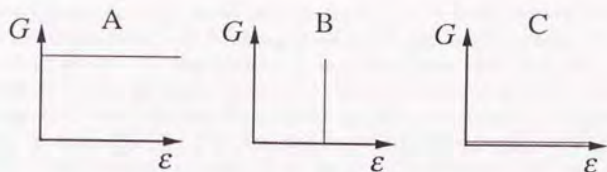


Figure 3.9: Line shape of a conductance peak at zero temperature. In the A (C) phase the conductance is $e^2\eta/2\pi$ (0) regardless of the gate voltage or ϵ . In the B phase the conductance is $e^2\eta/2\pi$ just on resonance ($\epsilon = 0$) but 0 otherwise. Thus the line width is zero.

ing equations for tunneling matrix elements through the left and the right barrier, t_l and t_r , which can be derived by extending the real-space renormalization group method explained in Sec. 3.4.1 [20]. The calculation is a natural extension of what is given in Sec. 3.4.1, so we do not repeat it here. It is shown that at least one of t_l and t_r is scaled to zero if $\eta < 1$, and that both of them are scaled to large if $\eta > 1$. Therefore the zero-temperature phase diagram of the asymmetric case is the same as that of the off-resonance phase diagram of the symmetric case (Fig. 3.3).

For sufficiently small t_l and t_r , a perturbative calculation of the conductance may be possible. By extending the argument in Sec. 3.4.2, for $T \ll \Delta\epsilon$ the conductance is calculated as

$$G = \frac{\beta e^2}{8\pi} \int dE \frac{\Gamma_r \Gamma_l}{(E - \epsilon)^2 + \frac{1}{4}(\Gamma_r + \Gamma_l)^2} \left| \frac{\Gamma(\frac{1}{2\eta} + i\frac{\beta E}{2\pi})}{\Gamma(\frac{1}{2\eta})} \right|^4, \quad (3.48)$$

where $\Gamma_{r(l)}$ is the tunneling rate through the right (left) tunnel barrier,

$$\Gamma_{r(l)} = \frac{2\sqrt{\pi} \Gamma(\frac{1}{2\eta}) t_{r(l)}^2}{\Gamma(\frac{1}{2\eta} + \frac{1}{2})} \left(\frac{\pi \Delta\epsilon}{\Lambda} \right)^{\frac{1}{\eta}} \left(\frac{\pi T}{\Lambda} \right)^{\frac{1}{\eta} - 1}. \quad (3.49)$$

Equation (3.48) realizes an extension of Eq. (3.12) to Luttinger liquids. Note, however, that this result is not always correct near zero temperature.

3.6 Summary

In this chapter we have studied the resonant tunneling through a double-barrier structure in a 1D interacting spinless fermion system. We summarize our findings below.

- The effective action for phase fields $\bar{\theta}$ and $\tilde{\theta}$ is obtained. $\bar{\theta}$ always suffers dissipation, while $\tilde{\theta}$ has a mass gap.
- At zero temperature the system is classified into three phases (Fig. 3.5) depending on η and V_0 . The phase boundary between the B and C phases is dependent on the strength of the barriers, while the boundary between the A and B phases is not. This is because $\tilde{\theta}$ is subject to the dissipation only when the barrier strength V_0/α is much larger than the cutoff Λ . The zero-temperature line shape of a conductance peak is quite different in each phase as shown in Fig. 3.9.

- The conductance is calculated perturbatively in both limits of weak barriers and strong barriers (weak links). At low temperatures the conductance shows anomalous power-law dependence on temperature. It is shown that, when the charging energy U is included, the temperature dependence changes around $T \approx \Delta\epsilon$. It is also found that, though for $T \ll \Gamma$ the line shape of the conductance peaks is quite strange (Fig. 3.9), for $T \gg \Gamma$ the line shape (ϵ dependence) in Luttinger liquids is very similar to that in the noninteracting system. It is the T dependence of the peak height or width that is dramatically changed by the interaction, and the nonmonotonic temperature dependence of the peak height is predicted for the moderate repulsive interaction.

Finally, we briefly comment on recent experiments on resonant tunneling [2, 36]. Kastner *et al.* measured conductance of a narrow wire patterned by using electron beam lithography in a two-dimensional electron gas of GaAs/AlGaAs heterostructure [2, 36]. The wire (length $\approx 3 \mu\text{m}$, nominal width $\approx 0.5 \mu\text{m}$) was argued to be one dimensional, i.e., only a single subband was occupied. They observed periodic oscillations of the conductance of a double constriction formed in the wire with changing a gate voltage. The line shape of resonance peaks could be fitted very well by the derivative of the Fermi distribution function, and the peak height grew roughly as $1/T$ when the temperature was decreased. These experimental results can be understood successfully by the Coulomb-blockade theory developed by Meir, Wingreen, and Lee [38] and, independently, Beenakker [39]. That is, the experiments can be understood from the Fermi-liquid picture, not from the Luttinger-liquid picture. As shown in the preceding section the most peculiar feature of the resonant tunneling in Luttinger liquids is that the line width vanishes as $\Gamma \propto T^{\frac{1}{2}-1}$ for repulsive interaction. This behavior is expected to be seen only below the temperature T^* at which $T = \Gamma$. The experiment was probably performed in the temperature range much higher than T^* , and hence they observed the line shape of the Fermi-liquid type.

Chapter 4

Anderson Localization

4.1 Introduction

In the preceding chapters we have discussed the tunneling through one or two tunnel barriers. The next step that one may naturally expect is to study the tunneling through three barriers. We, however, go far ahead and consider the case where there are *infinite* barriers (impurities). The aim of this chapter is then to investigate the electronic transport in a dirty 1D system, i.e., the Anderson localization [42].

In fact, the Anderson localization in 1D interacting systems is an old problem and has already been discussed in many articles as we reviewed in Sec. 1.3. Chui and Bray [13] and Apel and Rice [14] pointed out that a phase transition between insulating and conducting states occurs at zero temperature when the strength of electron-electron interaction is changed. Suzumura and Fukuyama [15] used the phase Hamiltonian and, to determine the phase boundary, they made use of an analogy between the pinning of charge-density wave (CDW) [28] and the pinning of phase fields. Giamarchi and Schultz [16] then discussed the phase transition extensively by using the RG calculation. These studies show that the interaction-induced Anderson transition occurs at $\eta_\rho + \eta_\sigma = 3$ in the limit where the impurity potential is very weak. It is also shown that in the localized phase the temperature dependence of the resistivity changes around some temperature T_{loc} below which the phase fields are pinned.

Our analysis given in Chap. 2 shows that for the single-barrier case the phase transition occurs at $\eta_\rho + \eta_\sigma = 2$ in the weak-potential limit. Clearly, this phase boundary differs from that of the Anderson localization, $\eta_\rho + \eta_\sigma = 3$. Then we ask a question: Why are these two boundaries different, and how do these two results reconcile with each other?

In most of the previous studies on the Anderson localization, it is assumed that the average spacing R between neighboring impurities is much shorter than a characteristic length scale of distortion of the phase fields by impurity potential. That is, these studies are based on the weak-pinning picture, if we use the analogy to the CDW pinning. On the contrary, our single-barrier problem is in the strong-pinning limit. We will see below that our strong-pinning picture holds true at high temperatures but gives way to the weak-pinning picture at low temperatures, and that this crossover occurs around $T = T_{dis} \equiv v/k_B R$, where v is the Fermi velocity. Above T_{dis} the impurity potentials act as the assembly of independent barriers and the 0D results are applicable. Below T_{dis} the recursion formulas for RG flows change to those discussed in Ref. [16]. This crossover, which manifests itself in the nonmonotonic temperature dependence of the resistivity, is described in a unified fashion.

4.2 Effective action

Suppose that N impurities are distributed dilutely at $x = x_j$ ($j = 1, 2, \dots, N$) with average interval R . Then the partition function of the system is given by

$$Z_0 = \int \mathcal{D}\theta \int \mathcal{D}\phi \exp\left(-\int_0^\beta d\tau [L_0(\tau) + L'(\tau)]\right), \quad (4.1)$$

where L_0 is the pure Lagrangian (2.2) and L' is given by

$$L' = -\sum_{x_j} \frac{2V_j}{\pi\alpha} \cos[\theta(x_j, \tau) + 2k_F x_j] \cos[\phi(x_j, \tau)]. \quad (4.2)$$

In the same way as in Chap. 2, we introduce the phase fields at impurity sites, $\theta_j(\tau)$ and $\phi_j(\tau)$, and auxiliary fields, $\lambda_{1j}(\tau)$ and $\lambda_{2j}(\tau)$, and then integrate out $\theta(x, \tau)$ and $\phi(x, \tau)$. The result is

$$\begin{aligned} Z_0 = \int \prod_j \mathcal{D}\theta_j \mathcal{D}\phi_j \mathcal{D}\lambda_{1j} \mathcal{D}\lambda_{2j} \exp\left(& -\frac{\pi\eta_\rho}{2\beta} \sum_{\omega_n} \sum_{x_j} \sum_{x_k} \frac{1}{|\omega_n|} \exp[-|\omega_n(x_j - x_k)|/v_\rho] \lambda_{1j}(\omega_n) \lambda_{1k}(-\omega_n) \right. \\ & -\frac{\pi\eta_\sigma}{2\beta} \sum_{\omega_n} \sum_{x_j} \sum_{x_k} \frac{1}{|\omega_n|} \exp[-|\omega_n(x_j - x_k)|/v_\sigma] \lambda_{2j}(\omega_n) \lambda_{2k}(-\omega_n) \\ & + \frac{i}{\beta} \sum_{\omega_n} \sum_{x_j} [\lambda_{1j}(\omega_n) \theta_j(-\omega_n) + \lambda_{2j}(\omega_n) \phi_j(-\omega_n)] \\ & \left. + \sum_{x_j} \frac{2V_j}{\pi\alpha} \int_0^\beta d\tau \cos[\theta_j(\tau) + 2k_F x_j] \cos \phi_j(\tau) \right), \end{aligned} \quad (4.3)$$

where we have used the relation

$$\int_{-\infty}^{\infty} \frac{dq}{2\pi} \frac{e^{-iqx}}{\omega_n^2 + v^2 q^2} = \frac{1}{2v|\omega_n|} \exp(-|\omega_n x|/v). \quad (4.4)$$

Assuming that the randomness of impurity distribution affects the electronic transport mainly through the random distribution of the phase $2k_F x_j$, we now approximate the x_j 's in $\exp[-|\omega_n(x_j - x_k)|/v_{\rho(\sigma)}]$ by $x_j = jR$ ($j = 1, 2, \dots, N$) while keeping $2k_F x_j$ to be a random variable. This is a crucial approximation.

We introduce the Fourier transforms,

$$\theta_j(\omega_n) = \frac{1}{\sqrt{N}} \sum_q e^{ijqR} \theta(q, \omega_n), \quad \phi_j(\omega_n) = \frac{1}{\sqrt{N}} \sum_q e^{ijqR} \phi(q, \omega_n), \quad (4.5)$$

$$\lambda_{1j}(\omega_n) = \frac{1}{\sqrt{N}} \sum_q e^{ijqR} \lambda_1(q, \omega_n), \quad \lambda_{2j}(\omega_n) = \frac{1}{\sqrt{N}} \sum_q e^{ijqR} \lambda_2(q, \omega_n), \quad (4.6)$$

where q belongs to the first Brillouin zone ($-\pi/R \leq q \leq \pi/R$). Substituting Eqs. (4.5) and (4.6) into Eq. (4.3) and integrating out $\lambda_1(q, \omega_n)$ and $\lambda_2(q, \omega_n)$, we get the effective Euclidean action for $\theta(q, \omega_n)$ and $\phi(q, \omega_n)$ as

$$S_{\text{eff}} = \frac{1}{\beta} \sum_{\omega_n} \sum_q (K_\rho(q, \omega_n) |\theta(q, \omega_n)|^2 + K_\sigma(q, \omega_n) |\phi(q, \omega_n)|^2)$$

$$-\sum_x \frac{2V_j}{\pi\alpha} \int_0^\beta d\tau \cos[\theta_j(\tau) + 2k_F x_j] \cos[\phi_j(\tau)] \quad (4.7)$$

with

$$K_\gamma(q, \omega_n) = \frac{|\omega_n|}{2\pi\eta_\gamma} \frac{1 - 2 \exp(-R|\omega_n|/v_\gamma) \cos qR + \exp(-2R|\omega_n|/v_\gamma)}{1 - \exp(-2R|\omega_n|/v_\gamma)} \quad (\gamma = \rho, \sigma). \quad (4.8)$$

This is the central result of this chapter. It is easily seen that the kernel $K_\gamma(q, \omega_n)$ is approximated as

$$K_\gamma(q, \omega_n) \approx \begin{cases} \frac{|\omega_n|}{2\pi\eta_\gamma}, & |\omega_n| \gg v_\gamma/R \\ \frac{R}{4\pi v_\gamma \eta_\gamma} (\omega_n^2 + v_\gamma^2 q^2), & |\omega_n| \ll v_\gamma/R \text{ and } |qR| \ll \pi. \end{cases} \quad (4.9)$$

4.3 Implications to transport properties

Now we assume that v_ρ and v_σ are of the same order of magnitude ($\sim v$). Then v/R is the discretization energy within the interval between two neighboring impurities. For $|\omega_n| \gg v/R$ the correlations between the different impurities are unimportant, and the effective action is just the sum of the action in Eq. (2.7) with respect to the impurity sites with a trivial modification, $V_0 \cos \theta_0(\tau) \cos \phi_0(\tau) \rightarrow V_j \cos[\theta_j(\tau) + 2k_F x_j] \cos \phi_j(\tau)$. On the other hand, if $|\omega_n| \ll v/R$, the correlation between the impurity sites must be properly treated. The effective action describing the long-wavelength ($|q| < \pi/R$) and low-frequency ($|\omega_n| < v/R$) phenomena is obtained by integrating out the high frequency ($|\omega_n| > v/R$) components by the RG method for the single-impurity problem discussed above. When the impurity potential V_j is weak enough, it is renormalized to $\bar{V}_j = V_j(R/a)^{1-\frac{1}{2}(v_\rho+v_\sigma)}$ with a being the lattice spacing. This \bar{V}_j exists at every site j in this coarse grained system, and we can now apply the previous analysis [14, 15, 16] assuming a random potential expressed as a continuous function of x . That is, for small q and ω_n the effective action (4.7) reduces to

$$\begin{aligned} S_{\text{eff}} &= \frac{1}{\beta} \sum_{\omega_n} \sum_q (K_\rho(q, \omega_n) |\theta(q, \omega_n)|^2 + K_\sigma(q, \omega_n) |\phi(q, \omega_n)|^2) \\ &\quad - \frac{2\bar{V}_j}{\pi\alpha} \int_0^\beta d\tau \cos[\theta_j(\tau) + 2k_F x_j] \cos[\phi_j(\tau)] \\ &\Rightarrow \int d\tau \int dx \left(\frac{1}{4\pi v_\rho \eta_\rho} [(\partial_\tau \theta(x, \tau))^2 + v_\rho^2 (\partial_x \theta(x, \tau))^2] \right. \\ &\quad \left. + \frac{1}{4\pi v_\sigma \eta_\sigma} [(\partial_\tau \phi(x, \tau))^2 + v_\sigma^2 (\partial_x \phi(x, \tau))^2] \right. \\ &\quad \left. - \frac{2n_i \bar{V}}{\pi\alpha} \cos[\theta(x, \tau) + 2k_F x] \cos[\phi(x, \tau)] \right), \quad (4.10) \end{aligned}$$

where n_i is the impurity density.

Thus we can expect to see a crossover from the single-impurity behavior to the dense-impurity behavior, when the relevant energy scale or, equivalently, the temperature is varied across $T_{\text{dis}} = v/k_B R$. We note that this crossover temperature T_{dis} is higher than T_{loc} because the localization length L_{loc} is always longer than R . It may be instructive to show that this

RG procedure is compatible with the previous theories on the localization length. According to the weak-pinning analysis [15], the localization length is given by

$$L_{loc} \sim n_i^{-1} (n_i \alpha)^{\frac{2-\eta}{3-\eta}} \left(\frac{V_0}{v} \right)^{-\frac{2}{3-\eta}}, \quad (4.11)$$

where $\eta = \eta_\rho + \eta_\sigma$, $n_i = 1/R$, and α is the short-distance cutoff. By integrating out the high-frequency modes $|\omega_n| > v/R$, the potential is renormalized to $\tilde{V}_j = V_0(R/a)^{1-\frac{1}{2}\eta}$. Substituting \tilde{V}_j for V_0 and R for α in Eq. (4.11), we get

$$L_{loc} \sim R \left[\frac{V_0}{v} \left(\frac{R}{a} \right)^{1-\frac{1}{2}\eta} \right]^{-\frac{2}{3-\eta}} = R \left(\frac{R}{a} \right)^{-\frac{2-\eta}{3-\eta}} \left(\frac{V_0}{v} \right)^{-\frac{2}{3-\eta}}, \quad (4.12)$$

which is exactly the same as Eq. (4.11) with $\alpha = a$. In this way our RG procedure matches the previous result.

Now we discuss the resistivity $\rho(T)$ of 1D Luttinger liquids with many impurities. Suppose that the impurity density is so low that around $T \approx v/R$ the phonon scattering is almost negligible. Then, without electron-electron interactions, $\rho(T)$ would be equal to residual resistivity, $m/ne^2\tau \approx 1/e^2R$ ($\tau \approx R/v$), for all T less than v/R . In Luttinger liquids the interaction effect will manifest itself in the resistivity at $T \leq v/R$ in the following way. The resistivity is related to the conductance by $\rho(T) \sim (LG_\rho)^{-1}$ where L is some characteristic length scale. L is estimated as R for $T > T_{dis}$, v_F/T for $T_{loc} < T < T_{dis}$, and L_{loc} for $T < T_{loc}$. For $T < T_{dis}$ G_ρ^{-1} is proportional to $V(T)^2$ with $V(T)$ being the renormalized potential strength down to the energy scale of the order of $k_B T$. As a particular example, suppose that interaction parameters lie in the range $2 < \eta_\rho + \eta_\sigma < 3$. At high temperature $T > T_{dis}$ both charge and spin phase fields are not pinned, and the resistivity $\rho(T)$ is proportional to the inverse of the conductance of a single impurity. As discussed by Fisher and Zwerger [25], when $\eta_\rho + \eta_\sigma > 2$, the resistivity is nonmonotonic as a function of the temperature, showing a maximum at some temperature T^* .¹ In the high temperature limit, it approaches $\rho_\infty \equiv (Re^2\eta_\rho/\pi)^{-1}$, which is just the residual resistivity. Below T^* the resistivity decreases again toward ρ_∞ with decreasing temperature. When the temperature is further reduced below T_{dis} , the resistivity changes to decrease to zero as $\rho(T) \propto T^{\eta_\rho + \eta_\sigma - 2}$ and then turns to increase around T_{loc} as $\rho(T) \propto T^{\eta_\rho + \eta_\sigma - 3}$, as the phase fields begin to be pinned [16]. Thus the temperature dependence of the resistivity has a fairly complicated structure with two crossover temperatures, T_{loc} and T_{dis} , and this scenario may be checked experimentally by changing the concentration of the impurities, i.e., R^{-1} . Schematic temperature dependence of the resistivity for general cases is shown in Fig. 4.1.

¹For $T > v/R$ the resistivity is proportional to the resistance of a single impurity potential. As shown in Chap. 2, the single-barrier case can be mapped to the problem of a quantum Brownian motion of a particle in a cosine potential. Fisher and Zwerger showed that the mobility of the particle has a nonmonotonic temperature dependence with a minimum at $T \approx T^*$. For $T \ll T^*$ the transport can be viewed as thermally resisted quantum tunneling between adjacent minima in the potential. For $T \gg T^*$, on the other hand, the transport is mainly due to thermally assisted hopping over the barrier. They estimated the crossover temperature as $T^* \approx c/mq_0^2$, where m is the mass of the particle, q_0 is a period of the cosine potential, and c is a constant of order 1 that depends on the friction. In our problem, $m \sim 1/\Lambda$ and $q_0 \sim \pi$, thereby $T^* \sim \Lambda/10$. Thus, in many cases the crossover temperature is so high that the main contribution to the resistivity comes from the scattering by phonons; the resistance maximum at $T \approx T^*$ will not be seen in such a case. However, if the electron density is sufficiently low, then T^* may become low enough to make the resistance maximum be present.

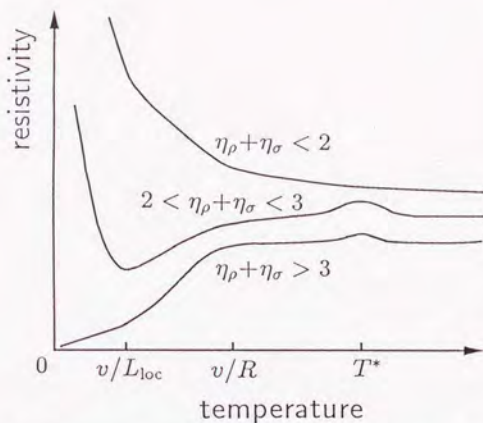


Figure 4.1: The schematic temperature dependence of the resistivity. In the high temperature limit it approaches $\rho_\infty = (Re^2\eta_\rho/\pi)^{-1}$. For $\eta_\rho + \eta_\sigma < 3$, it has a maximum at some temperature $T^* (> T_{\text{dis}})$. Below T_{dis} , $\rho(T) \propto T^{\eta_\rho + \eta_\sigma - 2}$ for $T_{\text{loc}} < T < T_{\text{dis}}$ and $\rho(T) \propto T^{\eta_\rho + \eta_\sigma - 3}$ for $T < T_{\text{loc}}$. The localization length is infinity for $\eta_\rho + \eta_\sigma > 3$.

4.4 Summary

In this chapter we have discussed the electronic transport in a 1D interacting electron system with many impurities. We have derived an effective action for the phase fields at the impurity sites, with which we can discuss a crossover from the strong-pinning (dilute-impurity) limit to the weak-pinning (dense-impurity) limit. This crossover has been disregarded in the previous studies on the Anderson transition because they are based on the collective-pinning picture and concerned with the low-temperature limit only. The theory also predicts a non-trivial temperature dependence of the resistivity.

Chapter 5

Concluding Remarks

5.1 Conclusions

Here we summarize the results obtained in this thesis.

We have discussed the tunneling through barriers for three models of 1D interacting electron systems (Luttinger liquids) by using the bosonization method. Integrating out phase fields away from the barriers, we have obtained effective actions for the phase fields on the barrier sites. These actions commonly contain the dissipation term. This dissipation arises from the low-lying collective excitations in the Luttinger liquids, which is reminiscent of the so-called Fermi-surface effect on the diffusion of heavy particles in a metal [43]. In fact, mathematics in our tunneling theory is very similar to that in the Kondo effect [26, 41, 44], the X-ray absorption problem [45], and, in particular, the macroscopic quantum coherence [23, 24, 25].

In the single-barrier case, the zero-temperature phase diagram is found to be separated into four regions (Figs. 2.1 and 2.3). These regions are classified in terms of zero-temperature values of the charge conductance G_ρ and the spin conductance G_σ . An interesting observation is that there are regions in which only one of the charge and spin phase fields is pinned by the barrier potential. This is a manifestation of the spin-charge separation in the Luttinger liquid. In contrast to the spinless model studied by Kane and Fisher [17], the phase boundaries are in general dependent on the strength of the barrier. The conductances G_ρ and G_σ are calculated perturbatively in powers of the barrier strength and of the tunneling matrix element; a power-law dependence on the temperature is found.

We have then examined the resonant tunneling of spinless fermions through a double-barrier structure. In the effective action, $\bar{\theta}$ is massless and subject to the dissipation while $\bar{\theta}$ is massive. This mass gap comes from the discreteness of energy levels in the region between two barriers. The zero-temperature phase diagram is classified into three regions in terms of the line shape of resonance peaks (Fig. 3.5). It is found that the well-known Lorentzian line shape is characteristic of the noninteracting case, in which the barrier potential is always a marginal perturbation except on resonance. We have introduced a charging-energy term and explored the temperature dependence of the resonance peaks both above and below $T = \Delta\epsilon/k_B$. In particular, for weakly repulsive interactions the peak height of conductance resonances is shown to be a nonmonotonic function of the temperature. Moreover, the ϵ dependence of the conductance is explicitly calculated for $T \gg \Gamma$, and the line shape is found to be similar to the derivative of the Fermi distribution function.

The Anderson localization is discussed with reference to the single-barrier result. We have

shown that correlation between the phase fields on neighboring impurity sites is negligible for high energy ($|\omega| \gg v/R$) but is of crucial importance for low energy ($|\omega| \ll v/R$). Accordingly, the resistivity shows complex temperature dependence (Fig. 4.1); the T dependence changes appreciably around $T = T_{\text{dis}}$ and T_{loc} .

5.2 Related problems

Listed below are some of possible extensions and topics closely related to the present work.

- In calculating conductance we assumed that electrostatic potential or chemical potential is constant in the leads, which allowed us to write the action in terms of the phase fields on the barrier sites only. This is an approximation whose validity is not clarified completely, though we could obtain reasonable results with the method. In principle, the distribution of the electric field in the leads must be determined self-consistently. This is a difficult and fundamental problem, and further study is clearly needed.
- We have examined one-dimensional Luttinger liquids as a model for very narrow, single-channel quantum wires. Another system that is considered as a Luttinger liquid is an edge state in a fractional quantum Hall system. In fact, it is argued [46, 47] that edge states are chiral Luttinger liquids. Thus it seems promising to study the tunneling between edge states with the bosonization method. Kinaret *et al.* [48] studied this problem by computing numerically the overlap integral for finite systems, and found that the tunneling is suppressed by electronic correlations.
- One-dimensional spin- $\frac{1}{2}$ Heisenberg antiferromagnetic chains with some defects are equivalent to the models discussed in this thesis. Eggert and Affleck [49] have studied such spin chains using the conformal field theory.
- In Chap. 3 we have studied the tunneling of *spinless* fermions through a double barrier. If these fermions had spin, then the Kondo effect would occur. The Kondo effect in the resonant tunneling has already been studied for the normal Fermi liquid [50, 51, 52]. The same effect in a Luttinger liquid is also studied by Kane and Fisher [20] and Lee and Toner [53] in the weak-coupling regime.
- The optical properties of Luttinger liquids are also of much interest. In particular, the Fermi-edge singularities in optical spectra have been discussed by using the bosonization method [54, 55].

The whole story of the tunneling in Luttinger liquids is being continued and will end when all these problems are worked out completely. This thesis may be just an introduction of the story.

Appendices

A.1 Derivation of Eq. (2.27)

Here we calculate the charge conductance G_ρ for $T \ll \Lambda$. From Eq. (2.26) the charge conductance is written as

$$G_\rho = \frac{e^2}{\pi} \eta_\rho - \frac{e^2}{2} \eta_\rho^2 \beta \left(\frac{V_0}{\pi \alpha} \right)^2 \int_{-\infty}^{\infty} dt \exp \left[-(\eta_\rho + \eta_\sigma) \int_0^\infty d\omega \frac{e^{-\omega/\Lambda}}{\omega} \left((1 - \cos \omega t) \coth \frac{\beta \omega}{2} + i \sin \omega t \right) \right].$$

We shall first evaluate the integral over ω . We divide the integral into two parts and calculate them separately:

$$\begin{aligned} \int_0^\infty d\omega \frac{e^{-\omega/\Lambda}}{\omega} (1 - e^{-i\omega t}) &= i \int_0^\infty d\omega \int_0^t dt_0 e^{-\omega/\Lambda - i\omega t_0} = i \int_0^t \frac{dt_0}{\frac{1}{\Lambda} + it_0} = \ln(1 + i\Lambda t) \\ \int_0^\infty d\omega \frac{e^{-\omega/\Lambda}}{\omega} (1 - \cos \omega t) \left(\coth \frac{\beta \omega}{2} - 1 \right) &= \int_0^\infty d\omega \frac{e^{-\omega/\Lambda}}{\omega} \sum_{n=1}^{\infty} \frac{(-1)^{n-1}}{(2n)!} (\omega t)^{2n} 2 \sum_{m=1}^{\infty} e^{-m\beta \omega} \\ &= 2 \sum_{m=1}^{\infty} \sum_{n=1}^{\infty} \frac{(-1)^{n-1}}{(2n)!} \left(\frac{\Lambda t}{1 + m\beta \Lambda} \right)^{2n} \int_0^\infty dx e^{-x} x^{2n-1} \\ &= \sum_{m=1}^{\infty} \ln \left[1 + \left(\frac{\Lambda t}{1 + m\beta \Lambda} \right)^2 \right] \\ &\approx \ln \left[\prod_{m=1}^{\infty} \left(1 + \frac{t^2}{m^2 \beta^2} \right) \right] \\ &= \ln \left(\frac{\beta}{\pi t} \sinh \frac{\pi t}{\beta} \right). \end{aligned}$$

Hence,

$$\exp \left[-(\eta_\rho + \eta_\sigma) \int_0^\infty d\omega \frac{e^{-\omega/\Lambda}}{\omega} \left((1 - \cos \omega t) \coth \frac{\beta \omega}{2} + i \sin \omega t \right) \right] = \left[(1 + i\Lambda t) \frac{\beta}{\pi t} \sinh \frac{\pi t}{\beta} \right]^{-\eta_\rho - \eta_\sigma}. \quad (\text{A.1})$$

The integral over t is thus written as

$$I_1 \equiv \int_{-\infty}^{\infty} dt \left[(1 + i\Lambda t) \frac{\beta}{\pi t} \sinh \frac{\pi t}{\beta} \right]^{-\eta_\rho - \eta_\sigma}.$$

Introducing a variable $z \equiv \frac{\pi}{\beta} \left(t + \frac{i\pi}{2} \right)$, we then write the integral as

$$I_1 = \frac{1}{\Lambda} \left(\frac{\pi}{\beta \Lambda} \right)^{\eta_\rho + \eta_\sigma - 1} \int_{-\infty + \frac{i\pi}{2}}^{\infty + \frac{i\pi}{2}} dz \left[\left(\frac{\pi}{\beta \Lambda} + \frac{\pi}{2} + iz \right) \frac{1}{z - \frac{i\pi}{2}} \sinh \left(z - \frac{i\pi}{2} \right) \right]^{-\eta_\rho - \eta_\sigma}$$

$$= \frac{1}{\Lambda} \left(\frac{\pi}{\beta\Lambda} \right)^{\eta_\rho + \eta_\sigma - 1} \int_{-\infty}^{\infty} dz \left[\left(\frac{\pi}{\beta\Lambda} + \frac{\pi}{2} + iz \right) \frac{1}{\frac{\pi}{2} + iz} \cosh z \right]^{-\eta_\rho - \eta_\sigma}$$

Since we are interested in the T dependence at low temperature ($\beta\Lambda \gg 1$), the integral is approximated as

$$\begin{aligned} I_1 &\approx \frac{1}{\Lambda} \left(\frac{\pi}{\beta\Lambda} \right)^{\eta_\rho + \eta_\sigma - 1} \int_{-\infty}^{\infty} dz (\cosh z)^{-\eta_\rho - \eta_\sigma} \\ &= \frac{1}{\Lambda} \left(\frac{\pi}{\beta\Lambda} \right)^{\eta_\rho + \eta_\sigma - 1} \int_0^1 y^{\frac{\eta_\rho + \eta_\sigma}{2} - 1} (1-y)^{-\frac{1}{2}} dy \quad (y = 1/\cosh^2 z) \\ &= \frac{1}{\Lambda} \left(\frac{\pi}{\beta\Lambda} \right)^{\eta_\rho + \eta_\sigma - 1} B\left(\frac{1}{2}(\eta_\rho + \eta_\sigma), \frac{1}{2}\right) \\ &= \frac{1}{\Lambda} \frac{\sqrt{\pi} \Gamma(\frac{1}{2}(\eta_\rho + \eta_\sigma))}{\Gamma(\frac{1}{2}(\eta_\rho + \eta_\sigma + 1))} \left(\frac{\pi}{\beta\Lambda} \right)^{\eta_\rho + \eta_\sigma - 1} \end{aligned}$$

Combining these results together, we get

$$G_\rho = \frac{e^2 \eta_\rho}{\pi} \left[1 - \frac{\sqrt{\pi}}{2} \eta_\rho \left(\frac{V_0}{\alpha\Lambda} \right)^2 \frac{\Gamma(\frac{1}{2}(\eta_\rho + \eta_\sigma))}{\Gamma(\frac{1}{2}(\eta_\rho + \eta_\sigma + 1))} \left(\frac{\pi T}{\Lambda} \right)^{\eta_\rho + \eta_\sigma - 2} \right]. \quad (\text{A.2})$$

A.2 Derivation of Eq. (2.29)

To derive Eq. (2.29), we must evaluate the following integral:

$$I_2 \equiv \int_{-\infty}^{\infty} dt \cos(\eta_1 e V t) \exp \left[-\eta_2 \int_0^{\infty} d\omega \frac{e^{-\omega/\Lambda}}{\omega} (1 - e^{-i\omega t}) \right],$$

where η_1 and η_2 are positive constants. From Eq. (A.1) I_2 can be written as

$$I_2 = \int_{-\infty}^{\infty} dt (1 + i\Lambda t)^{-\eta_2} \cos(\eta_1 e V t).$$

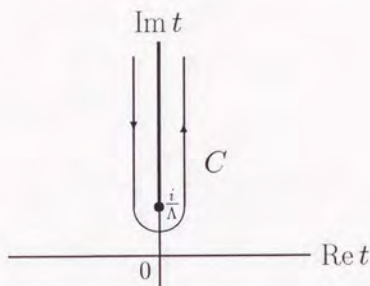
We then rewrite the integral as the integral along the contour C (Fig. A.1),

$$I_2 = \frac{1}{2} \int_C dt (1 + i\Lambda t)^{-\eta_2} \exp(i\eta_1 e V t),$$

and we calculate it as

$$\begin{aligned} I_2 &= \frac{1}{2} \int_0^{\infty} idy \exp \left[-\eta_1 e V \left(\frac{1}{\Lambda} + y \right) \right] (e^{-i\pi} y \Lambda)^{-\eta_2} + \frac{1}{2} \int_0^{\infty} idy \exp \left[-\eta_1 e V \left(\frac{1}{\Lambda} + y \right) \right] (e^{i\pi} y \Lambda)^{-\eta_2} \\ &= \frac{1}{\Lambda} \left(\frac{\eta_1 e V}{\Lambda} \right)^{\eta_2 - 1} \exp(-\eta_1 e V / \Lambda) \sin(\pi \eta_2) \Gamma(1 - \eta_2) \\ &= \frac{\pi}{\Lambda \Gamma(\eta_2)} \left(\frac{\eta_1 e V}{\Lambda} \right)^{\eta_2 - 1} \exp(-\eta_1 e V / \Lambda), \end{aligned}$$

where we have used the well-known identity for the Gamma function, $\Gamma(x)\Gamma(1-x) = \pi/\sin(\pi x)$. Equation (2.29) can be easily obtained from I_2 .

Figure A.1: The contour C of the integral I_2 .

A.3 Conductance from $\langle \bar{\theta}(\omega_n) \bar{\theta}(-\omega_n) \rangle$

We describe below how G_{2n} is obtained from $Q_{2n}(\omega_n)$ by analytic continuation $i\omega_n \rightarrow \omega + i\delta$.

From Eq. (3.24) $Q_2(\omega_n)$ is given by

$$\begin{aligned}
 Q_2(\omega_n) = & -\frac{\beta\pi^2\eta^2}{\omega_n^2} \left(1 + e^{-|\omega_n|/\Delta\epsilon}\right)^2 \left(\frac{V_0}{\pi\alpha}\right)^2 \\
 & \times \int_0^\beta d\tau (1 - \cos \omega_n \tau) \exp\left(-\frac{\pi\eta}{\beta} \sum_{\omega'_n} \frac{1 + e^{-|\omega'_n|/\Delta\epsilon}}{|\omega'_n|} [1 - \cos \omega'_n \tau]\right) \\
 & \times \left\{ \exp\left(-\frac{\pi\eta}{\beta} \sum_{\omega'_n} \frac{1 - \cos \omega'_n \tau}{\frac{2}{\pi}\eta U + \frac{|\omega'_n|}{1 - \exp(-|\omega'_n|/\Delta\epsilon)}}\right) \right. \\
 & \left. + \cos \varphi \exp\left(-\frac{\pi\eta}{\beta} \sum_{\omega'_n} \frac{1 + \cos \omega'_n \tau}{\frac{2}{\pi}\eta U + \frac{|\omega'_n|}{1 - \exp(-|\omega'_n|/\Delta\epsilon)}}\right) \right\}. \quad (\text{A.3})
 \end{aligned}$$

We first consider the simplest case where the charging energy U is negligible. In this case Eq. (A.3) is simplified to

$$\begin{aligned}
 Q_2(\omega_n) = & -\frac{\beta\pi^2\eta^2}{\omega_n^2} \left(1 + e^{-|\omega_n|/\Delta\epsilon}\right)^2 \left(\frac{V_0}{\pi\alpha}\right)^2 \\
 & \times \int_0^\beta d\tau (1 - \cos \omega_n \tau) \left\{ \exp\left(-\frac{2\pi\eta}{\beta} \sum_{\omega'_n} \frac{1}{|\omega'_n|} (1 - \cos \omega'_n \tau)\right) \right. \\
 & \left. + \cos \varphi \exp\left(-\frac{2\pi\eta}{\beta} \sum_{\omega'_n} \frac{1}{|\omega'_n|} (1 - e^{-|\omega'_n|/\Delta\epsilon} \cos \omega'_n \tau)\right) \right\}. \quad (\text{A.4})
 \end{aligned}$$

Note that the integrand is invariant for the transformation, $\tau \rightarrow \beta - \tau$, since $\omega_n = 2\pi n/\beta$. Thus $1 - \cos \omega_n \tau$ in Eq. (A.4) can be replaced by $1 - e^{i\omega_n \tau}$. We then transform the summations over ω'_n into integrals over a continuous variable ω' :

$$S_1(\tau) \equiv \frac{1}{\beta} \sum_{\omega'_n} \frac{1}{|\omega'_n|} (1 - \cos \omega'_n \tau)$$

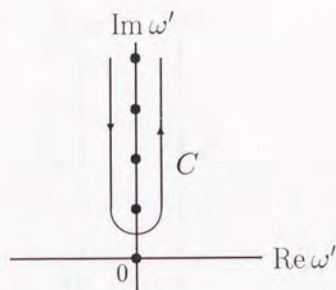


Figure A.2: The contour C . The filled circles are $\omega' = 2\pi nTi$.

$$\begin{aligned}
 &= \frac{1}{\beta} \sum_{\omega'_n > 0} \frac{1}{\omega'_n} \left(1 + e^{i\beta\omega'_n} - e^{i\omega'_n\tau} - e^{i\omega'_n(\beta-\tau)} \right) \\
 &= \frac{1}{2\pi} \int_C d\omega' \frac{1}{e^{\beta\omega'} - 1} \frac{1}{\omega'} \left(1 + e^{\beta\omega'} - e^{\omega'\tau} - e^{\omega'(\beta-\tau)} \right) \\
 &= \frac{1}{\pi} \int_0^\infty d\omega' \frac{e^{-\omega'/\Lambda}}{\omega'} \left(\coth \frac{\beta\omega'}{2} (1 - \cosh \omega'\tau) + \sinh \omega'\tau \right), \quad (\text{A.5})
 \end{aligned}$$

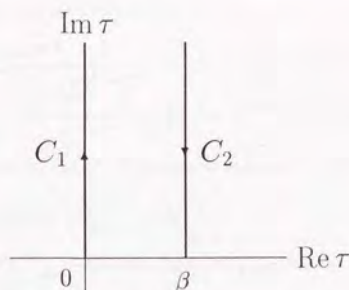
$$\begin{aligned}
 S_2(\tau) &\equiv \frac{1}{\beta} \sum_{\omega'_n} \frac{1}{|\omega'_n|} \left(1 - e^{-|\omega'_n|/\Delta\epsilon} \cos \omega'_n\tau \right) \\
 &= \frac{1}{\beta} \sum_{\omega'_n > 0} \frac{1}{\omega'_n} \left(1 + e^{i\beta\omega'_n} - e^{-\omega'_n/\Delta\epsilon + i\omega'_n\tau} - e^{-\omega'_n/\Delta\epsilon + i\omega'_n(\beta-\tau)} \right) + \frac{1}{\beta\Delta\epsilon} \\
 &= \frac{1}{2\pi} \int_C d\omega' \frac{1}{e^{\beta\omega'} - 1} \frac{1}{\omega'} \left(1 + e^{\beta\omega'} - e^{i\omega'/\Delta\epsilon + \omega'\tau} - e^{i\omega'/\Delta\epsilon + \omega'(\beta-\tau)} \right) + \frac{1}{\beta\Delta\epsilon} \\
 &= \frac{1}{\pi} \int_0^\infty d\omega' \frac{e^{-\omega'/\Lambda}}{\omega'} \frac{1}{e^{\beta\omega'} - 1} \left(1 + e^{\beta\omega'} - e^{\omega'\tau} \cos \frac{\omega'}{\Delta\epsilon} - e^{\omega'(\beta-\tau)} \cos \frac{\omega'}{\Delta\epsilon} \right), \quad (\text{A.6})
 \end{aligned}$$

where we have introduced a cutoff Λ to avoid ultraviolet divergences, and C is the contour depicted in Fig. A.2. Notice that these are still invariant with respect to $\tau \rightarrow \beta - \tau$. Hence we have

$$\begin{aligned}
 Q_2(\omega_n) &= -\frac{\beta\pi^2\eta^2}{\omega_n^2} \left(1 + e^{-|\omega_n|/\Delta\epsilon} \right)^2 \left(\frac{V_0}{\pi\alpha} \right)^2 \\
 &\quad \times \int_0^\beta d\tau \left(1 - e^{i\omega_n\tau} \right) \{ \exp[-2\pi\eta S_1(\tau)] + \cos \varphi \exp[-2\pi\eta S_2(\tau)] \}.
 \end{aligned}$$

We next transform the integral over τ into a contour integral along C_1 ($\tau = it$, $t \geq 0$) and C_2 ($\tau = \beta - it$, $t \leq 0$), which are illustrated in Fig. A.3:

$$\begin{aligned}
 \int_0^\beta d\tau \dots &= \int_{C_1+C_2} d\tau \dots \\
 &= i \int_0^\infty dt \left(1 - e^{-\omega_n t} \right) \{ \exp[-2\pi\eta S_1(it)] + \cos \varphi \exp[-2\pi\eta S_2(it)] \} \\
 &\quad - i \int_{-\infty}^0 dt \left(1 - e^{i\omega_n(\beta-it)} \right) \{ \exp[-2\pi\eta S_1(\beta-it)] + \cos \varphi \exp[-2\pi\eta S_2(\beta-it)] \}
 \end{aligned}$$

Figure A.3: The contour C_1 and C_2 .

$$= i \int_0^{\infty} dt (1 - e^{-\omega n t}) \{ \exp[-2\pi\eta S_1(it)] + \cos \varphi \exp[-2\pi\eta S_2(it)] \} \\ - i \int_{-\infty}^0 dt (1 - e^{\omega n t}) \{ \exp[-2\pi\eta S_1(it)] + \cos \varphi \exp[-2\pi\eta S_2(it)] \}.$$

The retarded correlation function $Q_2^R(\omega)$ is readily obtained just by setting $\omega_n \rightarrow -i\omega$:

$$Q_2^R(\omega) = i \frac{\beta \pi^2 \eta^2}{\omega^2} (1 + e^{i\omega/\Delta\epsilon})^2 \left(\frac{V_0}{\pi\alpha} \right)^2 \\ \times \left\{ \int_0^{\infty} dt (1 - e^{i\omega t}) (\exp[-2\pi\eta S_1(it)] + \cos \varphi \exp[-2\pi\eta S_2(it)]) \right. \\ \left. - \int_{-\infty}^0 dt (1 - e^{-i\omega t}) (\exp[-2\pi\eta S_1(it)] + \cos \varphi \exp[-2\pi\eta S_2(it)]) \right\}.$$

By definition, the conductance G_2 is obtained as

$$G_2 = -\frac{i}{\beta} \left(\frac{e}{2\pi} \right)^2 \lim_{\omega \rightarrow +0} \omega Q_2^R(\omega) \\ = -ie^2 \eta^2 \left(\frac{V_0}{\pi\alpha} \right)^2 \int_{-\infty}^{\infty} dt t \left\{ \exp[-2\pi\eta S_1(it)] + \cos \varphi \exp[-2\pi\eta S_2(it)] \right\}. \quad (\text{A.7})$$

Since the integrand in Eq. (A.7) is analytic in the region $-\beta \leq \text{Im } t \leq 0$, we can transform the integral as follows:

$$G_2 = -ie^2 \eta^2 \left(\frac{V_0}{\pi\alpha} \right)^2 \int_{-\infty}^{\infty} dt (t - i\beta) \left\{ \exp[-2\pi\eta S_1(it + \beta)] + \cos \varphi \exp[-2\pi\eta S_2(it + \beta)] \right\} \\ = ie^2 \eta^2 \left(\frac{V_0}{\pi\alpha} \right)^2 \int_{-\infty}^{\infty} dt (t + i\beta) \left\{ \exp[-2\pi\eta S_1(\beta - it)] + \cos \varphi \exp[-2\pi\eta S_2(\beta - it)] \right\} \\ = -\frac{1}{2} e^2 \eta^2 \beta \left(\frac{V_0}{\pi\alpha} \right)^2 \int_{-\infty}^{\infty} dt \left\{ \exp[-2\pi\eta S_1(it)] + \cos \varphi \exp[-2\pi\eta S_2(it)] \right\},$$

where we have used the identity, $S_j(\beta - it) = S_j(it)$. The remaining task is to perform the t -integration. To this end, we must know the explicit form of $S_1(it)$ and $S_2(it)$. $S_1(it)$ has already been calculated in Appendix A.1 and is given by

$$S_1(it) = \frac{1}{\pi} \ln \left[(1 + i\Delta t) \frac{\beta}{\pi t} \sinh \frac{\pi t}{\beta} \right].$$

The calculation of $S_2(it)$ proceeds as follows:

$$S_2(it) = \frac{1}{\pi} \int_0^\infty d\omega \frac{e^{-\omega/\Lambda}}{\omega} \frac{1}{e^{\beta\omega} - 1} \left(1 + e^{\beta\omega} - e^{i\omega t} - e^{\omega(\beta-it)} \right) \\ + \frac{1}{\pi} \int_0^\infty d\omega \frac{e^{-\omega/\Lambda}}{\omega} \frac{1}{e^{\beta\omega} - 1} \left(e^{i\omega t} + e^{\omega(\beta-it)} \right) \left(1 - \cos \frac{\omega}{\Delta\epsilon} \right),$$

where the first integral is equal to $S_1(\tau)$. The second integral is calculated as

$$\int_0^\infty d\omega \frac{e^{-\omega/\Lambda}}{\omega} \frac{1}{e^{\beta\omega} - 1} \left(e^{i\omega t} + e^{\omega(\beta-it)} \right) \left(1 - \cos \frac{\omega}{\Delta\epsilon} \right) \\ = \frac{1}{2i} \sum_{n=1}^\infty \int_0^{1/\Delta\epsilon} dx \int_0^\infty d\omega e^{-\omega/\Lambda - n\beta\omega} \left(e^{i\omega(x+t)} + e^{\omega(\beta+ix-it)} - e^{-i\omega(x-t)} - e^{\omega(\beta-ix-it)} \right) \\ \approx \int_0^{1/\Delta\epsilon} dx \frac{x}{\left(\frac{1}{\Lambda} + it\right)^2 + x^2} + \sum_{n=1}^\infty \int_0^{1/\Delta\epsilon} dx \left\{ \frac{x}{(n\beta - it)^2 + x^2} + \frac{x}{(n\beta + it)^2 + x^2} \right\} \\ = \frac{1}{2} \ln \left[\frac{(1 + i\Lambda t)^2 + (\Lambda/\Delta\epsilon)^2}{(1 + i\Lambda t)^2} \right] - \frac{1}{2} \ln \left[1 + \left(\frac{1}{it\Delta\epsilon} \right)^2 \right] + \frac{1}{2} \ln \left[\frac{\cosh \frac{2\pi}{\beta\Delta\epsilon} - \cosh \frac{2\pi t}{\beta}}{1 - \cosh \frac{2\pi t}{\beta}} \right],$$

where we have assumed that $\beta\Lambda$ is much larger than unity and used the identity,

$$\prod_{n=-\infty}^\infty \left[1 + \frac{x^2}{(a - 2n\pi)^2} \right] = \frac{\cosh x - \cos a}{1 - \cos a}.$$

Thus $S_2(it)$ is given by

$$S_2(it) = \frac{1}{2\pi} \ln \left[(1 + i\Lambda t)^2 + \left(\frac{\Lambda}{\Delta\epsilon} \right)^2 \right] + \frac{1}{2\pi} \ln \left[\frac{\sinh^2 \frac{\pi}{\beta\Delta\epsilon} - \sinh^2 \frac{\pi t}{\beta}}{\left(\frac{\pi}{\beta\Delta\epsilon} \right)^2 - \left(\frac{\pi t}{\beta} \right)^2} \right].$$

In calculating G_2 , we slide the integration path by $-i\beta/2$:

$$G_2 = -\frac{1}{2} e^2 \eta^2 \beta \left(\frac{V_0}{\pi\alpha} \right)^2 \int_{-\infty}^\infty dt \left\{ \exp[-2\pi\eta S_1(it + \frac{\beta}{2})] + \cos \varphi \exp[-2\pi\eta S_2(it + \frac{\beta}{2})] \right\}.$$

It then turns out that $S_1(it + \frac{\beta}{2})$ and $S_2(it + \frac{\beta}{2})$ can be approximated as

$$\exp[-2\pi\eta S_1(it + \frac{\beta}{2})] \approx \left[\frac{\beta\Lambda}{\pi} \cosh \frac{\pi t}{\beta} \right]^{-2\eta}, \\ \exp[-2\pi\eta S_2(it + \frac{\beta}{2})] \approx \left[\left(\frac{\beta\Lambda}{\pi} \right)^2 \left(\sinh^2 \frac{\pi}{\beta\Delta\epsilon} + \cosh^2 \frac{\pi t}{\beta} \right) \right]^{-\eta}.$$

Hence G_2 is given by

$$G_2 = -\frac{1}{2} e^2 \eta^2 \beta \left(\frac{V_0}{\pi\alpha} \right)^2 \left(\frac{\beta\Lambda}{\pi} \right)^{-2\eta} \int_{-\infty}^\infty dt \left\{ \left(\cosh \frac{\pi t}{\beta} \right)^{-2\eta} + \cos \varphi \left(\sinh^2 \frac{\pi}{\beta\Delta\epsilon} + \cosh^2 \frac{\pi t}{\beta} \right)^{-\eta} \right\}.$$

If $T \ll \Delta\epsilon$, then $\sinh \frac{\pi}{\beta\Delta\epsilon} \approx \pi/\beta\Delta\epsilon$. Thus G_2 is calculated as

$$G_2 = -\frac{1}{2} e^2 \eta^2 \beta \left(\frac{V_0}{\pi\alpha} \right)^2 \left(\frac{\beta\Lambda}{\pi} \right)^{-2\eta}$$

$$\begin{aligned} & \times \int_{-\infty}^{\infty} dt \left\{ \left(\cosh \frac{\pi t}{\beta} \right)^{-2\eta} + \cos \varphi \left[\left(\cosh \frac{\pi t}{\beta} \right)^{-2\eta} - \eta \left(\frac{\pi}{\beta \Delta \epsilon} \right)^2 \left(\cosh \frac{\pi t}{\beta} \right)^{-2\eta-2} - \dots \right] \right\} \\ & = -\frac{e^2 \eta^2 \sqrt{\pi} \Gamma(\eta)}{2\pi \Gamma(\eta + \frac{1}{2})} \left(\frac{V_0}{\alpha \Lambda} \right)^2 \left(\frac{\pi T}{\Lambda} \right)^{2\eta-2} \left\{ 1 + \cos \varphi \left[1 - \frac{2\eta^2}{2\eta + 1} \left(\frac{\pi T}{\Delta \epsilon} \right)^2 - \dots \right] \right\}. \quad (\text{A.8}) \end{aligned}$$

If $T \gg \Delta \epsilon$, on the other hand, G_2 is

$$G_2 = -\frac{e^2 \eta^2 \sqrt{\pi} \Gamma(\eta)}{2\pi \Gamma(\eta + \frac{1}{2})} \left(\frac{V_0}{\alpha \Lambda} \right)^2 \left(\frac{\pi T}{\Lambda} \right)^{2\eta-2} \left\{ 1 + c \frac{T}{\Delta \epsilon} \exp(-2\pi\eta T/\Delta \epsilon) \cos \varphi \right\}, \quad (\text{A.9})$$

where c is a dimensionless constant of order 1. Notice that Eqs. (A.8) and (A.9) reproduce the correct results for the noninteracting case [(3.5) and (3.6)] if we set $\eta = 1$ and $V_0/\alpha\Lambda = V/2W$.

Another useful but approximate method to obtain the above results is to do the following replacement in Eq. (A.3):

$$\frac{1}{\omega_n} \int_0^\beta d\tau (1 - \cos \omega_n \tau) \Rightarrow A\beta^2, \quad (\text{A.10})$$

$$\exp\left(-\frac{\pi\eta}{\beta} \sum_{\omega'_n} \frac{1 + e^{-|\omega'_n|/\Delta \epsilon}}{|\omega'_n|} [1 - \cos \omega'_n \tau]\right) \Rightarrow \begin{cases} \left(\frac{\pi T}{\Lambda}\right)^\eta, & T \gg \Delta \epsilon \\ \left(\frac{\pi T}{\Lambda} \frac{\pi T}{\Delta \epsilon}\right)^\eta, & T \ll \Delta \epsilon, \end{cases} \quad (\text{A.11})$$

$$\exp\left(-\frac{\pi\eta}{\beta} \sum_{\omega'_n} \frac{1 - e^{-|\omega'_n|/\Delta \epsilon}}{|\omega'_n|}\right) \Rightarrow \begin{cases} \left(\frac{\pi T}{\Lambda}\right)^\eta \exp(-\pi\eta T/\Delta \epsilon), & T \gg \Delta \epsilon \\ \left(\frac{\Delta \epsilon}{\Lambda}\right)^\eta, & T \ll \Delta \epsilon, \end{cases} \quad (\text{A.12})$$

$$\exp\left(-\frac{\pi\eta}{\beta} \sum_{\omega'_n} \frac{1 - e^{-|\omega'_n|/\Delta \epsilon}}{|\omega'_n|} \cos \omega'_n \tau\right) \Rightarrow \begin{cases} \exp(-\pi\eta T/\Delta \epsilon), & T \gg \Delta \epsilon \\ 1 + O((T/\Delta \epsilon)^2), & T \ll \Delta \epsilon, \end{cases} \quad (\text{A.13})$$

where A is a constant of order 1. The conductance is symbolically given by $G \Leftrightarrow (\omega_n/\beta)(e/2\pi)^2 Q(\omega_n)$. For example, the T dependence of the first term in Eq. (A.8) is obtained from Eqs. (A.10)–(A.13) as $(V_0/\alpha)^2 \cdot A\beta^2 \cdot [(\pi T/\Lambda)(\pi T/\Delta \epsilon)]^\eta \cdot (\Delta \epsilon/\Lambda)^\eta = A(V_0/\alpha\Lambda)^2 \times (\pi T/\Lambda)^{2\eta-2}$. We must note that, though this method is useful, we cannot get the higher-order correction terms, such as the term proportional to $(\pi T/\Delta \epsilon)^2$ in Eq. (A.8).

When $U \gg \Delta \epsilon$, it is difficult to calculate G_2 explicitly from Eq. (A.3). Thus we use the simplified method described above. In this case the propagator for $\bar{\theta}$ changes from $(1 - e^{-|\omega_n|/\Delta \epsilon})/|\omega_n|$ to $(\frac{|\omega_n|}{1 - \exp(-|\omega_n|/\Delta \epsilon)} + \frac{2}{\pi}\eta U)^{-1}$. Accordingly, Eqs. (A.12) and (A.13) are modified as follows.

$$\exp\left(-\frac{\pi\eta}{\beta} \sum_{\omega'_n} \left[\frac{|\omega'_n|}{1 - e^{-|\omega'_n|/\Delta \epsilon}} + \frac{2}{\pi}\eta U \right]^{-1}\right) \Rightarrow \begin{cases} \left(\frac{\pi T}{\Lambda}\right)^\eta \exp(-\pi^2 T/U), & T \gg U \\ \left(\frac{2\eta U}{\pi\Lambda}\right)^\eta, & T \ll U, \end{cases} \quad (\text{A.14})$$

$$\exp\left(-\frac{\pi\eta}{\beta} \sum_{\omega'_n} \left[\frac{|\omega'_n|}{1 - e^{-|\omega'_n|/\Delta \epsilon}} + \frac{2}{\pi}\eta U \right]^{-1} \cos \omega'_n \tau\right) \Rightarrow \begin{cases} \exp(-\pi^2 T/2U), & T \gg U \\ 1 + O((T/U)^2), & T \ll U. \end{cases} \quad (\text{A.15})$$

On the other hand, the propagator for $\bar{\theta}$ does not change, and thus Eq. (A.11) is applicable also for nonzero U . From these correspondences (A.10), (A.11), (A.14), and (A.15), we can

easily estimate G_2 . The T dependence of G_2 is different for three temperature ranges:

$$G_2 = \begin{cases} -A_1 e^2 \left(\frac{V_0}{\alpha\Lambda}\right)^2 \left(\frac{\pi T}{\Lambda}\right)^{2\eta-2} \left(\frac{2\eta U}{\Delta\epsilon}\right)^\eta (1 + \cos\varphi), & T \ll \Delta\epsilon \\ -A_2 e^2 \left(\frac{V_0}{\alpha\Lambda}\right)^2 \left(\frac{\pi T}{\Lambda}\right)^{\eta-2} \left(\frac{2\eta U}{\pi\Lambda}\right)^\eta (1 + \cos\varphi), & \Delta\epsilon \ll T \ll U \\ -A_3 e^2 \left(\frac{V_0}{\alpha\Lambda}\right)^2 \left(\frac{\pi T}{\Lambda}\right)^{2\eta-2}, & T \gg U, \end{cases} \quad (\text{A.16})$$

where the A_i 's are dimensionless constants of order 1. Note that Eq. (A.16) contains only the leading term.

Next we shall evaluate the 4th-order term. From Eq. (3.24) $Q_4(\omega_n)$ is obtained as

$$\begin{aligned} Q_4(\omega_n) &= \frac{\pi^2 \eta^2}{2\omega_n^2} \left(1 + e^{-|\omega_n|/\Delta\epsilon}\right)^2 \left(\frac{V_0}{\pi\alpha}\right)^4 \\ &\quad \times \int_0^\beta d\tau_1 \int_0^\beta d\tau_2 \int_0^\beta d\tau_3 \int_0^\beta d\tau_4 (1 - \cos\omega_n\tau_{12}) \\ &\quad \times \exp\left(-\frac{\pi\eta}{\beta} \sum_{\omega'_n} \tilde{g}(\omega'_n)(1 - \cos\omega'_n\tau_{12}) - \frac{\pi\eta}{\beta} \sum_{\omega'_n} \tilde{g}(\omega'_n)(1 - \cos\omega'_n\tau_{34})\right) \\ &\quad \times \left\{ \exp\left(-\frac{\pi\eta}{\beta} \sum_{\omega'_n} \tilde{g}(\omega'_n)(1 - \cos\omega'_n\tau_{12})\right) + \cos\varphi \exp\left(-\frac{\pi\eta}{\beta} \sum_{\omega'_n} \tilde{g}(\omega'_n)(1 + \cos\omega'_n\tau_{12})\right) \right\} \\ &\quad \times \left\{ \exp\left(-\frac{\pi\eta}{\beta} \sum_{\omega'_n} \tilde{g}(\omega'_n)(1 - \cos\omega'_n\tau_{34})\right) + \cos\varphi \exp\left(-\frac{\pi\eta}{\beta} \sum_{\omega'_n} \tilde{g}(\omega'_n)(1 + \cos\omega'_n\tau_{34})\right) \right\} \\ &= \frac{\pi^2 \eta^2}{\omega_n^2} \left(1 + e^{-|\omega_n|/\Delta\epsilon}\right)^2 \left(\frac{V_0}{2\pi\alpha}\right)^4 \int_0^\beta d\tau_1 \int_0^\beta d\tau_2 \int_0^\beta d\tau_3 \int_0^\beta d\tau_4 \\ &\quad \times (2 + \cos\omega_n\tau_{12} + \cos\omega_n\tau_{34} - \cos\omega_n\tau_{13} - \cos\omega_n\tau_{14} - \cos\omega_n\tau_{23} - \cos\omega_n\tau_{24}) \\ &\quad \times \exp\left(-\frac{\pi\eta}{\beta} \sum_{\omega'_n} \tilde{g}(\omega'_n)(2 + \cos\omega'_n\tau_{12} + \cos\omega'_n\tau_{34} - \cos\omega'_n\tau_{13} \right. \\ &\quad \left. - \cos\omega'_n\tau_{14} - \cos\omega'_n\tau_{23} - \cos\omega'_n\tau_{24})\right) \\ &\quad \times \left\{ \cos 2\varphi \exp\left(-\frac{\pi\eta}{\beta} \sum_{\omega'_n} \tilde{g}(\omega'_n)(2 + \cos\omega'_n\tau_{12} + \cos\omega'_n\tau_{13} + \cos\omega'_n\tau_{14} \right. \right. \\ &\quad \left. \left. + \cos\omega'_n\tau_{23} + \cos\omega'_n\tau_{24} + \cos\omega'_n\tau_{34})\right) \right. \\ &\quad \left. + \cos\varphi \exp\left(-\frac{\pi\eta}{\beta} \sum_{\omega'_n} \tilde{g}(\omega'_n)(2 + \cos\omega'_n\tau_{12} + \cos\omega'_n\tau_{13} + \cos\omega'_n\tau_{23} \right. \right. \\ &\quad \left. \left. - \cos\omega'_n\tau_{14} - \cos\omega'_n\tau_{24} - \cos\omega'_n\tau_{34})\right) \right. \\ &\quad \left. + \cos\varphi \exp\left(-\frac{\pi\eta}{\beta} \sum_{\omega'_n} \tilde{g}(\omega'_n)(2 + \cos\omega'_n\tau_{12} + \cos\omega'_n\tau_{14} + \cos\omega'_n\tau_{24} \right. \right. \\ &\quad \left. \left. - \cos\omega'_n\tau_{13} - \cos\omega'_n\tau_{23} - \cos\omega'_n\tau_{34})\right) \right. \\ &\quad \left. + \cos\varphi \exp\left(-\frac{\pi\eta}{\beta} \sum_{\omega'_n} \tilde{g}(\omega'_n)(2 + \cos\omega'_n\tau_{13} + \cos\omega'_n\tau_{14} + \cos\omega'_n\tau_{34} \right. \right. \\ &\quad \left. \left. - \cos\omega'_n\tau_{12} - \cos\omega'_n\tau_{23} - \cos\omega'_n\tau_{24})\right) \right. \\ &\quad \left. + \cos\varphi \exp\left(-\frac{\pi\eta}{\beta} \sum_{\omega'_n} \tilde{g}(\omega'_n)(2 + \cos\omega'_n\tau_{23} + \cos\omega'_n\tau_{24} + \cos\omega'_n\tau_{34} \right. \right. \\ &\quad \left. \left. - \cos\omega'_n\tau_{12} - \cos\omega'_n\tau_{13} - \cos\omega'_n\tau_{14})\right) \right\} \end{aligned}$$

$$\begin{aligned}
& + \exp\left(-\frac{\pi\eta}{\beta} \sum_{\omega'_n} \bar{g}(\omega'_n) (2 + \cos \omega'_n \tau_{12} + \cos \omega'_n \tau_{34} - \cos \omega'_n \tau_{13} \right. \\
& \quad \left. - \cos \omega'_n \tau_{14} - \cos \omega'_n \tau_{23} - \cos \omega'_n \tau_{24})\right) \\
& + \exp\left(-\frac{\pi\eta}{\beta} \sum_{\omega'_n} \bar{g}(\omega'_n) (2 + \cos \omega'_n \tau_{13} + \cos \omega'_n \tau_{24} - \cos \omega'_n \tau_{12} \right. \\
& \quad \left. - \cos \omega'_n \tau_{14} - \cos \omega'_n \tau_{23} - \cos \omega'_n \tau_{34})\right) \\
& + \exp\left(-\frac{\pi\eta}{\beta} \sum_{\omega'_n} \bar{g}(\omega'_n) (2 + \cos \omega'_n \tau_{14} + \cos \omega'_n \tau_{23} - \cos \omega'_n \tau_{12} \right. \\
& \quad \left. - \cos \omega'_n \tau_{13} - \cos \omega'_n \tau_{24} - \cos \omega'_n \tau_{34})\right) \Big\} \quad (\text{A.17})
\end{aligned}$$

$$\equiv Q_{4,1}(\omega_n) + Q_{4,2}(\omega_n),$$

where

$$\tau_{ij} = \tau_i - \tau_j, \quad \bar{g}(\omega_n) = \frac{1 + e^{-|\omega_n|/\Delta\epsilon}}{|\omega_n|}, \quad \tilde{g}(\omega_n) = \left(\frac{2\eta U}{\pi} + \frac{|\omega_n|}{1 - e^{-|\omega_n|/\Delta\epsilon}} \right)^{-1}.$$

Accordingly, the 4th-order conductance consists of two parts: $G_4 = G_{4,1} + G_{4,2}$, where $G_{4,i} = -(i/\beta)(e/2\pi)^2 \lim_{\omega \rightarrow 0} \omega Q_{4,i}^R(\omega)$. Using Eqs. (A.11)–(A.15) and the replacement

$$\frac{1}{\omega_n} \int_0^\beta d\tau_1 \int_0^\beta d\tau_2 \int_0^\beta d\tau_3 \int_0^\beta d\tau_4 (1 - \cos \omega_n \tau_{12}) \Rightarrow \beta^5,$$

we can easily estimate $G_{4,1}$ as

$$G_{4,1} = B e^2 \left(\frac{G_2}{e^2} \right)^2, \quad (\text{A.18})$$

where B is a dimensionless constant.

As shown in Sec. 3.3.1, the second-order cumulant expansion of the barrier potential $V_0 \cos \bar{\theta} \cos \hat{\theta}$ yields the effective potential $V_2 \cos 2\hat{\theta}$. It seems natural to expect that the most important contribution in $G_{4,2}$ comes from this effective action. To extract its contribution, we proceed in the following way. We first set $\tau_1 = \tau_2$ and $\tau_3 = \tau_4$ in the integrand of $Q_{4,2}$ and replace both $\int d\tau_2$ and $\int d\tau_4$ by $\tau_0 \equiv 1/[U + \frac{\pi}{2\eta}\Delta\epsilon]$ to get

$$\begin{aligned}
Q_{4,2} \Rightarrow & -\frac{\pi^2 \eta^2}{\omega_n^2} (1 + e^{-|\omega_n|/\Delta\epsilon})^2 \left(\frac{V_0}{2\pi\alpha} \right)^4 \\
& \times \tau_0^2 \int_0^\beta d\tau_1 \int_0^\beta d\tau_3^2 (1 - \cos \omega_n \tau_{13}) \exp\left(-\frac{4\pi\eta}{\beta} \sum_{\omega'_n} \bar{g}(\omega'_n) (1 - \cos \omega'_n \tau_{13})\right) \\
& \times \left\{ \cos 2\varphi \exp\left(-\frac{4\pi\eta}{\beta} \sum_{\omega'_n} \tilde{g}(\omega'_n) (1 + \cos \omega'_n \tau_{13})\right) \right. \\
& \quad + 4 \cos \varphi \exp\left(-\frac{2\pi\eta}{\beta} \sum_{\omega'_n} \tilde{g}(\omega'_n)\right) \\
& \quad \left. + \exp\left(-\frac{4\pi\eta}{\beta} \sum_{\omega'_n} \tilde{g}(\omega'_n) (1 - \cos \omega'_n \tau_{13})\right) + 2 \right\}.
\end{aligned}$$

We then apply the replacement rules (A.10)–(A.15) to the above equation. Hence $G_{4,2}$ is estimated for $U \gg \Delta\epsilon$ as

$$G_{4,2} = -C_1 e^2 \left(\frac{V_0}{\pi\alpha\Lambda} \right)^4 \left(\frac{\Lambda}{U} \right)^2 \left(\frac{\pi T}{\Delta\epsilon} \right)^{4\eta} \left(\frac{\pi T}{\Lambda} \right)^{4\eta-2} \left[1 + \left(\frac{2\eta U}{\pi\Lambda} \right)^{2\eta} \cos \varphi \right]^2 \quad (\text{A.19})$$

for $T \ll \Delta\epsilon$ and

$$G_{4,2} = -C_2 e^2 \left(\frac{V_0}{\pi\alpha\Lambda} \right)^4 \left(\frac{\Lambda}{U} \right)^2 \left(\frac{\pi T}{\Lambda} \right)^{4\eta-2} \left[1 + \left(\frac{2\eta U}{\pi\Lambda} \right)^{2\eta} \cos\varphi \right]^2 \quad (\text{A.20})$$

for $\Delta\epsilon \ll T \ll U$. C_1 and C_2 are dimensionless constants. If $U = 0$, then $G_{4,2}$ is estimated for $T \ll \Delta\epsilon$ as

$$G_{4,2} = -C_3 e^2 \left(\frac{V_0}{\pi\alpha\Lambda} \right)^4 \left(\frac{\Lambda}{\Delta\epsilon} \right)^2 \left(\frac{\pi T}{\Delta\epsilon} \right)^{4\eta} \left(\frac{\pi T}{\Lambda} \right)^{4\eta-2} \left[1 + \left(\frac{\Delta\epsilon}{\Lambda} \right)^{2\eta} \cos\varphi \right]^2, \quad (\text{A.21})$$

where C_3 is a dimensionless constant. Note that in Eqs. (A.19)–(A.21) $G_{4,2}$ is proportional to $[1 + \cos\varphi \exp(-\frac{2\eta}{\beta} \sum \tilde{g})]^2$. This factor can be traced to $(\cos(\frac{1}{2}\tilde{\theta} + k_F R) \cos(\frac{1}{2}\tilde{\theta} + k_F R))$ in Eq. (3.17). We should also note that Eqs. (A.19)–(A.21) are only parts of the whole conductance coming from $Q_{4,2}$. That is, there are other terms in $G_{4,2}$ that are less important at low temperatures.

A.4 Equivalence between two models

In this appendix, we demonstrate the equivalence between the model described by the effective action (3.13) and the system described by the Hamiltonian (3.40).

We first integrate out the harmonic oscillators $\{X_\alpha\}$ and $\{x_\beta\}$:

$$\begin{aligned} & \int \prod_\alpha \mathcal{D}X_\alpha \int \prod_\beta \mathcal{D}x_\beta \exp \left[-\sum_\alpha \int_0^\beta d\tau \left(\frac{M_\alpha}{2} (\partial_\tau X_\alpha)^2 + \frac{1}{2} M_\alpha \Omega_\alpha^2 X_\alpha^2 + \tilde{\lambda}_\alpha \tilde{\theta} X_\alpha + \frac{\tilde{\lambda}^2 \tilde{\theta}^2}{2M_\alpha \Omega_\alpha^2} \right) \right. \\ & \quad - \sum_\beta \int_0^\beta d\tau \left(\frac{m_\beta}{2} (\partial_\tau x_\beta)^2 + \frac{1}{2} m_\beta \omega_\beta^2 x_\beta^2 + \tilde{\lambda}_\beta \tilde{\theta} x_\beta + \frac{\tilde{\lambda}^2 \tilde{\theta}^2}{2m_\beta \omega_\beta^2} \right) \\ & \quad - \frac{1}{8\pi^2} \left(2U + \frac{\pi}{\eta} \Delta\epsilon \right) \int_0^\beta d\tau \tilde{\theta}^2 + \frac{e}{2\pi} \int_0^\beta d\tau (V\tilde{\theta} + V_g \tilde{\theta}) \\ & \quad \left. - \frac{2V_0}{\pi\alpha} \int_0^\beta d\tau \left(1 - \cos\tilde{\theta} \cos\frac{\tilde{\theta}}{2} \right) \right] \\ & \propto \exp \left[-\frac{1}{\beta} \sum_{\omega_n} \sum_\alpha \frac{\omega_n^2 \tilde{\lambda}_\alpha^2}{2M_\alpha \Omega_\alpha^2 (\Omega_\alpha^2 + \omega_n^2)} |\tilde{\theta}(\omega_n)|^2 - \frac{1}{\beta} \sum_{\omega_n} \sum_\beta \frac{\omega_n^2 \tilde{\lambda}_\beta^2}{2m_\beta \omega_\beta^2 (\omega_\beta^2 + \omega_n^2)} |\tilde{\theta}(\omega_n)|^2 \right. \\ & \quad - \frac{1}{8\pi^2} \left(2U + \frac{\pi}{\eta} \Delta\epsilon \right) \int_0^\beta d\tau \tilde{\theta}^2 + \frac{e}{2\pi} \int_0^\beta d\tau (V\tilde{\theta} + V_g \tilde{\theta}) \\ & \quad \left. - \frac{2V_0}{\pi\alpha} \int_0^\beta d\tau \left(1 - \cos\tilde{\theta} \cos\frac{\tilde{\theta}}{2} \right) \right]. \quad (\text{A.22}) \end{aligned}$$

Using the spectral function (3.41), we get

$$\begin{aligned} \sum_\alpha \frac{\omega_n^2 \tilde{\lambda}_\alpha^2}{2M_\alpha \Omega_\alpha^2 (\Omega_\alpha^2 + \omega_n^2)} &= \frac{\omega_n^2}{\pi} \int_0^\infty d\omega \frac{\tilde{J}(\omega)}{\omega(\omega^2 + \omega_n^2)} \\ &= \frac{\omega_n^2}{\pi^2 \eta} \left\{ \frac{1}{2} \int_0^\infty \frac{d\omega}{\omega^2 + \omega_n^2} + \pi \Delta\epsilon \sum_{n=1}^\infty \frac{1}{\omega_n^2 + [\pi \Delta\epsilon (2n-1)]^2} \right\} \\ &= \frac{\omega_n^2}{\pi^2 \eta} \left(\frac{\pi}{4|\omega_n|} + \frac{\pi}{4|\omega_n|} \tanh \frac{|\omega_n|}{2\Delta\epsilon} \right) \end{aligned}$$

$$= \frac{1}{2\pi\eta} \frac{|\omega_n|}{1 + \exp(-|\omega_n|/\Delta\epsilon)}. \quad (\text{A.23})$$

In the same way, from Eq. (3.42) we obtain

$$\begin{aligned} \sum_{\beta} \frac{\omega_n^2}{2m_{\beta}\omega_{\beta}^2(\omega_{\beta}^2 + \omega_n^2)} &= \frac{\omega_n^2}{\pi} \int_0^{\infty} d\omega \frac{\tilde{J}(\omega)}{\omega(\omega^2 + \omega_n^2)} \\ &= \frac{1}{8\pi\eta} \frac{|\omega_n|}{1 + \exp(-|\omega_n|/\Delta\epsilon)} - \frac{\Delta\epsilon}{8\pi\eta}. \end{aligned} \quad (\text{A.24})$$

From Eqs. (A.22), (A.23), and (A.24), we see that the right-hand side of Eq. (A.22) is $\exp(-S_{\text{eff}})$.

A.5 Derivation of Eqs. (3.43) and (3.45)

The Hamiltonians H_i , H_m , and H_f used in the calculation of Γ and G in Sec. 3.4.2 can be rewritten in terms of boson creation (annihilation) operators, a_{α}^{\dagger} and b_{β}^{\dagger} (a_{α} and b_{β}), of the harmonic oscillators:

$$\begin{aligned} H_i &= \sum_{\alpha} \Omega_{\alpha} \left(a_{\alpha}^{\dagger} a_{\alpha} + \frac{1}{2} \right) + \sum_{\beta} \omega_{\beta} \left(b_{\beta}^{\dagger} b_{\beta} + \frac{1}{2} \right), \\ H_m &= \sum_{\alpha} \left[\Omega_{\alpha} \left(a_{\alpha}^{\dagger} a_{\alpha} + \frac{1}{2} \right) + \frac{\pi \bar{\lambda}_{\alpha}}{\sqrt{2M_{\alpha}\Omega_{\alpha}}} (a_{\alpha}^{\dagger} + a_{\alpha}) + \frac{\pi^2 \bar{\lambda}_{\alpha}^2}{2M_{\alpha}\Omega_{\alpha}^2} \right] \\ &\quad + \sum_{\beta} \left[\omega_{\beta} \left(b_{\beta}^{\dagger} b_{\beta} + \frac{1}{2} \right) - \frac{2\pi \bar{\lambda}_{\beta}}{\sqrt{2m_{\beta}\omega_{\beta}}} (b_{\beta}^{\dagger} + b_{\beta}) + \frac{2\pi^2 \bar{\lambda}_{\beta}^2}{m_{\beta}\omega_{\beta}^2} \right] + U + \frac{\pi}{2\eta} \Delta\epsilon + eV_g - \frac{1}{2}eV \\ &= O_m^{\dagger} H_i O_m + \varepsilon - \frac{1}{2}eV, \\ H_f &= \sum_{\alpha} \left[\Omega_{\alpha} \left(a_{\alpha}^{\dagger} a_{\alpha} + \frac{1}{2} \right) + \frac{2\pi \bar{\lambda}_{\alpha}}{\sqrt{2M_{\alpha}\Omega_{\alpha}}} (a_{\alpha}^{\dagger} + a_{\alpha}) + \frac{2\pi^2 \bar{\lambda}_{\alpha}^2}{M_{\alpha}\Omega_{\alpha}^2} \right] + \sum_{\beta} \omega_{\beta} \left(b_{\beta}^{\dagger} b_{\beta} + \frac{1}{2} \right) - eV \\ &= O_f^{\dagger} H_i O_f - eV, \end{aligned}$$

where

$$\begin{aligned} O_m &= \exp \left[\sum_{\alpha} \frac{\pi \bar{\lambda}_{\alpha}}{\sqrt{2M_{\alpha}\Omega_{\alpha}^3}} (a_{\alpha}^{\dagger} - a_{\alpha}) - \sum_{\beta} \frac{2\pi \bar{\lambda}_{\beta}}{\sqrt{2m_{\beta}\omega_{\beta}^3}} (b_{\beta}^{\dagger} - b_{\beta}) \right], \\ O_f &= \exp \left[\sum_{\alpha} \frac{2\pi \bar{\lambda}_{\alpha}}{\sqrt{2M_{\alpha}\Omega_{\alpha}^3}} (a_{\alpha}^{\dagger} - a_{\alpha}) \right]. \end{aligned}$$

Using these relations, Eq. (3.43) can be written as

$$\Gamma = 2t^2 \int_{-\infty}^{\infty} dt_0 \langle O_m^{\dagger} e^{-iH_i t_0} O_m e^{iH_i t_0} \rangle_i, \quad (\text{A.25})$$

where we have neglected ε because, only when $\varepsilon \approx 0$, Γ plays an important role in the calculation of G . The integrand in Eq. (A.25) can be calculated as follows:

$$\langle O_m^{\dagger} e^{-iH_i t_0} O_m e^{iH_i t_0} \rangle_i = \left\langle \exp \left[- \sum_{\alpha} \frac{\pi \bar{\lambda}_{\alpha}}{2M_{\alpha}\Omega_{\alpha}^3} (a_{\alpha}^{\dagger} - a_{\alpha}) + \sum_{\beta} \frac{2\pi \bar{\lambda}_{\beta}}{\sqrt{2m_{\beta}\omega_{\beta}^3}} (b_{\beta}^{\dagger} - b_{\beta}) \right] \right\rangle_i$$

$$\begin{aligned}
& \times \exp \left[\sum_{\alpha} \frac{\pi \bar{\lambda}_{\alpha}}{2M_{\alpha} \Omega_{\alpha}^3} (a_{\alpha}^{\dagger} e^{-i\Omega_{\alpha} t_0} - a_{\alpha} e^{i\Omega_{\alpha} t_0}) \right. \\
& \quad \left. - \sum_{\beta} \frac{2\pi \bar{\lambda}_{\beta}}{\sqrt{2m_{\beta} \omega_{\beta}^3}} (b_{\beta}^{\dagger} e^{-i\omega_{\beta} t_0} - b_{\beta} e^{i\omega_{\beta} t_0}) \right] \Bigg\}_i \\
& = \exp \left[- \sum_{\alpha} \frac{\pi^2 \bar{\lambda}_{\alpha}^2}{2M_{\alpha} \Omega_{\alpha}^3} (1 - e^{-i\Omega_{\alpha} t_0}) - \sum_{\beta} \frac{2\pi^2 \bar{\lambda}_{\beta}^2}{2m_{\beta} \omega_{\beta}^3} (1 - e^{-i\omega_{\beta} t_0}) \right] \\
& \quad \times \left\langle \exp \left[- \sum_{\alpha} \frac{\pi \bar{\lambda}_{\alpha}}{\sqrt{2M_{\alpha} \Omega_{\alpha}^3}} a_{\alpha}^{\dagger} (1 - e^{-i\Omega_{\alpha} t_0}) + \sum_{\beta} \frac{2\pi \bar{\lambda}_{\beta}}{\sqrt{2m_{\beta} \omega_{\beta}^3}} b_{\beta}^{\dagger} (1 - e^{-i\omega_{\beta} t_0}) \right] \right. \\
& \quad \left. \times \exp \left[\sum_{\alpha} \frac{\pi \bar{\lambda}_{\alpha}}{\sqrt{2M_{\alpha} \Omega_{\alpha}^3}} a_{\alpha} (1 - e^{i\Omega_{\alpha} t_0}) - \sum_{\beta} \frac{2\pi \bar{\lambda}_{\beta}}{\sqrt{2m_{\beta} \omega_{\beta}^3}} b_{\beta} (1 - e^{i\omega_{\beta} t_0}) \right] \right\rangle_i \\
& = \exp \left[- \sum_{\alpha} \frac{\pi^2 \bar{\lambda}_{\alpha}^2}{2M_{\alpha} \Omega_{\alpha}^3} \left(1 - e^{-i\Omega_{\alpha} t_0} + \frac{2}{e^{\beta \Omega_{\alpha}} - 1} (1 - \cos \Omega_{\alpha} t_0) \right) \right. \\
& \quad \left. - \sum_{\beta} \frac{2\pi^2 \bar{\lambda}_{\beta}^2}{m_{\beta} \omega_{\beta}^3} \left(1 - e^{-i\omega_{\beta} t_0} + \frac{2}{e^{\beta \omega_{\beta}} - 1} (1 - \cos \omega_{\beta} t_0) \right) \right].
\end{aligned}$$

In the above we have used the identities, $\exp(A+B) = \exp(A)\exp(B)\exp(-\frac{1}{2}[A,B])$ and $\langle \exp(-z^* a^{\dagger}) \exp(za) \rangle = \exp[-|z|^2/(e^{\beta \omega} - 1)]$, where a (a^{\dagger}) is an annihilation (creation) operator of a boson and $\langle \dots \rangle$ represents the thermal average with respect to the Hamiltonian $H = \omega a^{\dagger} a$. Hence Eq. (A.25) is rewritten as

$$\begin{aligned}
\Gamma & = 2t^2 \int_{-\infty}^{\infty} dt_0 \exp \left[-\pi \int_0^{\infty} d\omega \frac{e^{-\omega/\Lambda}}{\omega^2} [\bar{J}(\omega) + 4\bar{J}(\omega)] \left(\coth \frac{\beta \omega}{2} (1 - \cos \omega t_0) + i \sin \omega t_0 \right) \right] \\
& = 2t^2 \int_{-\infty}^{\infty} dt_0 \exp \left[-\frac{1}{\eta} \int_0^{\infty} d\omega \frac{e^{-\omega/\Lambda}}{\omega} \left(\coth \frac{\beta \omega}{2} (1 - \cos \omega t_0) + i \sin \omega t_0 \right) \right. \\
& \quad \left. - \frac{1}{\eta} \sum_{n=1}^{\infty} \frac{e^{-n\pi \Delta \epsilon / \Lambda}}{n} \left(\coth \frac{n\pi \beta \Delta \epsilon}{2} [1 - \cos(n\pi \Delta \epsilon t_0)] + i \sin(n\pi \Delta \epsilon t_0) \right) \right].
\end{aligned} \tag{A.26}$$

In the same way, the conductance G (3.44) is calculated as follows:

$$\begin{aligned}
G & = \beta e^2 t^4 \int_{-\infty}^{\infty} dt_0 \int_0^{\infty} dt_1 \int_0^{\infty} dt_2 e^{i\epsilon(t_1 - t_2) - \Gamma(t_1 + t_2)} \\
& \quad \times \langle e^{iH_i(t_0 - t_1 + t_2)} O_m^{\dagger} e^{iH_i t_1} O_m O_f^{\dagger} e^{-iH_i t_0} O_f O_m^{\dagger} e^{-iH_m t_2} O_m \rangle_i \\
& = \beta e^2 t^4 \int_{-\infty}^{\infty} dt_0 \int_0^{\infty} dt_1 \int_0^{\infty} dt_2 e^{i\epsilon(t_1 - t_2) - \Gamma(t_1 + t_2)} \\
& \quad \times \exp \left[-\pi \int_0^{\infty} d\omega \frac{e^{-\omega/\Lambda}}{\omega^2} \left\{ [\bar{J}(\omega) + 4\bar{J}(\omega)] K_+(\omega; t_0, t_1, t_2) \right. \right. \\
& \quad \left. \left. + [\bar{J}(\omega) - 4\bar{J}(\omega)] K_-(\omega; t_0, t_1, t_2) \right\} \right] \\
& = \beta e^2 t^4 \int_{-\infty}^{\infty} dt_0 \int_0^{\infty} dt_1 \int_0^{\infty} dt_2 \exp \left[i\epsilon(t_1 - t_2) - \Gamma(t_1 + t_2) - \frac{1}{\eta} \int_0^{\infty} d\omega \frac{e^{-\omega/\Lambda}}{\omega} K_+(\omega; t_0, t_1, t_2) \right. \\
& \quad \left. - \frac{1}{\eta} \sum_{n=1}^{\infty} \frac{e^{-n\pi \Delta \epsilon / \Lambda}}{n} K_+(n\pi \Delta \epsilon; t_0, t_1, t_2) \right. \\
& \quad \left. - \frac{1}{\eta} \sum_{n=1}^{\infty} (-1)^{n-1} \frac{e^{-n\pi \Delta \epsilon / \Lambda}}{n} K_-(n\pi \Delta \epsilon; t_0, t_1, t_2) \right], \tag{A.27}
\end{aligned}$$

where

$$K_+(\omega; t_0, t_1, t_2) \equiv \coth \frac{\beta\omega}{2} \left[2 - \cos \omega t_0 - \cos \omega(t_0 - t_1 + t_2) \right] + i \left[\sin \omega t_0 + \sin \omega(t_0 - t_1 + t_2) \right],$$

$$K_-(\omega; t_0, t_1, t_2) \equiv \coth \frac{\beta\omega}{2} \left[\cos \omega t_1 + \cos \omega t_2 - \cos \omega(t_0 - t_1) - \cos \omega(t_0 + t_2) \right]$$

$$+ i \left[\sin \omega t_1 - \sin \omega t_2 + \sin \omega(t_0 - t_1) + \sin \omega(t_0 + t_2) \right].$$

It is interesting to note that the summations in Eqs. (A.26) and (A.27) arise from the discreteness of resonant levels.

We will estimate Γ and G for two limiting cases: (i) $T \ll \Delta\epsilon$ and (ii) $\Delta\epsilon \ll T \ll U$.

(i) $T \ll \Delta\epsilon$.

In this case we may neglect the oscillating terms in the discrete summations in Eqs. (A.26) and (A.27). Then Γ is calculated as

$$\Gamma \approx 2t^2 \int_{-\infty}^{\infty} dt_0 \exp \left[-\frac{1}{\eta} \int_0^{\infty} d\omega \frac{e^{-\omega/\Lambda}}{\omega} \left(\coth \frac{\beta\omega}{2} (1 - \cos \omega t_0) + i \sin \omega t_0 \right) - \frac{1}{\eta} \sum_{n=1}^{\infty} \frac{e^{-n\pi\Delta\epsilon/\Lambda}}{n} \right]^{-\frac{1}{\eta}}$$

$$\approx 2t^2 \left(\frac{\pi\Delta\epsilon}{\Lambda} \right)^{\frac{1}{\eta}} \int_{-\infty}^{\infty} dt_0 \left[(1 + i\Lambda t_0) \frac{\beta}{\pi t_0} \sinh \frac{\pi t_0}{\beta} \right]$$

$$\approx \frac{2\sqrt{\pi} \Gamma(\frac{1}{2\eta}) t^2}{\Gamma(\frac{1}{2\eta} + \frac{1}{2}) \Lambda} \left(\frac{\pi\Delta\epsilon}{\Lambda} \right)^{\frac{1}{\eta}} \left(\frac{\pi T}{\Lambda} \right)^{\frac{1}{\eta} - 1}$$

$$= \frac{2\sqrt{\pi} \Gamma(\frac{1}{2\eta})}{\Gamma(\frac{1}{2\eta} + \frac{1}{2})} \pi\Delta\epsilon \left(\frac{t}{\Lambda} \right)^2 \left(\frac{\pi^2 \Delta\epsilon T}{\Lambda^2} \right)^{\frac{1}{\eta} - 1}.$$

The evaluation of the conductance G is more complicated but straight-forward:

$$G \approx \beta e^2 t^4 \int_{-\infty}^{\infty} dt_0 \int_0^{\infty} dt_1 \int_0^{\infty} dt_2 \exp \left[i\epsilon(t_1 - t_2) - \Gamma(t_1 + t_2) - \frac{2}{\eta} \sum_{n=1}^{\infty} \frac{e^{-n\pi\Delta\epsilon/\Lambda}}{n} \right]$$

$$- \frac{1}{\eta} \int_0^{\infty} d\omega \frac{e^{-\omega/\Lambda}}{\omega} K_+(\omega; t_0, t_1, t_2) \Big]$$

$$\approx \beta e^2 t^4 \left(\frac{\pi\Delta\epsilon}{\Lambda} \right)^{\frac{2}{\eta}} \int_{-\infty}^{\infty} dt_0 \left[(1 + i\Lambda t_0) \frac{\beta}{\pi t_0} \sinh \frac{\pi t_0}{\beta} \right]^{-\frac{1}{\eta}}$$

$$\times \int_{-\infty}^{\infty} d\tilde{t} \exp(i\epsilon\tilde{t}) \left([1 + i\Lambda(t_0 - \tilde{t})] \frac{\beta}{\pi(t_0 - \tilde{t})} \sinh \frac{\pi(t_0 - \tilde{t})}{\beta} \right)^{-\frac{1}{\eta}} \int_{|\tilde{t}|/2}^{\infty} d\tilde{t} \exp(-2\Gamma\tilde{t})$$

$$(\tilde{t} \equiv (t_1 + t_2)/2, \tilde{t} \equiv t_1 - t_2)$$

$$= \frac{\beta e^2 t^4}{2\Gamma} \left(\frac{\pi\Delta\epsilon}{\Lambda} \right)^{\frac{2}{\eta}} \int_{-\infty}^{\infty} d\tilde{t} \exp(i\epsilon\tilde{t} - \Gamma|\tilde{t}|)$$

$$\times \int_{-\infty}^{\infty} dt_0 \left((1 + i\Lambda t_0) \frac{\beta}{\pi t_0} \sinh \frac{\pi t_0}{\beta} [1 + i\Lambda(t_0 - \tilde{t})] \frac{\beta}{\pi(t_0 - \tilde{t})} \sinh \frac{\pi(t_0 - \tilde{t})}{\beta} \right)^{-\frac{1}{\eta}}$$

$$= \frac{\beta e^2 t^4}{2\pi} \left(\frac{\pi\Delta\epsilon}{\Lambda} \right)^{\frac{2}{\eta}} \int_{-\infty}^{\infty} d\tilde{t} \int_{-\infty}^{\infty} dE \frac{e^{iE\tilde{t}}}{(E - \epsilon)^2 + \Gamma^2}$$

$$\times \int_{-\infty + \frac{1}{2}\beta}^{\infty + \frac{1}{2}\beta} dt_0 \left((1 + i\Lambda t_0) \frac{\beta}{\pi t_0} \sinh \frac{\pi t_0}{\beta} [1 + i\Lambda(t_0 - \tilde{t})] \frac{\beta}{\pi(t_0 - \tilde{t})} \sinh \frac{\pi(t_0 - \tilde{t})}{\beta} \right)^{-\frac{1}{\eta}}$$

$$= \frac{\beta e^2 t^4}{2\pi} \left(\frac{\pi \Delta \epsilon}{\Lambda} \right)^{\frac{2}{\eta}} \left(\frac{\pi T}{\Lambda} \right)^{\frac{2}{\eta}} \int_{-\infty}^{\infty} dE \frac{1}{(E - \epsilon)^2 + \Gamma^2} \left[\int_{-\infty}^{\infty} dt_0 e^{iEt_0} \left(\cosh \frac{\pi t_0}{\beta} \right)^{-\frac{1}{\eta}} \right]^2.$$

The Fourier transform of $[\cosh(\pi t_0/\beta)]^{-\frac{1}{\eta}}$ is related to the Gamma function:

$$\begin{aligned} \int_{-\infty}^{\infty} dt_0 e^{iEt_0} \left(\cosh \frac{\pi t_0}{\beta} \right)^{-\frac{1}{\eta}} &= \frac{2^{\frac{1}{\eta}-1}}{\pi} \beta B\left(\frac{1}{2\eta} - i\frac{\beta E}{2\pi}, \frac{1}{2\eta} + i\frac{\beta E}{2\pi}\right) \\ &= \frac{2^{\frac{1}{\eta}-1}}{\pi T} \frac{|\Gamma(\frac{1}{2\eta} + i\frac{\beta E}{2\pi})|^2}{\Gamma(\frac{1}{\eta})}. \end{aligned}$$

Hence the conductance G is obtained as

$$\begin{aligned} G &= \frac{2^{\frac{2}{\eta}-3}}{(\pi T)^3} e^2 t^4 \left(\frac{\pi \Delta \epsilon}{\Lambda} \right)^{\frac{2}{\eta}} \left(\frac{\pi T}{\Lambda} \right)^{\frac{2}{\eta}} \int_{-\infty}^{\infty} dE \frac{1}{(E - \epsilon)^2 + \Gamma^2} \frac{|\Gamma(\frac{1}{2\eta} + i\frac{\beta E}{2\pi})|^4}{[\Gamma(\frac{1}{\eta})]^2} \\ &= \frac{2^{\frac{2}{\eta}-5}}{\pi^2} \beta e^2 \left(\frac{\Gamma(\frac{1}{2\eta} + \frac{1}{2})}{\Gamma(\frac{1}{2\eta})\Gamma(\frac{1}{\eta})} \right)^2 \int_{-\infty}^{\infty} dE \frac{\Gamma^2}{(E - \epsilon)^2 + \Gamma^2} |\Gamma(\frac{1}{2\eta} + i\frac{\beta E}{2\pi})|^4 \\ &= \frac{\beta e^2}{8\pi} \int_{-\infty}^{\infty} dE \frac{\Gamma^2}{(E - \epsilon)^2 + \Gamma^2} \left| \frac{\Gamma(\frac{1}{2\eta} + i\frac{\beta E}{2\pi})}{\Gamma(\frac{1}{2\eta})} \right|^4, \end{aligned}$$

where we have used the identity, $\Gamma(2z) = 2^{2z-1} \pi^{-\frac{1}{2}} \Gamma(z) \Gamma(z + \frac{1}{2})$.

Now we define a function $F(E)$ by

$$F(E) \equiv \frac{\beta}{4\pi^2} \left| \Gamma\left(\frac{1}{2\eta} + i\frac{\beta E}{2\pi}\right) \right|^4.$$

For $\eta = 1$, $F(E)$ is equal to $-f'(E)$, where $f(E)$ is the Fermi distribution function. In this sense $F(E)$ may be considered as a generalization of the derivative of the Fermi distribution function to Luttinger liquids. Furthermore, it is easily shown that

$$\begin{aligned} F(E) &\sim \beta \left(\frac{\beta |E|}{2\pi} \right)^{\frac{2}{\eta}-2} \exp(-\beta |E|) \quad \text{for } \beta |E| \rightarrow \infty, \\ \int_{-\infty}^{\infty} F(E) dE &= \frac{[\Gamma(\frac{1}{\eta})]^4}{\Gamma(\frac{2}{\eta})}. \end{aligned}$$

(ii) $\Delta \epsilon \ll T \ll U$.

In this temperature range, the discrete summations in Eqs. (A.26) and (A.27) may be replaced by integrals over ω . Accordingly, the temperature dependence of Γ and G is changed.

The level width Γ is calculated as follows.

$$\begin{aligned} \Gamma &\approx 2t^2 \int_{-\infty}^{\infty} dt_0 \exp \left[-\frac{2}{\eta} \int_0^{\infty} d\omega \frac{e^{-\omega/\Lambda}}{\omega} \left(\coth \frac{\beta \omega}{2} (1 - \cos \omega t_0) + i \sin \omega t_0 \right) \right] \\ &\approx \frac{2\sqrt{\pi} \Gamma(\frac{1}{\eta}) t^2}{\Gamma(\frac{1}{\eta} + \frac{1}{2}) \Lambda} \left(\frac{\pi T}{\Lambda} \right)^{\frac{2}{\eta}-1} \\ &= \frac{2\sqrt{\pi} \Gamma(\frac{1}{\eta})}{\Gamma(\frac{1}{\eta} + \frac{1}{2})} \pi T \left(\frac{t}{\Lambda} \right)^2 \left(\frac{\pi T}{\Lambda} \right)^{\frac{2}{\eta}-2}. \end{aligned}$$

The conductance G is also obtained as

$$\begin{aligned}
 G &\approx \beta e^2 t^4 \int_{-\infty}^{\infty} dt_0 \int_0^{\infty} dt_1 \int_0^{\infty} dt_2 \exp \left[i\varepsilon(t_1 - t_2) - \Gamma(t_1 + t_2) - \frac{2}{\eta} \int_0^{\infty} d\omega \frac{e^{-\omega/\Lambda}}{\omega} K_+(\omega; t_0, t_1, t_2) \right] \\
 &\approx \frac{2^{\frac{4}{\eta}-3}}{(\pi t)^3} e^2 t^4 \left(\frac{\pi T}{\Lambda} \right)^{\frac{4}{\eta}} \int_{-\infty}^{\infty} dE \frac{1}{(E - \varepsilon)^2 + \Gamma^2} \frac{|\Gamma(\frac{1}{\eta} + i\frac{\beta E}{2\pi})|^4}{[\Gamma(\frac{2}{\eta})]^2} \\
 &= \frac{2^{\frac{4}{\eta}-5}}{\pi^2} \beta e^2 \left(\frac{\Gamma(\frac{1}{\eta} + \frac{1}{2})}{\Gamma(\frac{1}{\eta})\Gamma(\frac{2}{\eta})} \right)^2 \int_{-\infty}^{\infty} dE \frac{\Gamma^2}{(E - \varepsilon)^2 + \Gamma^2} |\Gamma(\frac{1}{\eta} + i\frac{\beta E}{2\pi})|^4 \\
 &= \frac{\beta e^2}{8\pi} \int_{-\infty}^{\infty} dE \frac{\Gamma^2}{(E - \varepsilon)^2 + \Gamma^2} \left| \frac{\Gamma(\frac{1}{\eta} + i\frac{\beta E}{2\pi})}{\Gamma(\frac{1}{\eta})} \right|^4.
 \end{aligned}$$

References

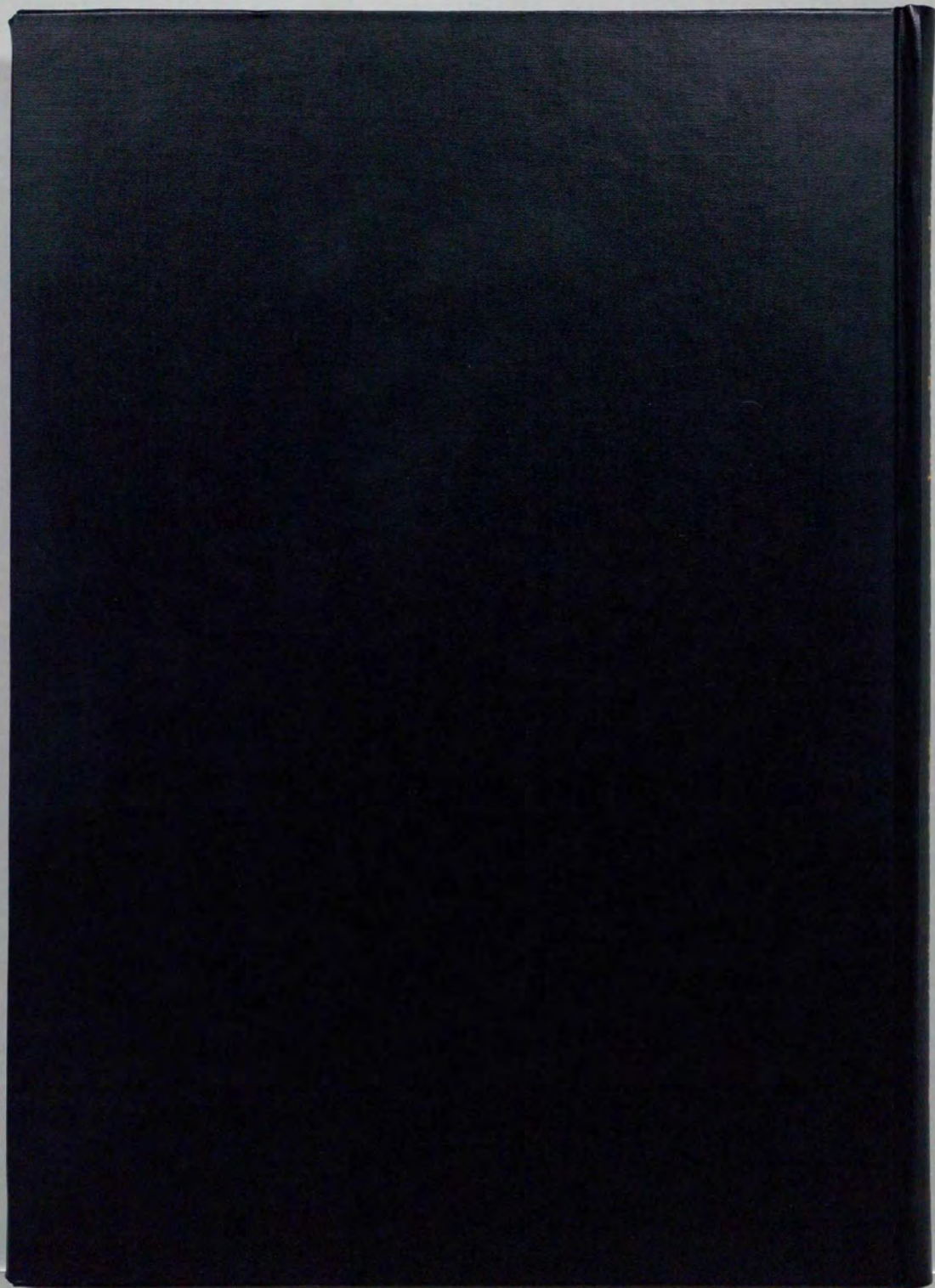
- [1] J. J. More and R. S. Sargent, *Optimization of Process Control Systems*, Wiley-Interscience, New York, 1979.
- [2] J. J. More and R. S. Sargent, *Optimization of Process Control Systems*, Wiley-Interscience, New York, 1979.
- [3] J. J. More and R. S. Sargent, *Optimization of Process Control Systems*, Wiley-Interscience, New York, 1979.
- [4] J. J. More and R. S. Sargent, *Optimization of Process Control Systems*, Wiley-Interscience, New York, 1979.
- [5] J. J. More and R. S. Sargent, *Optimization of Process Control Systems*, Wiley-Interscience, New York, 1979.
- [6] J. J. More and R. S. Sargent, *Optimization of Process Control Systems*, Wiley-Interscience, New York, 1979.
- [7] J. J. More and R. S. Sargent, *Optimization of Process Control Systems*, Wiley-Interscience, New York, 1979.
- [8] J. J. More and R. S. Sargent, *Optimization of Process Control Systems*, Wiley-Interscience, New York, 1979.
- [9] J. J. More and R. S. Sargent, *Optimization of Process Control Systems*, Wiley-Interscience, New York, 1979.
- [10] J. J. More and R. S. Sargent, *Optimization of Process Control Systems*, Wiley-Interscience, New York, 1979.
- [11] J. J. More and R. S. Sargent, *Optimization of Process Control Systems*, Wiley-Interscience, New York, 1979.
- [12] J. J. More and R. S. Sargent, *Optimization of Process Control Systems*, Wiley-Interscience, New York, 1979.
- [13] J. J. More and R. S. Sargent, *Optimization of Process Control Systems*, Wiley-Interscience, New York, 1979.
- [14] J. J. More and R. S. Sargent, *Optimization of Process Control Systems*, Wiley-Interscience, New York, 1979.
- [15] J. J. More and R. S. Sargent, *Optimization of Process Control Systems*, Wiley-Interscience, New York, 1979.
- [16] J. J. More and R. S. Sargent, *Optimization of Process Control Systems*, Wiley-Interscience, New York, 1979.
- [17] J. J. More and R. S. Sargent, *Optimization of Process Control Systems*, Wiley-Interscience, New York, 1979.
- [18] J. J. More and R. S. Sargent, *Optimization of Process Control Systems*, Wiley-Interscience, New York, 1979.
- [19] J. J. More and R. S. Sargent, *Optimization of Process Control Systems*, Wiley-Interscience, New York, 1979.
- [20] J. J. More and R. S. Sargent, *Optimization of Process Control Systems*, Wiley-Interscience, New York, 1979.

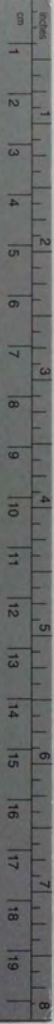
References

- [1] D. V. Averin and K. K. Likharev, in *Mesoscopic Phenomena in Solids*, edited by B. L. Altshuler, P. A. Lee, and R. A. Webb (Elsevier, Amsterdam, 1990).
- [2] M. A. Kastner, *Rev. Mod. Phys.* **64**, 849 (1992).
- [3] F. D. M. Haldane, *J. Phys. C* **14**, 2585 (1981).
- [4] Y. Suzumura, *Prog. Theor. Phys.* **61**, 1 (1978).
- [5] V. J. Emery, in *Highly Conducting One-Dimensional Solids*, edited by J. T. Devreese *et al.* (Plenum, New York, 1979).
- [6] J. Sólyom, *Adv. Phys.* **28**, 209 (1979).
- [7] H. Fukuyama and H. Takayama, in *Dynamical Properties of Quasi-One-Dimensional Conductors*, edited by P. Monceau (Reidel, 1984).
- [8] I. Affleck, in *Fields, Strings and Critical Phenomena*, edited by E. Brézin and J. Zinn-Justin (Elsevier, Amsterdam, 1989), p. 563.
- [9] N. Kawakami and S.-K. Yang, *Prog. Theor. Phys. Suppl.* **107**, 59 (1992).
- [10] S. Tomonaga, *Prog. Theor. Phys.* **5**, 544 (1950).
- [11] J. M. Luttinger, *J. Math. Phys.* **4**, 1154 (1963).
- [12] G. D. Mahan, *Many-Particle Physics* (Plenum, New York, 1981), 2nd ed.
- [13] S. T. Chui and J. W. Bray, *Phys. Rev. B* **16**, 1329 (1977); *Phys. Rev. B* **19**, 4020 (1979).
- [14] W. Apel, *J. Phys. C* **15**, 1973 (1982); W. Apel and T. M. Rice, *Phys. Rev. B* **26**, 7063 (1982).
- [15] Y. Suzumura and H. Fukuyama, *J. Phys. Soc. Jpn.* **52**, 2870 (1983); **53**, 3918 (1984); T. Saso, Y. Suzumura, and H. Fukuyama, *Prog. Theor. Phys. Suppl.* **84**, 269 (1985).
- [16] T. Giamarchi and H. J. Schultz, *Phys. Rev. B* **37**, 325 (1988).
- [17] C. L. Kane and M. P. A. Fisher, *Phys. Rev. Lett.* **68**, 1220 (1992).
- [18] A. Furusaki and N. Nagaosa, *Phys. Rev. B* **47**, 4631 (1993).
- [19] C. L. Kane and M. P. A. Fisher, *Phys. Rev. B* **46**, 7268 (1992).

- [20] C. L. Kane and M. P. A. Fisher, Phys. Rev. B **46**, 15233 (1992).
- [21] A. Furusaki and N. Nagaosa, Phys. Rev. B **47**, 3827 (1993).
- [22] A. O. Caldeira and A. J. Leggett, Ann. Phys. (N.Y.) **149**, 374 (1983).
- [23] A. Schmid, Phys. Rev. Lett. **51**, 1506 (1983).
- [24] F. Guinea, V. Hakim, and A. Muramatsu, Phys. Rev. Lett. **54**, 263 (1985).
- [25] M. P. A. Fisher and W. Zwerger, Phys. Rev. B **32**, 6190 (1985).
- [26] J. Kondo, Prog. Theor. Phys. **32**, 37 (1964).
- [27] A. Luther and I. Peschel, Phys. Rev. B **9**, 2911 (1974).
- [28] H. Fukuyama and P. A. Lee, Phys. Rev. B **17**, 535 (1978).
- [29] R. Landauer, IBM J. Res. Dev. **1**, 223 (1957); Phil. Mag. **21**, 863 (1970).
- [30] L. I. Glazman, I. M. Ruzin, and B. I. Shklovskii, Phys. Rev. B **45**, 8454 (1992).
- [31] A. I. Larkin and P. A. Lee, Phys. Rev. B **17**, 1596 (1978).
- [32] S.-k. Ma, *Modern Theory of Critical Phenomena* (Benjamin/Cummings, Reading, Massachusetts, 1976).
- [33] R. P. Feynman and F. L. Vernon, Ann. Phys. (N.Y.) **24**, 118 (1963).
- [34] M. H. Devoret, D. Esteve, H. Grabert, G.-L. Ingold, H. Pothier, and C. Urbina, Phys. Rev. Lett. **64**, 1824 (1990).
- [35] S. M. Girvin, L. I. Glazman, M. Jonson, D. R. Penn, M. D. Stiles, Phys. Rev. Lett. **64**, 3183 (1990).
- [36] J. H. F. Scott-Thomas, B. Field, M. A. Kastner, H. I. Smith, D. A. Antoniadis, Phys. Rev. Lett. **62**, 583 (1989); U. Meirav, M. A. Kastner, and S. J. Wind, Phys. Rev. Lett. **65**, 771 (1990); P. L. McEuen, E. B. Foxman, U. Meirav, M. A. Kastner, Y. Meir, N. S. Wingreen, and S. J. Wind, Phys. Rev. Lett. **66**, 1926 (1991); U. Meirav, P. L. McEuen, M. A. Kastner, E. B. Foxman, A. Kumar, and S. J. Wind, Z. Phys. B **85**, 357 (1991) and references therein.
- [37] H. van Houten and C. W. J. Beenakker, Phys. Rev. Lett. **63**, 1893 (1989).
- [38] Y. Meir, N. Wingreen, and P. A. Lee, Phys. Rev. Lett. **66**, 3048 (1991).
- [39] C. W. J. Beenakker, Phys. Rev. B **44**, 1646 (1991).
- [40] M. Büttiker, IBM J. Res. Dev. **32**, 63 (1988).
- [41] P. W. Anderson, G. Yuval, and D. R. Hamann, Phys. Rev. B **1**, 4464 (1970).
- [42] See, for example, P. A. Lee and T. V. Ramakrishnan, Rev. Mod. Phys. **57**, 287 (1985).
- [43] J. Kondo, Physica **84B**, 40 (1976); **125B**, 279 (1984); **126B**, 377 (1984).

- [44] K. G. Wilson, *Rev. Mod. Phys.* **47**, 773 (1975).
- [45] P. Nozières and C. T. de Dominicis, *Phys. Rev.* **178**, 1097 (1969).
- [46] X. G. Wen, *Phys. Rev. Lett.* **64**, 2206 (1990); *Phys. Rev. B* **41**, 12838 (1990).
- [47] M. Stone, *Phys. Rev. B* **42**, 8399 (1990).
- [48] J. M. Kinaret, Y. Meir, N. S. Wingreen, P. Lee, and X.-G. Wen, *Phys. Rev. B* **45**, 9489 (1992); **46**, 4681 (1992).
- [49] S. Eggert and I. Affleck, *Phys. Rev. B* **46**, 10866 (1992).
- [50] L. I. Glazman and M. E. Raikh, *Pis'ma Zh. Eksp. Teor. Fiz.* **47**, 378 (1988) [*JETP Lett.* **47**, 452 (1988)].
- [51] T. K. Ng and P. A. Lee, *Phys. Rev. Lett.* **61**, 1768 (1988).
- [52] A. Kawabata, *J. Phys. Soc. Jpn.* **60** 3222 (1991).
- [53] D.-H. Lee and J. Toner, *Phys. Rev. Lett.* **69**, 3378 (1992).
- [54] T. Ogawa, A. Furusaki, and N. Nagaosa, *Phys. Rev. Lett.* **68**, 3638 (1992).
- [55] D. K. K. Lee and Y. Chen, *Phys. Rev. Lett.* **69**, 1399 (1992).





Kodak Color Control Patches

Blue Cyan Green Yellow Red Magenta White 3/Color Black



Kodak Gray Scale

A 1 2 3 4 5 6 M 8 9 10 11 12 13 14 15 B 17 18 19



© Kodak, 2007 TM Kodak